Appendix A.6:

Vivian St – CPT 5586

Table 1: Site Description for Vivian St (CC LIQ 1 – CPT 5586).

Attribute	Yes/No			Description/Date	Symbol in Figure 1
	10-m Buffer	20-m Buffer	50-m Buffer		
Near a body of surface water or other free face features?	No	No	No	The center of the site is 450 meters away from the Avon River. The direction of the free face is roughly NW-SE, while its height is approximately 1.5 m.	NA
Lateral spreading observed during the CES?	No	No	No	Ground cracks that are <10mm and 10-50mm (plus one crack of 50-200mm) in length and indicating lateral stretching within the 10-m, 20-m, and 50-m buffers, respectively, were observed by the mapping team.[1] However, these cracks likely represent creep of slightly elevated ground toward the road with the relatively lower elevation, and as such appear to be only a local feature. Cracks in concrete pavement due to undulating land are also possible.	NA
Nearby buildings or structures?	Yes	Yes	Yes	Building coverage of the 10-m, 20-m, and 50-m buffers is 12%, 22%, and 26%, respectively.	White Fill + Brown Outline
Sloping land?	No	No	No	Flat land, residential area	NA
Step changes in the ground surface?	No	No	No	NA	NA
Retaining walls?	No	No	No	NA	NA
Vegetation?	Yes	Yes	Yes	Trees and bushes cover 37% of the 10-m buffer, 15% of the 20-m buffer and 22% of the 50-m buffer. They are in all quadrants of the buffers.	White Fill + Green Outline
Anthropogenic changes to the site between the LiDAR surveys?	No	No	No	NA	NA
Other important factors?	No	Yes	Yes	Low-motor-vehicle-volume, two-way roadway (street) occupies 18% of the 20-m buffer and stretches throughout the NE and SE quadrants. It covers 10% of the 50-m buffer and stretches throughout the NE and SE quadrants. Trampoline is in the NW quadrant of the 50-m buffer.	Trampoline: White Fill +Blue Outline Road: Gray Fill + Red Outline

Note: Buffer is the area within a circle of a specified radius with CPT investigations done at its center (172.689983°, -43.496445°).

[1] Canterbury Geotechnical Database. (2012). "Observed Ground Crack Locations", Map Layer CGD0400 - 23 July 2012, retrieved July 09, 2018 from https://canterburygeotechnicaldatabase.projectorbit.com/

Figure 1: Site plan with patches where LiDAR survey data is considered.

Note 1: Ten patches (outlined in red) in free field were initially selected for settlement assessment as areas free of vegetation and structures. Further analyses such as proximity of a patch to a CPT, proximity of a patch to a property subjected to addition and/or demolition of a structure, front yard/backyard alterations (e.g., ploughing, rubble, scrap), aerial distribution of sediment ejecta, and density of LiDAR points for 2003 resulted in Patches A, B, and C being selected for detailed settlement assessment and other patches being discarded in detailed settlement assessment. In addition, since significant amounts of ejecta were observed on roads in the CES, the entire portion of the road within the 50-m buffer was considered for settlement assessment. Roads as hard, relatively flat surfaces provide many ground-classified points. Therefore, it is very useful to compare settlement estimates on roads with settlement estimates for the selected patches.

Table 2: LiDAR flight error adjustments, global adjustments for the difference between average LiDAR point elevations and benchmark survey elevations, and vertical tectonic movement adjustments.

	Adjustments (mm)		
Earthquake Event(s)	LiDAR Flight Error	Global Offset[2]	Tectonic Vertical Movement
Sep-10	-100	-3	0
Feb-11	0	16	-43
Jun-11	0	38	-42
Dec-11	0	-65	0
CES	-100	-14	-85
Post Sep 2010 LiDAR survey affected by ejecta?			No

Note: The negative sign indicates the subtraction from the ground surface subsidence, while the positive sign indicates the addition to the ground surface subsidence.

Table 3a: LiDAR Measurement Error for Patch A.

Surveys	Buffer	Area Averaged Difference Indicating Repeat Measurement Error (mm)	$\sigma^*_{\text{individual LiDAR points}}$ (mm)	%Reduction in σ due to Area Averaging of LiDAR Points
Post Feb 2011: Mar 2011 and May 2011	10-m	57	59	[97,97]
	20-m	57		
	50-m	57		
Post Dec 2011: Feb 2012 and Oct 2015	10-m	49	70	[70,70]
	20-m	49		
	50-m	49		

*Standard deviation.

[2] Russell, J., & van Ballegooy, S. (2015). *Canterbury Earthquake Sequence: Increased liquefaction vulnerability assessment methodology*. New Zealand: Tonkin & Taylor Ltd.

Table 3b: LiDAR Measurement Error for Patch B.

Surveys	Buffer	Area Averaged Difference Indicating Repeat Measurement Error (mm)	$\sigma^*_{\text{individual LiDAR points}}$ (mm)	%Reduction in σ due to Area Averaging of LiDAR Points
Post Feb 2011: Mar 2011 and May 2011	10-m	NA	59	[31,31]
	20-m	18		
	50-m	18		
Post Dec 2011: Feb 2012 and Oct 2015	10-m	NA	70	[19,19]
	20-m	13		
	50-m	13		

*Standard deviation.

Table 3c: LiDAR Measurement Error for Patch C.

Surveys	Buffer	Area Averaged Difference Indicating Repeat Measurement Error (mm)	$\sigma^*_{\text{individual LiDAR points}}$ (mm)	%Reduction in σ due to Area Averaging of LiDAR Points
Post Feb 2011: Mar 2011 and May 2011	10-m	NA	59	[56,56]
	20-m	NA		
	50-m	33		
Post Dec 2011: Feb 2012 and Oct 2015	10-m	NA	70	[7,7]
	20-m	NA		
	50-m	5		

*Standard deviation.

Table 3d: LiDAR Measurement Error for Road.

Surveys	Buffer	Area Averaged Difference Indicating Repeat Measurement Error (mm)	$\sigma^*_{\text{individual LiDAR points}}$ (mm)	%Reduction in σ due to Area Averaging of LiDAR Points
Post Feb 2011: Mar 2011 and May 2011	10-m	NA	59	[44, 64]
	20-m	26		
	50-m	38		
Post Dec 2011: Feb 2012 and Oct 2015	10-m	NA	70	[3,3]
	20-m	2		
	50-m	2		

*Standard deviation.

Table 4a: Ground surface subsidence adjustments due to LiDAR measurement error for Patch A.

Earthquake Event(s)	$\sigma_{\text{pre-EQ LiDAR survey}}$ (mm)	$\sigma_{\text{post-EQ LiDAR survey}}$ (mm)	σ_{total} (mm)	Area Average Adjusted σ (mm) **
Sep-10	158	56	134	±130
Feb-11	56	59	59	±57
Jun-11	59	61	62	±60
Dec-11	61	70	87	±84
CES	158	70	124	±120

**Based on the highest %Reduction in Table 3a.

Table 4b: Ground surface subsidence adjustments due to LiDAR measurement error for Patch B.

Earthquake Event(s)	$\sigma_{\text{pre-EQ LiDAR survey}}$ (mm)	$\sigma_{\text{post-EQ LiDAR survey}}$ (mm)	σ_{total} (mm)	Area Average Adjusted σ (mm) **
Sep-10	158	56	134	±41
Feb-11	56	59	59	±18
Jun-11	59	61	62	±19
Dec-11	61	70	87	±26
CES	158	70	124	±38

**Based on the highest %Reduction in Table 3b.

Table 4c: Ground surface subsidence adjustments due to LiDAR measurement error for Patch C.

Earthquake Event(s)	$\sigma_{pre\text{-}EQ\ LiDAR\ survey}$ (mm)	$\sigma_{post\text{-}EQ\ LiDAR\ survey}$ (mm)	σ_{total} (mm)	Area Average Adjusted σ (mm) **
Sep-10	158	56	134	±75
Feb-11	56	59	59	±33
Jun-11	59	61	62	±35
Dec-11	61	70	87	±48
CES	158	70	124	±70

**Based on the highest %Reduction in Table 3c.

Table 4d: Ground surface subsidence adjustments due to LiDAR measurement error for Road.

Earthquake Event(s)	$\sigma_{pre\text{-}EQ\ LiDAR\ survey}$ (mm)	$\sigma_{post\text{-}EQ\ LiDAR\ survey}$ (mm)	σ_{total} (mm)	Area Average Adjusted σ (mm) **
Sep-10	158	56	134	±86
Feb-11	56	59	59	±38
Jun-11	59	61	62	±40
Dec-11	61	70	87	±56
CES	158	70	124	±80

**Based on the highest %Reduction in Table 3d.

Table 5a: Raw liquefaction-related ground surface subsidence using original LiDAR points for Patch A.

	Average Ground Surface Subsidence (mm)		
Earthquake Event(s)	10-m Buffer	20-m Buffer	50-m Buffer
Sep-10	-1	-1	-1
Feb-11	244	244	244
Jun-11	85	85	85
Dec-11	85	85	85
CES	413	413	413

Table 5b: Raw liquefaction-related ground surface subsidence using original LiDAR points for Patch B.

	Average Ground Surface Subsidence (mm)		
Earthquake Event(s)	10-m Buffer	20-m Buffer	50-m Buffer
Sep-10	NA	260	260
Feb-11	NA	168	168
Jun-11	NA	56	56
Dec-11	NA	90	90
CES	NA	575	575

Table 5c: Raw liquefaction-related ground surface subsidence using original LiDAR points for Patch C.

	Average Ground Surface Subsidence (mm)		
Earthquake Event(s)	10-m Buffer	20-m Buffer	50-m Buffer
Sep-10	NA	NA	75
Feb-11	NA	NA	241
Jun-11	NA	NA	85
Dec-11	NA	NA	54
CES	NA	NA	455

Table 5d: Raw liquefaction-related ground surface subsidence using original LiDAR points for Road.

	Average Ground Surface Subsidence (mm)		
Earthquake Event(s)	10-m Buffer	20-m Buffer	50-m Buffer
Sep-10	NA	91	106
Feb-11	NA	154	125
Jun-11	NA	83	87
Dec-11	NA	62	58
CES	NA	390	376

Table 6a: Corrected liquefaction-related ground surface subsidence using original LiDAR points for Patch A with the calculated adjustments in Table 2.

	Average Calculated Ground Surface Subsidence (mm)		
Earthquake Event(s)	10-m Buffer	20-m Buffer	50-m Buffer
Sep-10	-104 ± 125	-104 ± 125	-104 ± 125
Feb-11	217 ± 50	217 ± 50	217 ± 50
Jun-11	81 ± 50	81 ± 50	81 ± 50
Dec-11	20 ± 75	20 ± 75	20 ± 75
CES	214 ± 125	214 ± 125	214 ± 125

Notes: Plus/minus values are same as those in Table 4a, but rounded to the nearest 25; Positive overall values indicate ground surface subsidence, while negative overall values indicate ground surface uplift.

Table 6b: Corrected liquefaction-related ground surface subsidence using original LiDAR points for Patch B with the calculated adjustments in Table 2.

	Average Calculated Ground Surface Subsidence (mm)		
Earthquake Event(s)	10-m Buffer	20-m Buffer	50-m Buffer
Sep-10	NA	157±50	157±50
Feb-11	NA	141±25	141±25
Jun-11	NA	52±25	52±25
Dec-11	NA	25±25	25±25
CES	NA	376±50	376±50

Notes: Plus/minus values are same as those in Table 4b, but rounded to the nearest 25; Positive overall values indicate ground surface subsidence, while negative overall values indicate ground surface uplift.

Table 6c: Corrected liquefaction-related ground surface subsidence using original LiDAR points for Patch C with the calculated adjustments in Table 2.

	Average Calculated Ground Surface Subsidence (mm)		
Earthquake Event(s)	10-m Buffer	20-m Buffer	50-m Buffer
Sep-10	NA	NA	-28 ± 75
Feb-11	NA	NA	214 ± 25
Jun-11	NA	NA	81 ± 25
Dec-11	NA	NA	-11 ± 50
CES	NA	NA	256 ± 75

Notes: Plus/minus values are same as those in Table 4c, but rounded to the nearest 25; Positive overall values indicate ground surface subsidence, while negative overall values indicate ground surface uplift.

Table 6d: Corrected liquefaction-related ground surface subsidence using original LiDAR points for Road with the calculated adjustments in Table 2.

	Average Calculated Ground Surface Subsidence (mm)		
Earthquake Event(s)	10-m Buffer	20-m Buffer	50-m Buffer
Sep-10	NA	-12 ± 75	3 ± 75
Feb-11	NA	127 ± 50	98 ± 50
Jun-11	NA	79 ± 50	83 ± 50
Dec-11	NA	-3 ± 50	-7 ± 50
CES	NA	191 ± 75	177 ± 75

Notes: Plus/minus values are same as those in Table 4c, but rounded to the nearest 25; Positive overall values indicate ground surface subsidence, while negative overall values indicate ground surface uplift.

Table 7a: Corrected liquefaction-related ground surface subsidence for Patch A using LiDAR DEMs.

	Estimated Ground Surface Subsidence (mm)								
	10-m Buffer			20-m Buffer			50-m Buffer		
Earthquake Event(s)	16th %ile	50th %ile	84th %ile	16th %ile	50th %ile	84th %ile	16th %ile	50th %ile	84th %ile
Sep-10	<50	<50	<50	<50	<50	<50	<50	<50	<50
Feb-11	150	150	150	150	150	150	150	150	150
Jun-11	50	50	50	50	50	50	50	50	50
Dec-11	50	50	50	50	50	50	50	50	50
CES	350	350	350	350	350	350	350	350	350

Note: These percentiles are not the exact statistical measures; they indicate the spatial variability of ground surface subsidence.

Table 7b: Corrected liquefaction-related ground surface subsidence for Patch B using LiDAR DEMs.

	Estimated Ground Surface Subsidence (mm)								
	10-m Buffer			20-m Buffer			50-m Buffer		
Earthquake Event(s)	16th %ile	50th %ile	84th %ile	16th %ile	50th %ile	84th %ile	16th %ile	50th %ile	84th %ile
Sep-10	NA	NA	NA	<50	<50	<50	<50	<50	<50
Feb-11	NA	NA	NA	150	150	150	150	150	150
Jun-11	NA	NA	NA	50	50	50	50	50	50
Dec-11	NA	NA	NA	50	50	50	50	50	50
CES	NA	NA	NA	350	400	400	350	400	400

Note: These percentiles are not the exact statistical measures; they indicate the spatial variability of ground surface subsidence.

Table 7c: Corrected liquefaction-related ground surface subsidence for Patch C using LiDAR DEMs.

	Estimated Ground Surface Subsidence (mm)								
	10-m Buffer			20-m Buffer			50-m Buffer		
Earthquake Event(s)	16th %ile	50th %ile	84th %ile	16th %ile	50th %ile	84th %ile	16th %ile	50th %ile	84th %ile
Sep-10	NA	NA	NA	NA	NA	NA	<50	<50	<50
Feb-11	NA	NA	NA	NA	NA	NA	150	150	150
Jun-11	NA	NA	NA	NA	NA	NA	50	50	50
Dec-11	NA	NA	NA	NA	NA	NA	50	50	50
CES	NA	NA	NA	NA	NA	NA	200	200	250

Note: These percentiles are not the exact statistical measures; they indicate the spatial variability of ground surface subsidence.

Table 7d: Corrected liquefaction-related ground surface subsidence for Road using LiDAR DEMs.

	Estimated Ground Surface Subsidence (mm)								
	10-m Buffer			20-m Buffer			50-m Buffer		
Earthquake Event(s)	16th %ile	50th %ile	84th %ile	16th %ile	50th %ile	84th %ile	16th %ile	50th %ile	84th %ile
Sep-10	NA	NA	NA	<50	<50	50	<50	<50	50
Feb-11	NA	NA	NA	50	150	150	50	150	150
Jun-11	NA	NA	NA	50	50	50	50	50	50
Dec-11	NA	NA	NA	50	50	150	50	50	150
CES	NA	NA	NA	250	250	350	150	250	400

Note: These percentiles are not the exact statistical measures; they indicate the spatial variability of ground surface subsidence.

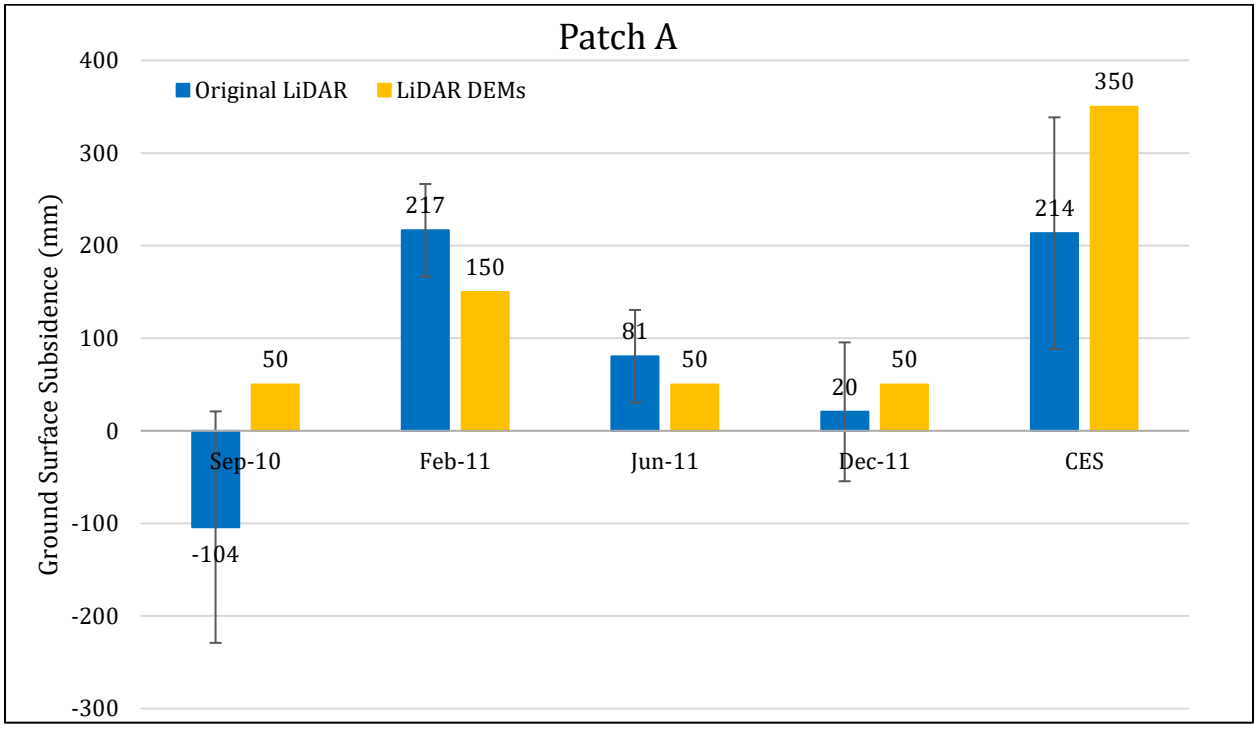

Figure 2: Comparison between ground surface subsidence determined from original LiDAR survey points and ground surface subsidence (50th %ile) estimated using LiDAR DEMs for Patch A.

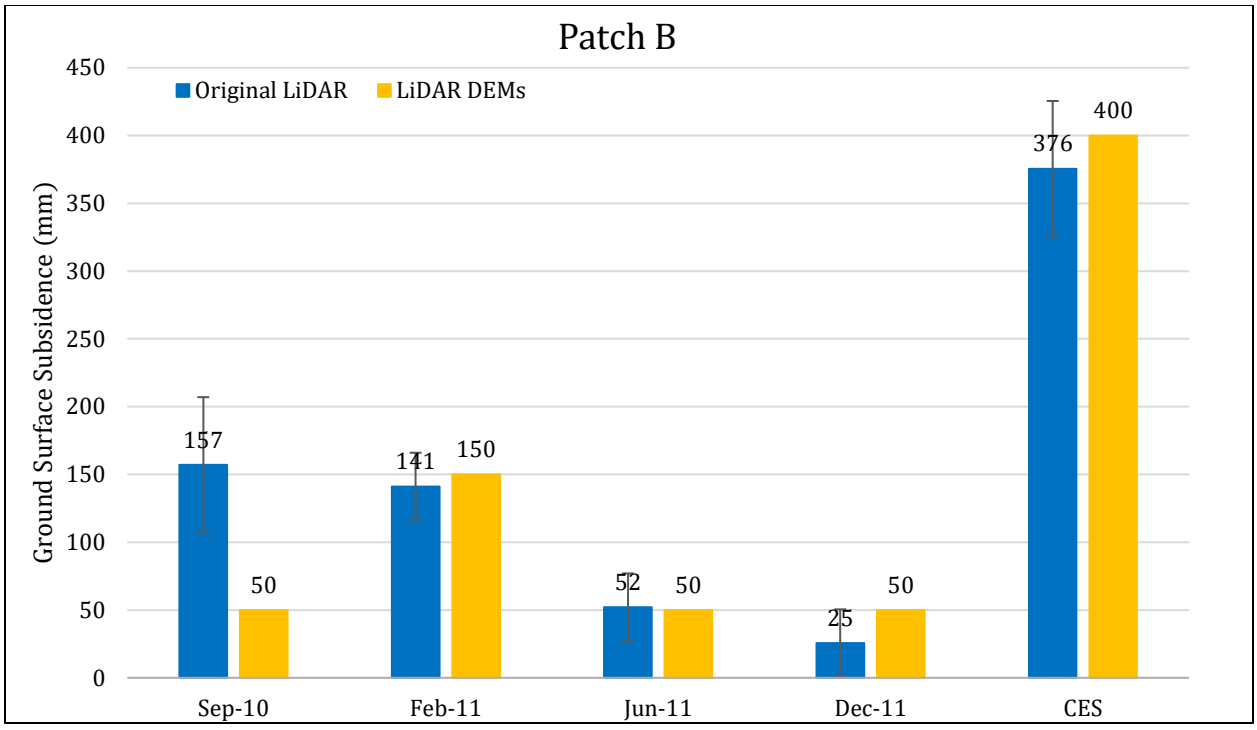

Figure 3: Comparison between ground surface subsidence determined from original LiDAR survey points and ground surface subsidence (50th %ile) estimated using LiDAR DEMs for Patch B.

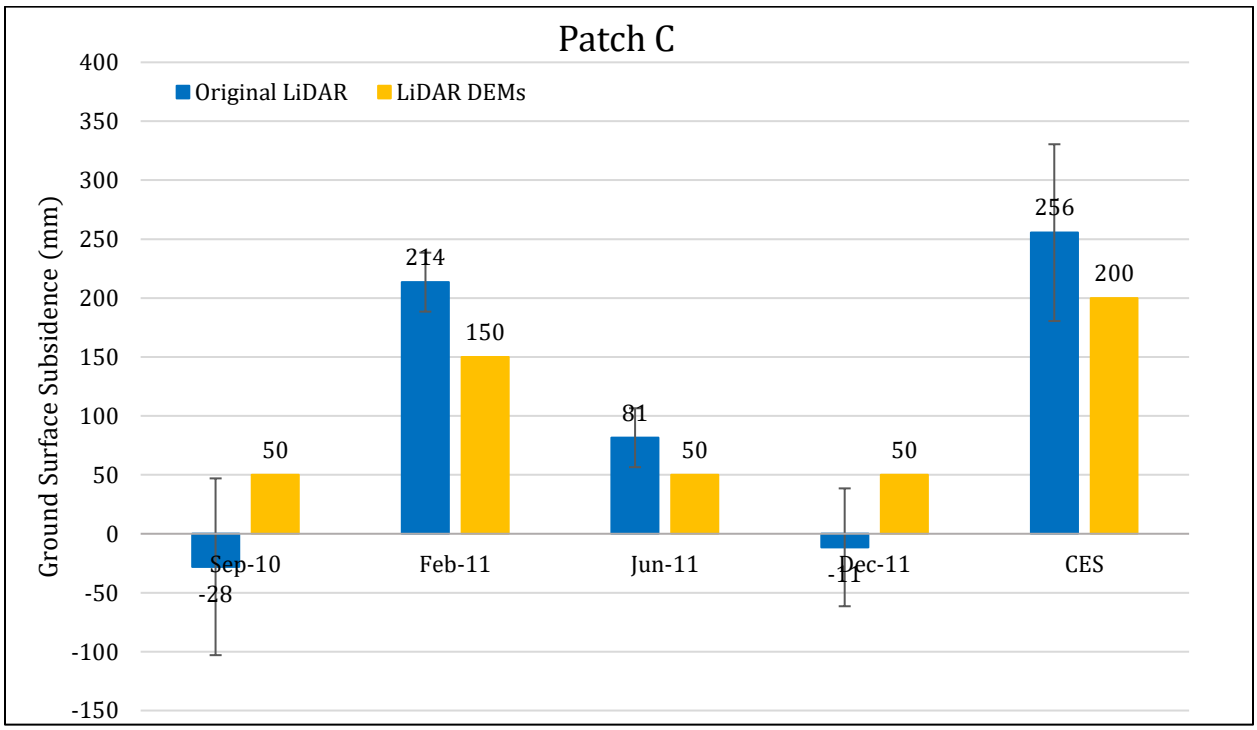

Figure 4: Comparison between ground surface subsidence determined from original LiDAR survey points and ground surface subsidence (50th %ile) estimated using LiDAR DEMs for Patch C.

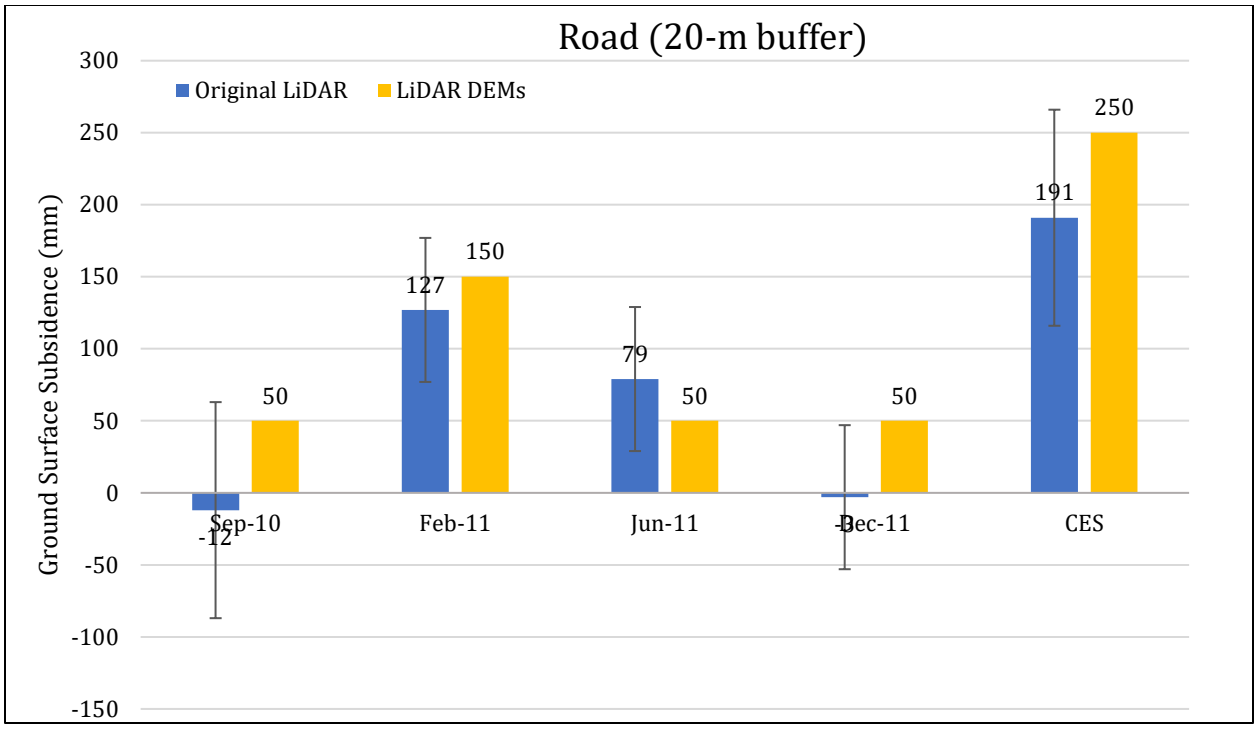

Figure 5: Comparison between ground surface subsidence determined from original LiDAR survey points and ground surface subsidence (50th %ile) estimated using LiDAR DEMs for Road for the 20-m buffer.

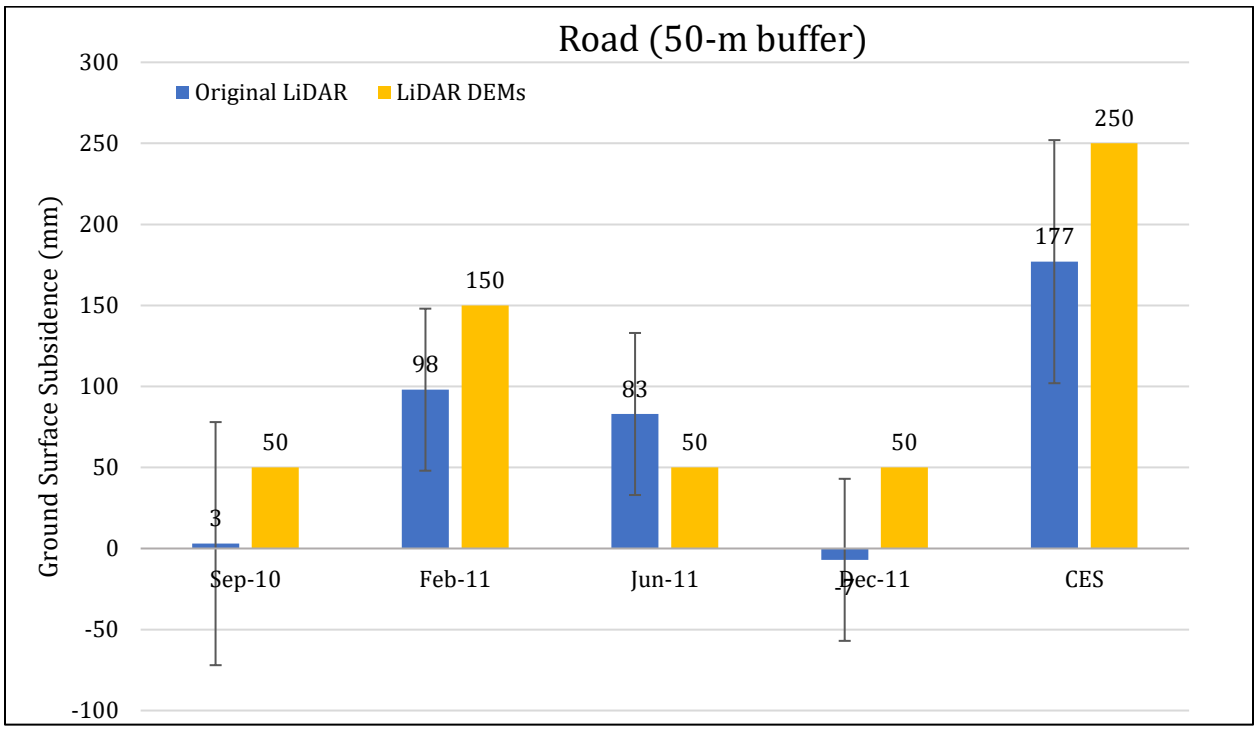

Figure 6: Comparison between ground surface subsidence determined from original LiDAR survey points and ground surface subsidence (50th %ile) estimated using LiDAR DEMs for Road for the 50-m buffer.

Note 2: The ground surface subsidence values determined from original LiDAR survey points are similar to the ground surface subsidence values estimated using LiDAR DEMs for all earthquake events. The exception to this trend occurs for the Sep-10 earthquake for Patch B as the estimated ground surface subsidence using the LiDAR DEM is three times smaller than the ground surface subsidence computed using the original LiDAR survey points (50 mm versus 157 mm, respectively).

Table 8a: Ejecta-Induced settlement for the top 20 m of the soil profile for Patch A for the 50th %ile PGA, P_L=50%, and C_{FC}=0.13 using BI-2014, ZRB-2002, and I_C cutoff of 2.6.

Earthquake Event(s)	M_W	PGA (g)	Depth to Groundwater (m)	S_T (mm)	S_{V1D} (mm)	$S_{E,L}$ (mm)
Sep-10	7.1	0.17	2.5	-104±125	9±20	-113±127
Feb-11	6.2	0.34	2.5	217±50	81±50	136±71
Jun-11	6.2	0.23	2.2	81±50	27±25	54±56
Dec-11	6.1	0.31	1.5	20±75	84±50	-64±90

Notes: S_T = Total settlement (Table 6); S_{V1D} = Average vertical settlement due to volumetric compression using Boulanger and Idriss (2014) (BI-2014), Zhang et al. (2002) (ZRB-2002) procedures and de Greef and Lengkeek (2018) thin-layer correction; $S_{E,L}$ = Ejecta-induced settlement as the difference between the LiDAR-based S_T and S_{V1D}.

Table 8b: Ejecta-Induced settlement for the top 20 m of the soil profile for Patch B for the 50th %ile PGA, P_L=50%, and C_{FC}=0.13 using BI-2014, ZRB-2002, and I_C cutoff of 2.6.

Earthquake Event(s)	M_W	PGA (g)	Depth to Groundwater (m)	S_T (mm)	S_{V1D} (mm)	$S_{E,L}$ (mm)
Sep-10	7.1	0.17	2.5	157±50	6±20	151±54
Feb-11	6.2	0.34	2.5	141±25	62±50	79±56
Jun-11	6.2	0.23	2.2	52±25	19±25	33±35
Dec-11	6.1	0.31	1.5	25±25	66±50	-41±56

Notes: S_T = Total settlement (Table 6); S_{V1D} = Average vertical settlement due to volumetric compression using Boulanger and Idriss (2014) (BI-2014), Zhang et al. (2002) (ZRB-2002) procedures and de Greef and Lengkeek (2018) thin-layer correction; $S_{E,L}$ = Ejecta-induced settlement as the difference between the LiDAR-based S_T and S_{V1D}.

Table 8c: Ejecta-Induced settlement for the top 20 m of the soil profile for Patch C for the 50th %ile PGA, P_L=50%, and C_{FC}=0.13 using BI-2014, ZRB-2002, and I_C cutoff of 2.6.

Earthquake Event(s)	M_W	PGA (g)	Depth to Groundwater (m)	S_T (mm)	S_{V1D} (mm)	$S_{E,L}$ (mm)
Sep-10	7.1	0.17	2.5	-28±75	6±20	-34±78
Feb-11	6.2	0.34	2.5	214±25	58±50	156±56
Jun-11	6.2	0.23	2.2	81±25	20±25	61±35
Dec-11	6.1	0.31	1.5	-11±50	72±50	-83±71

Notes: S_T = Total settlement (Table 6); S_{V1D} = Average vertical settlement due to volumetric compression using Boulanger and Idriss (2014) (BI-2014), Zhang et al. (2002) (ZRB-2002) procedures and de Greef and Lengkeek (2018) thin-layer correction; $S_{E,L}$ = Ejecta-induced settlement as the difference between the LiDAR-based S_T and S_{V1D}.

Table 8d: Ejecta-Induced settlement for the top 20 m of the soil profile for Road within the 20-m buffer for the 50th %ile PGA, P_L=50%, and C_{FC}=0.13 using BI-2014, ZRB-2002, and I_C cutoff of 2.6.

Earthquake Event(s)	M_W	PGA (g)	Depth to Groundwater (m)	S_T (mm)	S_{V1D} (mm)	$S_{E,L}$ (mm)
Sep-10	7.1	0.17	2.5	-12±75	8±20	-20±78
Feb-11	6.2	0.34	2.5	127±50	62±50	65±71
Jun-11	6.2	0.23	2.2	79±50	21±25	58±56
Dec-11	6.1	0.31	1.5	-3±50	65±50	-68±71

Notes: S_T = Total settlement (Table 6); S_{V1D} = Average vertical settlement due to volumetric compression using Boulanger and Idriss (2014) (BI-2014), Zhang et al. (2002) (ZRB-2002) procedures and de Greef and Lengkeek (2018) thin-layer correction; $S_{E,L}$ = Ejecta-induced settlement as the difference between the LiDAR-based S_T and S_{V1D}.

Table 8e: Ejecta-Induced settlement for the top 20 m of the soil profile for Road within the 50-m buffer for the 50th %ile PGA, P_L=50%, and C_{FC}=0.13 using BI-2014, ZRB-2002, and I_C cutoff of 2.6.

Earthquake Event(s)	M_W	PGA (g)	Depth to Groundwater (m)	S_T (mm)	S_{V1D} (mm)	$S_{E,L}$ (mm)
Sep-10	7.1	0.17	2.5	3±75	7±20	-4±78
Feb-11	6.2	0.34	2.5	98±50	59±50	39±71
Jun-11	6.2	0.23	2.2	83±50	19±25	64±56
Dec-11	6.1	0.31	1.5	-7±50	64±50	-71±71

Notes: S_T = Total settlement (Table 6); S_{V1D} = Average vertical settlement due to volumetric compression using Boulanger and Idriss (2014) (BI-2014), Zhang et al. (2002) (ZRB-2002) procedures and de Greef and Lengkeek (2018) thin-layer correction; $S_{E,L}$ = Ejecta-induced settlement as the difference between the LiDAR-based S_T and S_{V1D}.

Note 3: The uncertainty for volumetric settlement was derived based on the sensitivity of volumetric settlement to PGA, C_{FC}, and P_L for each earthquake event for VsVp 57203 *Shirley Intermediate School* and CC LIQ 1 – CPT 5586 – *Vivian St* sites. Taking the 50th percentile as the baseline case, the minimum and maximum values corresponding to the difference between the 25th percentile and the 50th percentile and the 75th percentile and the 50th percentile were determined. The arithmetic mean of the range of the minimum and maximum difference was evaluated for each patch at the two sites. The maximum arithmetic mean for each earthquake event was rounded to the nearest five and used as the uncertainty value. Accordingly, the 1-D volumetric settlement uncertainties of ±20, ±50, ±25, and ±50 mm for the Sep-10, Feb-11, Jun-11, and Dec-11 earthquake events, respectively, were used for all sites in this study.

Table 9a: Coverage area and height of ejecta estimates for Patch A using photographs.

Earthquake Event	$A_{E,thick}$ (m^2)	$H_{E,thick}$ (mm)	$A_{E,thin}$ (m^2)	$H_{E,thin}$ (mm)	A_T (m^2)
Sep-10	0	0	0	0	32
Feb-11	0	0	0	0	32
Jun-11	0	0	0	0	32
Dec-11	0	0	0	0	21*

Notes: $A_{E,thick/thin}$ = Coverage area of thick/thin ejecta layers; $H_{E,thick/thin}$ = Lower-upper estimate of height of thick/thin ejecta layers; A_T = Total assessment area of a buffer being considered; Thin and thick layers correspond to light gray and dark gray colors of ejecta observed in aerial photographs.

Table 9b: Coverage area and height of ejecta estimates for Patch B using photographs.

Earthquake Event	$H_{E,cone}$ (mm)	$A_{E,cone}$ (m^2)	$H_{E,thin}$ (mm)	$A_{E,thin}$ (m^2)	$H_{E,thick}$ (mm)	$A_{E,thick}$ (m^2)	A_T (m^2)
Sep-10	0	0	0	0	0	0	87
Feb-11	250-500	14	20-40	3.2	70-150	47	87
Jun-11	0	0	0	0	0	0	87
Dec-11	0	0	0	0	0	0	87

Notes: $A_{E,thick/thin}$ = Coverage area of thick/thin ejecta layers; $H_{E,thick/thin}$ = Lower-upper estimate of height of thick/thin ejecta layers; Thin and thick layers correspond to light gray and dark gray colors of ejecta observed in aerial photographs; $H_{E,cone}$ = Lower-upper estimate of height of conically shaped ejecta layers; $A_{E,cone}$ = Coverage area of conically shaped ejecta layers; A_T = Total assessment area of a buffer being considered.

Table 9c: Coverage area and height of ejecta estimates for Patch C using photographs.

Earthquake Event	$A_{E,thick}$ (m^2)	$H_{E,thick}$ (m)	$A_{E,thin}$ (m^2)	$H_{E,thin}$ (m)	A_T (m^2)
Sep-10	0	0	0	0	43
Feb-11	0	0	0	0	37
Jun-11	0	0	0	0	43
Dec-11	0	0	0	0	43

Notes: $A_{E,thick/thin}$ =Coverage area of thick/thin ejecta layers; $H_{E,thick/thin}$ = Lower-upper estimate of height of thick/thin ejecta layers; A_T= Total assessment area of a buffer being considered; Thin and thick layers correspond to light gray and dark gray colors of ejecta observed in aerial photographs.

Table 9d: Coverage area and height of ejecta estimates for Road within the 20-m buffer using photographs.

EQ Event	$H_{E,c}$ $H_{E,thin}$ (mm)	$A_{E,c}^{*}$ $A_{E,thin}$ (m^2)	$H_{E,cc}$ (mm)	$V_{E,cc}^{**}$ (m^3)	$H_{E,prism}$ (mm)	$V_{E,prism}$ (m^3)	$H_{E,pyr}$ (mm)	$V_{E,pyr}$ (m^3)	A_T (m^2)
Sep-10	0	0	0	0	0	0	0	0	223
Feb-11	300-500 5-10	23 36.4	283-537	2.68	4-113	0.595-1.19	9-66	0.018-0.036	223
Jun-11	0 5-10	63	277-901	8.61	11-97	0.302-0.604	12-23	0.002-0.005	236
Dec-11	100-200 0	2	0	0	7-62	0.031-0.061	9-18	0.001-0.002	240

Notes: $H_{E,c}$ = Lower-upper estimate of height of conically shaped ejecta layers; $A_{E,c}$ = Coverage area of conically shaped ejecta layers; * indicates that only a half of the cone's volume was used in the ejecta-induced settlement analysis; $A_{E,thin}$ = Coverage area of thin ejecta layers; $H_{E,\ thin}$ = Lower-upper estimate of height of thin ejecta layers; $H_{E,cc}$ = Lower-upper estimate of height of conically shaped ejecta pile components (based on the repose angle of 30°); $V_{E,cc}$ = Volume of conically shaped ejecta pile components; **indicates uncertainty in the place of origin of ejecta; $H_{E,prism/pyr}$ = Lower-upper estimate of ejecta height near the curb based on 2-4% cross slope of normal crown; $V_{E,prism}$ = Lower-upper estimate of total volume of prismatic-shape ejecta; $V_{E,pyr}$ = Lower-upper estimate of total volume of pyramidal-shape ejecta; A_T= Total assessment area of a buffer being considered.

Table 9e: Coverage area and height of ejecta estimates for Road within the 50-m buffer (without the 20-m buffer) using photographs.

EQ Event	$H_{E,c}$ (mm)	$V_{E,c}$ (m^3)	$H_{E,pile}$ (mm)	$V_{E,pile}^*$ (m^3)	$H_{E,prism/pyr}$ (mm)	$V_{E,prism+pyr}$ (m^3)	$H_{E,thin}$ (mm)	$A_{E,thin}$ (m^2)	A_T (m^2)
Sep-10	0	0	0	0	0	0	0	0	785
Feb-11	150-300	0.334-0.667	300-370	1.01-1.24	7-119	0.593-1.19	5-10	122	779
Jun-11	0	0	0	0	9-53	0.271-0.542	5-10	256	829
Dec-11	0	0	0	0	6-158	0.504-1.01	3-6	2.2	812

Notes: $V_{E,c}$ = Lower-upper estimate of conically shaped ejecta layers; $H_{E,c}$ = Lower-upper estimate of height of conically shaped ejecta layers; $H_{E,pile}$ = Lower-upper estimate of height of ejecta piles; $V_{E,pile}$ = Volume of ejecta piles; * indicates uncertainty in the place of origin of ejecta; $H_{E,prism/pyr}$ = Lower-upper estimate of ejecta height near the curb based on 2-4% cross slope of normal crown; $V_{E,prism+pyr}$ = Lower-upper estimate of total volume of prismatic- and pyramidal-shape ejecta; $A_{E,thin}$ =Coverage area of thin ejecta layers; $H_{E,\ thin}$ = Lower-upper estimate of height of thin ejecta layers; A_T= Total assessment area of a buffer being considered.

Note 4: The values in Table 9 correspond to the coverage area of ejecta outlined in aerial photographs (Figures 82 through 85) and the lower and upper estimates of ejecta height based on geometrical approximations, ground photographs, and EQC LDAT property inspection reports. The ejecta-induced settlement using photographs and engineering judgment, $S_{E,P}$, is estimated as

$$S_{E,P} = \frac{\sum_{i=1}^{a} A_{E,thick,i} * H_{E,thick,i} + \sum_{j=1}^{b} A_{E,thin,j} * H_{E,thin,j} + \frac{1}{3}\sum_{k=1}^{c} A_{E,pile,k} * R_{E,pile,k} * tan30°}{A_T} + \frac{\sum_{l=1}^{d}\left(\frac{1}{3}(A_{E,conical\ end\ 1,l} + A_{E,conical\ end\ 2,l}) * H_{E,pile,l} + \frac{1}{2} A_{E,prismatic\ middle,l} * H_{E,pile,l}\right)}{A_T} + \frac{\frac{1}{3}\sum_{m=1}^{e} A_{E,cone,m} * H_{E,cone,m} + \frac{1}{2}\sum_{n=1}^{f} W_{E,prism,n} * H_{E,prism,n} * L_{E,prism,n}}{A_T} + \frac{\frac{1}{3}\sum_{p=1}^{g} W_{E,pyramid,p} * H_{E,pyramid} * L_{E,pyramid}}{A_T}$$

$$= \frac{\sum_{i=1}^{a} V_{E,thick,i} + \sum_{j=1}^{b} V_{E,thin,j} + \sum_{k=1}^{c} V_{E,conical\ component,k} + \sum_{l=1}^{d} V_{E,pile,l}}{A_T} + \frac{\sum_{m=1}^{e} V_{E,cone,m} + \sum_{n=1}^{f} V_{E,prism,n} + \sum_{p=1}^{g} V_{E,pyramid,p}}{A_T}$$

where

- $A_{E,thick,i}$ and $H_{E,thick,i}$ are the area and the height of a thick ejecta layer, respectively;
- $A_{E,thin,j}$ and $H_{E,thin,j}$ are the area and the height of a thin ejecta layer, respectively;
- $A_{E,pile,k}$ and $R_{E,pile,k}$ are the area and the radius of an ejecta pile component, respectively, shaped as a cone with the repose angle of 30°;
- $A_{E,conical\ end\ 1/2,l}$ and $A_{E,prismatic\ middle,l}$ are the areas of half-cone ends of an ejecta pile and the area of a middle of an ejecta pile shaped as a triangular prism, respectively, while $H_{E,pile,l}$ is the height of an ejecta pile;

- $A_{E,cone,m}$ and $H_{E,cone,m}$ are the aerea and the height of a conically shaped ejecta, respectively;
- $W_{E,prism,n}$ and $L_{E,prism,n}$ are the width and the length of the coverage area of a prismatically shaped ejecta layer, respectively, and $H_{E,prism,n}$ is the height of a prism-like ejecta layer;
- $W_{E,pyr,p}$ and $L_{E,pyr,p}$ are the width and the length of the coverage area of a pyramid-like ejecta layer, respectively, and $H_{E,pyr,p}$ is the height of a pyramid-like ejecta layer;
- A_T is the total assessment area for a buffer being considered (Figure 1).

Table 10a: Ejecta-induced settlement estimates for Patches A, B, and C based on photographs.

Earthquake Event	Patch A		Patch B		Patch C	
	$S_{E,P,lower}$ (mm)	$S_{E,P,upper}$ (mm)	$S_{E,P,lower}$ (mm)	$S_{E,P,upper}$ (mm)	$S_{E,P,lower}$ (mm)	$S_{E,P,upper}$ (mm)
Sep-10	0	0	0	0	0	0
Feb-11	0	0	52	110	0	0
Jun-11	0	0	0	0	0	0
Dec-11	0	0	0	0	0	0

Note: $S_{E,P,lower}$ and $S_{E,P,upper}$ correspond to lower and upper estimates of $S_{E,P}$, respectively.

Table 10b: Ejecta-induced settlement estimates for Road (20-m and 50-m buffers) based on photographs.

Earthquake Event	Road (20-m buffer)		Road (50-m buffer)	
	$S_{E,P,lower}$ (mm)	$S_{E,P,upper}$ (mm)	$S_{E,P,lower}$ (mm)	$S_{E,P,upper}$ (mm)
Sep-10	0	0	0	0
Feb-11	21	28	9	13
Jun-11	38	40	13	15
Dec-11	≈0	1	1	2

Note: $S_{E,P,lower}$ and $S_{E,P,upper}$ correspond to lower and upper estimates of $S_{E,P}$, respectively.

Table 11a: Best final estimates of ejecta-induced settlement for Patches A, B, and C.

EQ Event	Patch A			Patch B			Patch C		
	$S_{E,L}$ (mm)	$S_{E,P}$ (mm)	$S_{E,final}$ (mm)	$S_{E,L}$ (mm)	$S_{E,P}$ (mm)	$S_{E,final}$ (mm)	$S_{E,L}$ (mm)	$S_{E,P}$ (mm)	$S_{E,final}$ (mm)
Sep-10	-113±127	0	0	151±54	0	0	-34±78	0	0
Feb-11	136±71	0	0	79±56	81±29	80±30	156±56	0	0
Jun-11	54±56	0	0	33±35	0	0	61±35	0	0
Dec-11	-64±90	0	0	-41±56	0	0	-83±71	0	0

Notes: $S_{E,L}$ = Ejecta-induced settlement based on LiDAR data reported in Table 8; $S_{E,P}$ = Median ejecta-induced settlement for the range of values reported in Table 10; $S_{E,final}$ = Best final estimate of ejecta-induced settlement rounded to the nearest 5; Final plus/minus values are also rounded to the nearest 5.

Table 11b: Best final estimates of ejecta-induced settlement for Road (20-m and 50-m buffers).

Earthquake Event	Road (20-m buffer)			Road (50-m buffer)		
	$S_{E,L}$ (mm)	$S_{E,P}$ (mm)	$S_{E,final}$ (mm)	$S_{E,L}$ (mm)	$S_{E,P}$ (mm)	$S_{E,final}$ (mm)
Sep-10	-20±78	0	0	-4±78	0	0
Feb-11	65±71	25±3	45±35	39±71	11±2	25±35
Jun-11	58±56	39±1	50±30	64±56	14±1	40±30
Dec-11	-68±71	0.5±0.5	<5	-71±71	1.5±0.5	<5

Notes: $S_{E,L}$ = Ejecta-induced settlement based on LiDAR data reported in Table 8; $S_{E,P}$ = Median ejecta-induced settlement for the range of values reported in Table 10; $S_{E,final}$ = Best final estimate of ejecta-induced settlement rounded to the nearest 5; Final plus/minus values are also rounded to the nearest 5.

Note 5:

- $S_{E,final}$ for Patches A and C is based solely on $S_{E,P}$ for all earthquake events.
- $S_{E,final}$ for Patch B for the Feb-11 EQ is a weighted average of $S_{E,L}$ and $S_{E,P}$ with weights of 1/2 and 1/2, respectively. The uncertainty associated with $S_{E,final}$ for Patch B is also a weighted average of uncertainties associated with $S_{E,L}$ and $S_{E,P}$ with the same weights of 1/2 and 1/2, respectively. For the Sep-10, Jun-11, and Dec-11 EQs, $S_{E,final}$ for Patch B is equal to $S_{E,P}$.
- $S_{E,final}$ for Road for the Feb-11 and Jun-11 EQs is a weighted average of $S_{E,L}$ and $S_{E,P}$ with weight coefficients of 1/2 and 1/2, respectively. Likewise, the uncertainty associated with $S_{E,final}$ for Road is a weighted average of uncertainties associated with $S_{E,L}$ and $S_{E,P}$ with the same weights of 1/2 and 1/2, respectively.
- The weight coefficients are based on the LiDAR error bands, LPI prediction error (Maurer et al. 2014[3]), presence of ejecta at the time of LiDAR surveys, density of July 2003 LiDAR points, and completeness of visual evidence (i.e., ground and aerial photographs and EQC LDAT property inspection reports for the site). The Vivian St site is in the apparent zone of higher ground surface subsidence for the Sep-10 EQ (i.e., the overestimate of the ground surface elevation by the Jul-03 LiDAR survey). The site is also in the zone of slight to moderate LPI overprediction of liquefaction severity for the Sep-10 and Feb-11 EQ. The LDAT property inspection report is available for Patch B, as well as the property occupant's statement of ejecta being 500 mm high. There are no ground photographs of the road.

Summary 1:

- **The best estimate of the ejecta-induced free-field ground settlement at the Vivian St site for the SEP 2010, JUN 2011, and DEC 2011 earthquake is 0 mm, 0 mm, and 0 mm, respectively. For the FEB 2011 earthquake, ejecta were absent from numerous properties; however, for properties with ejecta (about 35% of the unobstructed area of the site), the best estimate of the ejecta-induced free-field ground settlement is 80±30 mm.**

[3] Maurer, B. W., Green, R. A., Cubrinovski, M., & Bradley, B. A. (2014). Evaluation of the Liquefaction Potential Index for Assessing Liquefaction Hazard in Christchurch, New Zealand. *Journal of Geotechnical and Geoenvironmental Engineering*, 140(7), 04014032-1-11. doi:10.1061/(asce)gt.1943-5606.0001117

- **The best estimate of the ejecta-induced free-field ground settlement of the road at the Vivian St site for the SEP 2010, FEB 2011, JUN 2011, and DEC 2011 earthquake is 0 mm, 45±35 mm, 50±30 mm, and <5 mm, respectively.**

Figure 7: Location of the site.

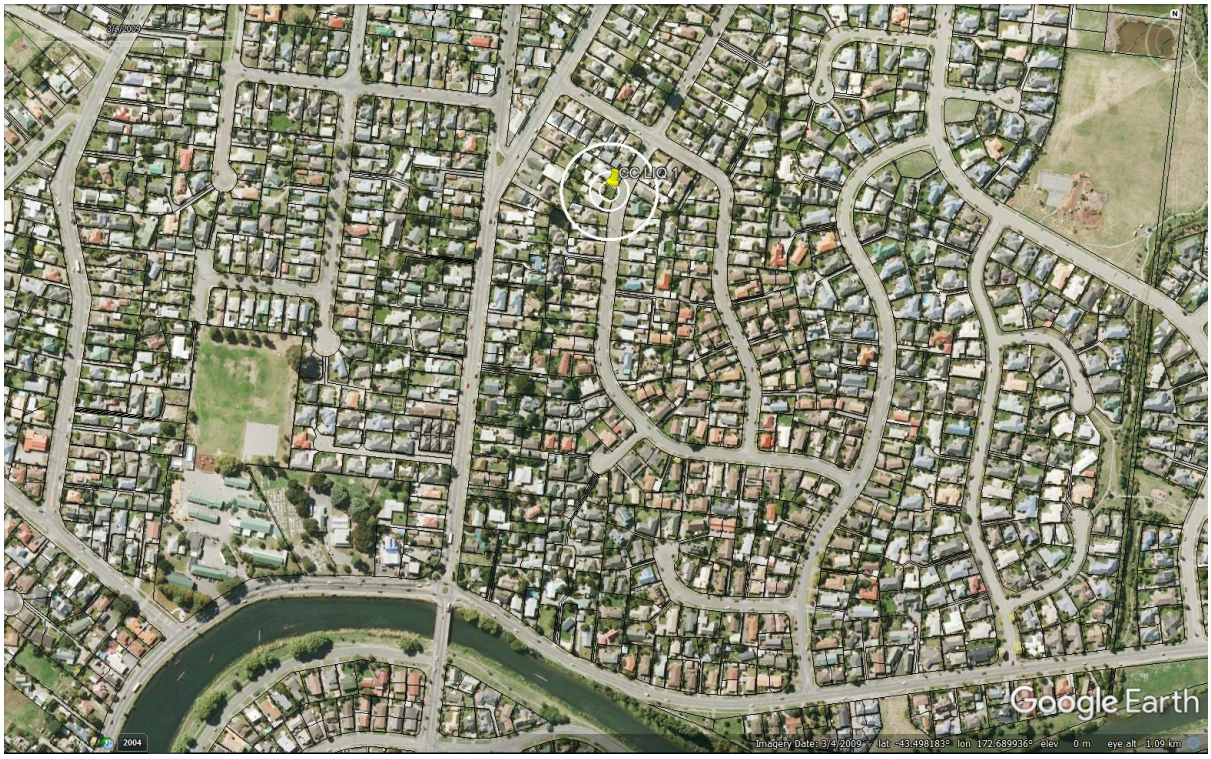

Figure 8: Position of the site relative to nearby buildings, vegetation, and free-face features.

Figure 9: Street view of the flat land.

Figure 10: Aerial photograph of the site taken in Dec 2004.

Figure 11: Aerial photograph of the site taken in Mar 2009.

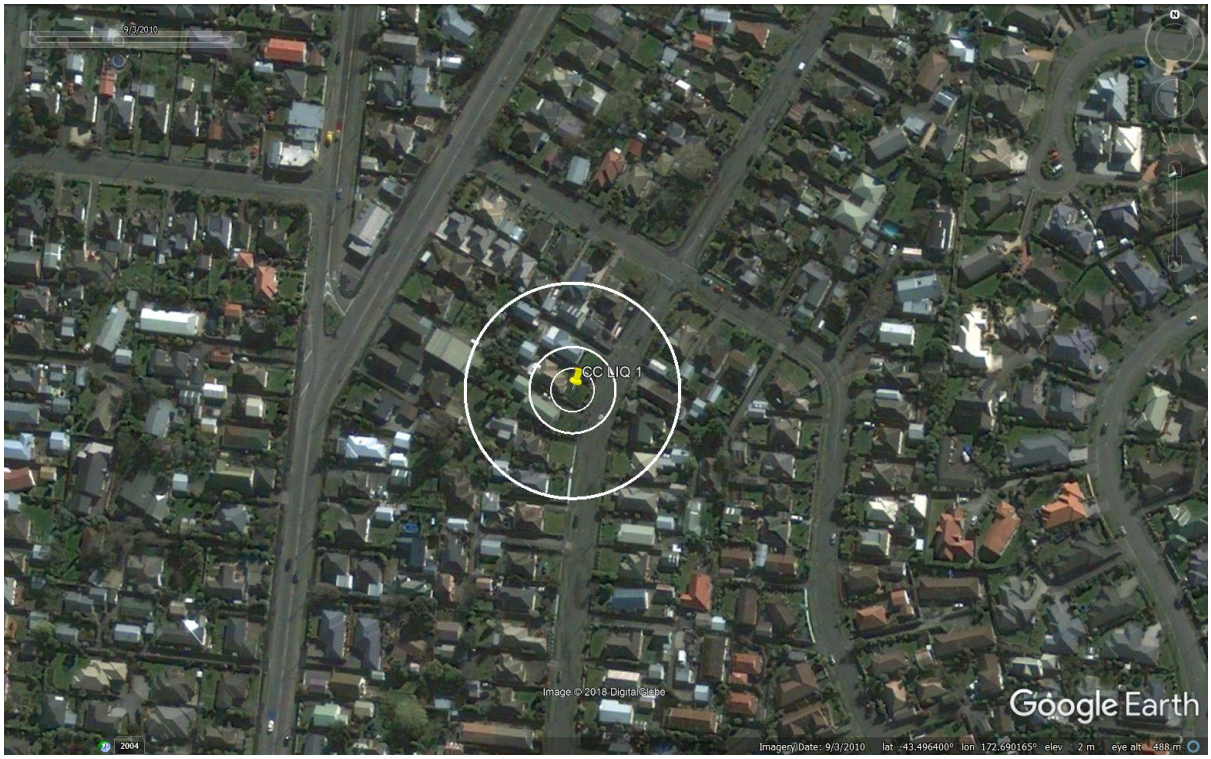

Figure 12: Aerial photograph of the site taken in Sep 2010.

Figure 13: Aerial photograph of the site taken in Nov 2015.

Figure 14: Aerial photograph of the site taken on Sep 4, 2010.

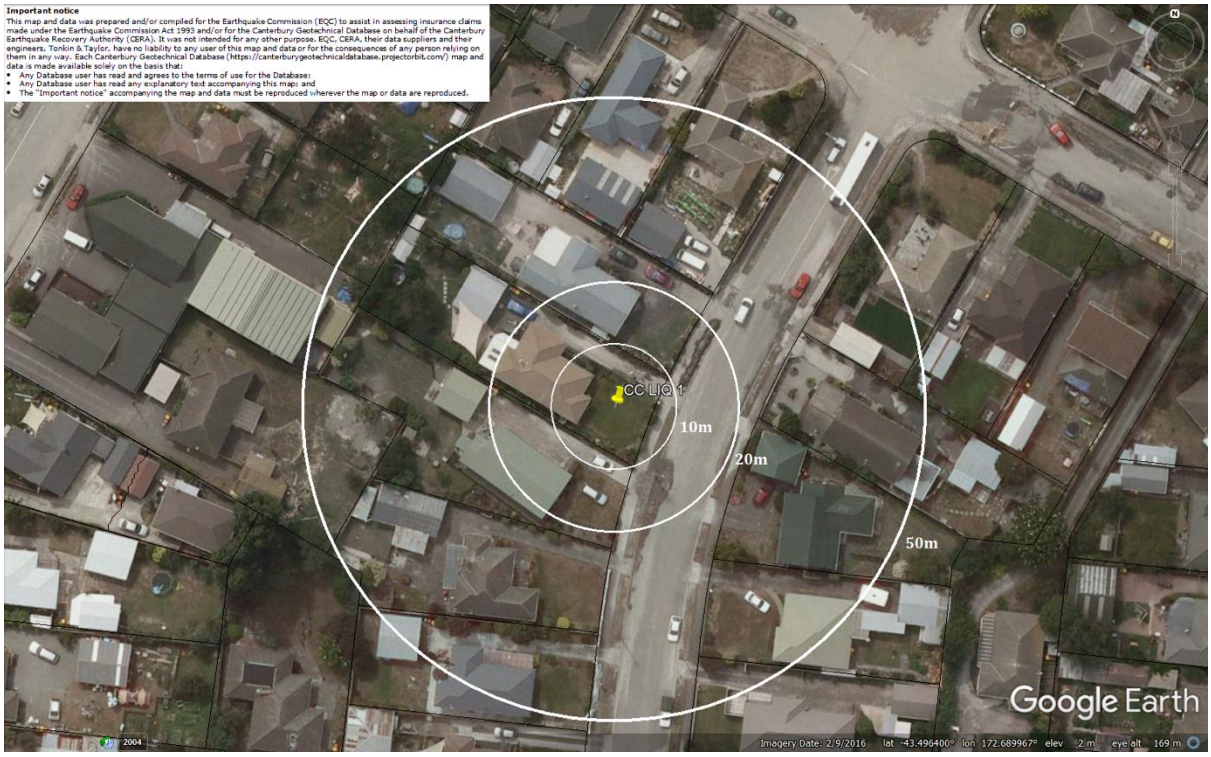

Figure 15: Aerial photograph of the site taken on Feb 24, 2011.

Figure 16: Aerial photograph of the site taken on June 14-15, 2011.

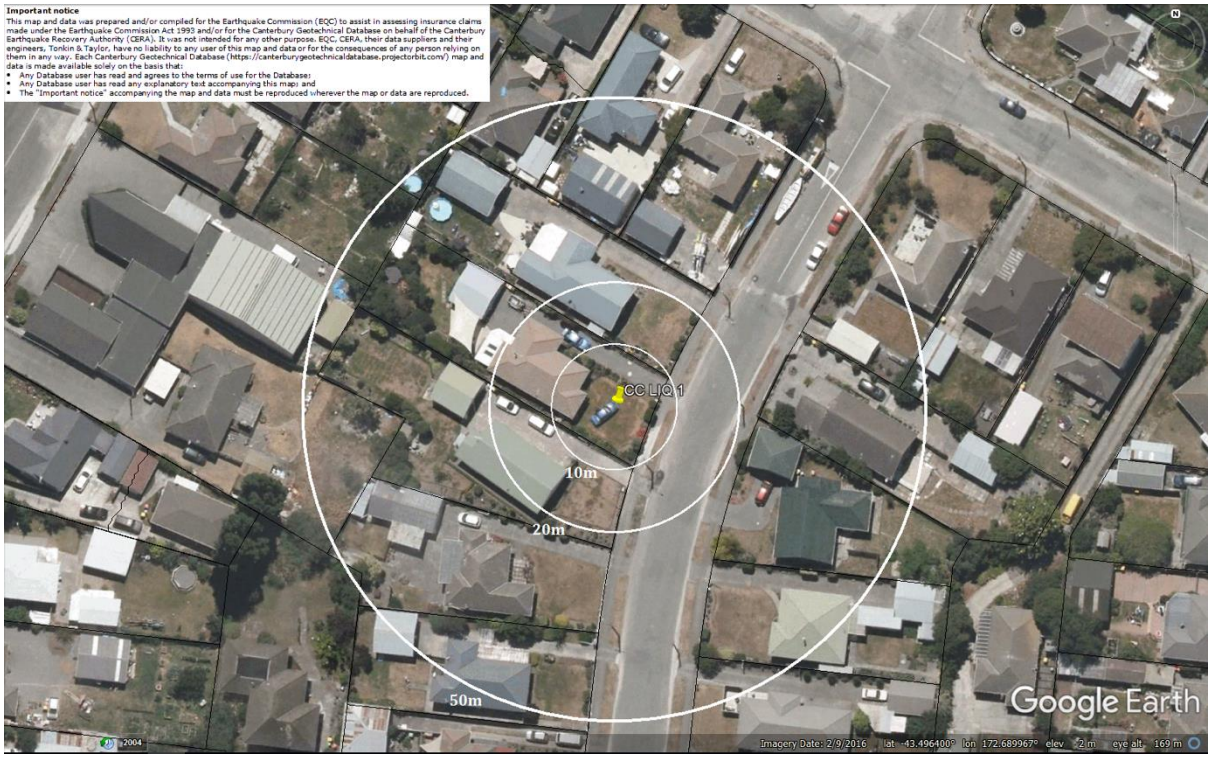

Figure 17: Aerial photograph of the site taken on Dec 24, 2011.

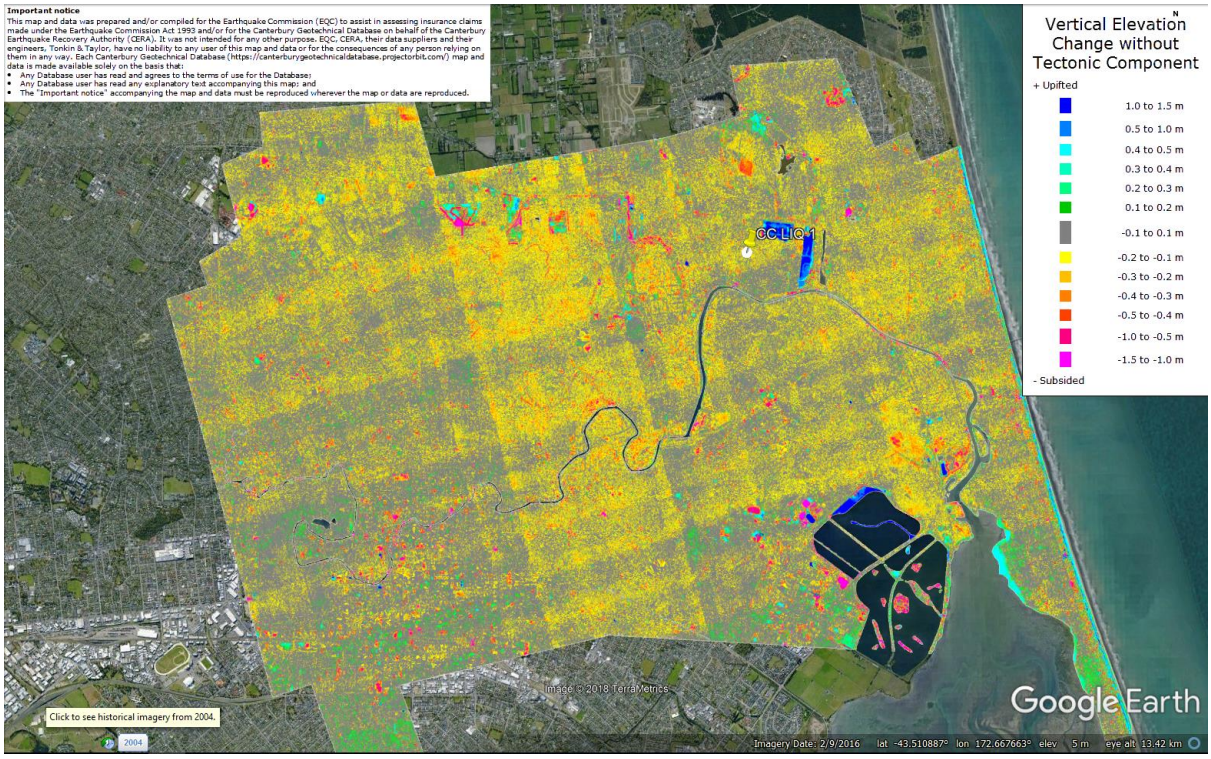

Figure 18: Vertical Ground Movements (Surface – Tectonic) for Sep 2010 Earthquake – the site is in the apparent zone of overestimated ground surface subsidence (i.e., flight error band for July 2003).

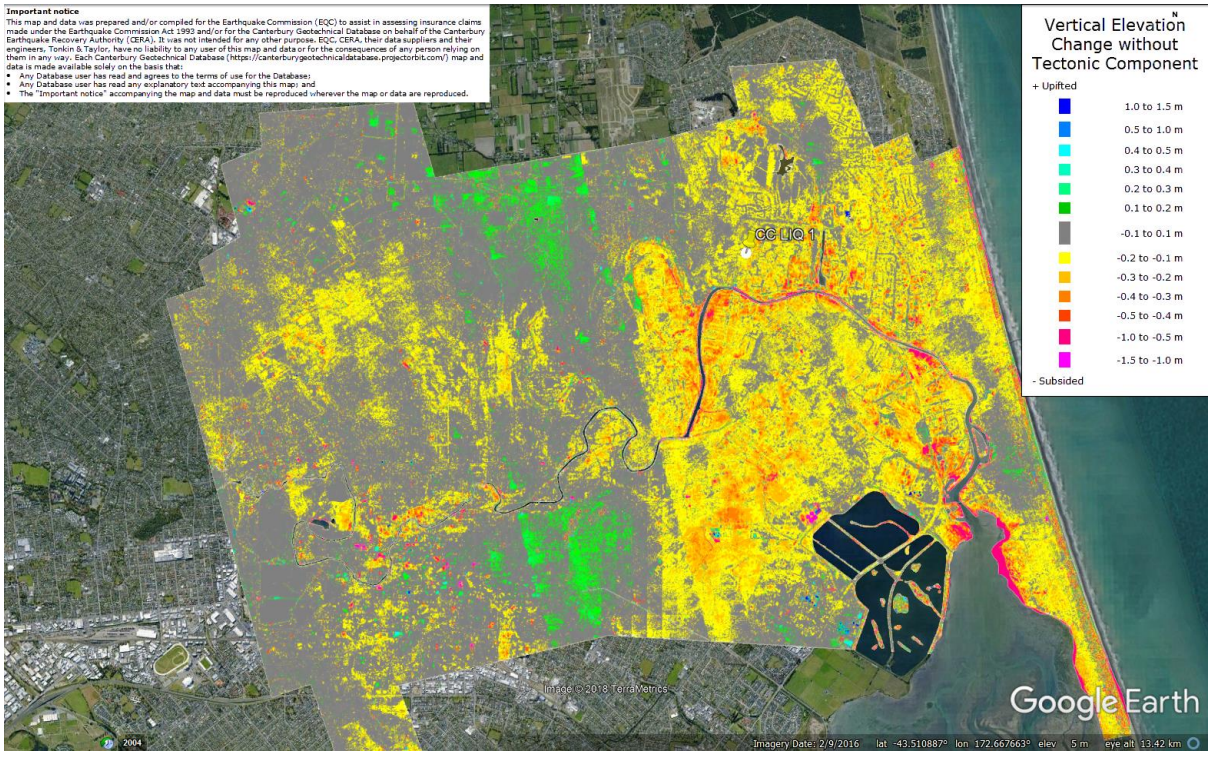

Figure 19: Vertical Ground Movements (Surface – Tectonic) for Feb 2011 Earthquake – the site is not in the apparent zone of underestimated ground surface subsidence.

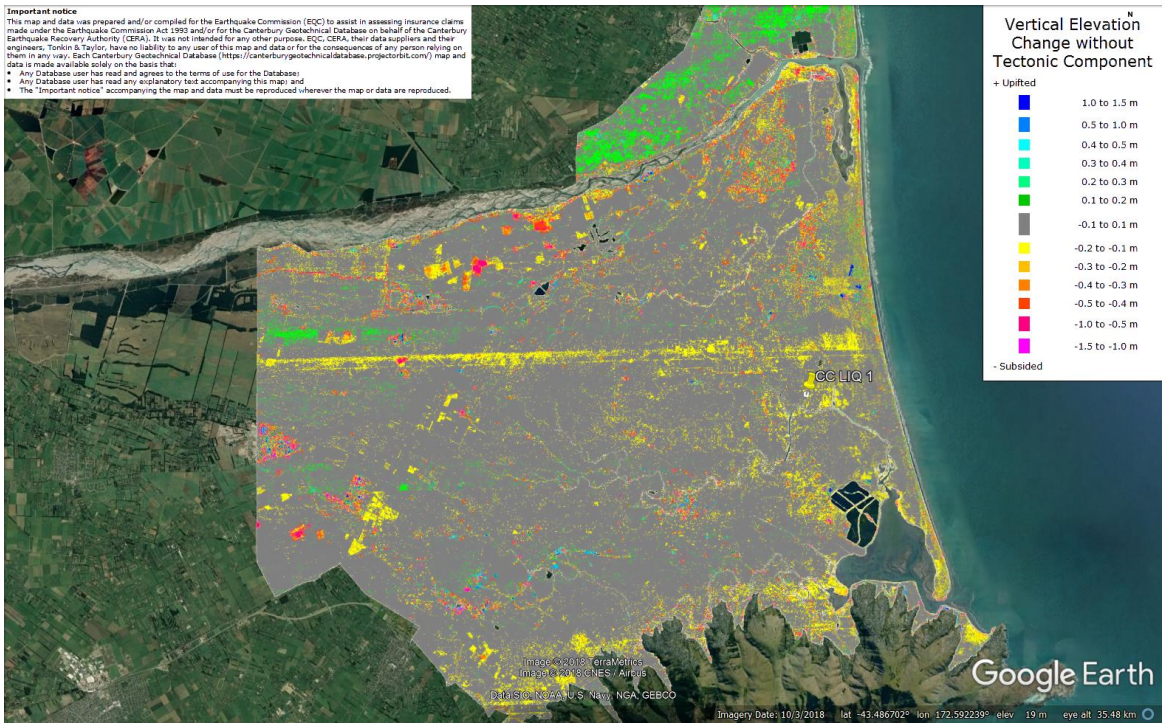

Figure 20: Vertical Ground Movements (Surface – Tectonic) for June 2011 Earthquake – the site is not in the apparent zone of overestimated or underestimated ground surface subsidence.

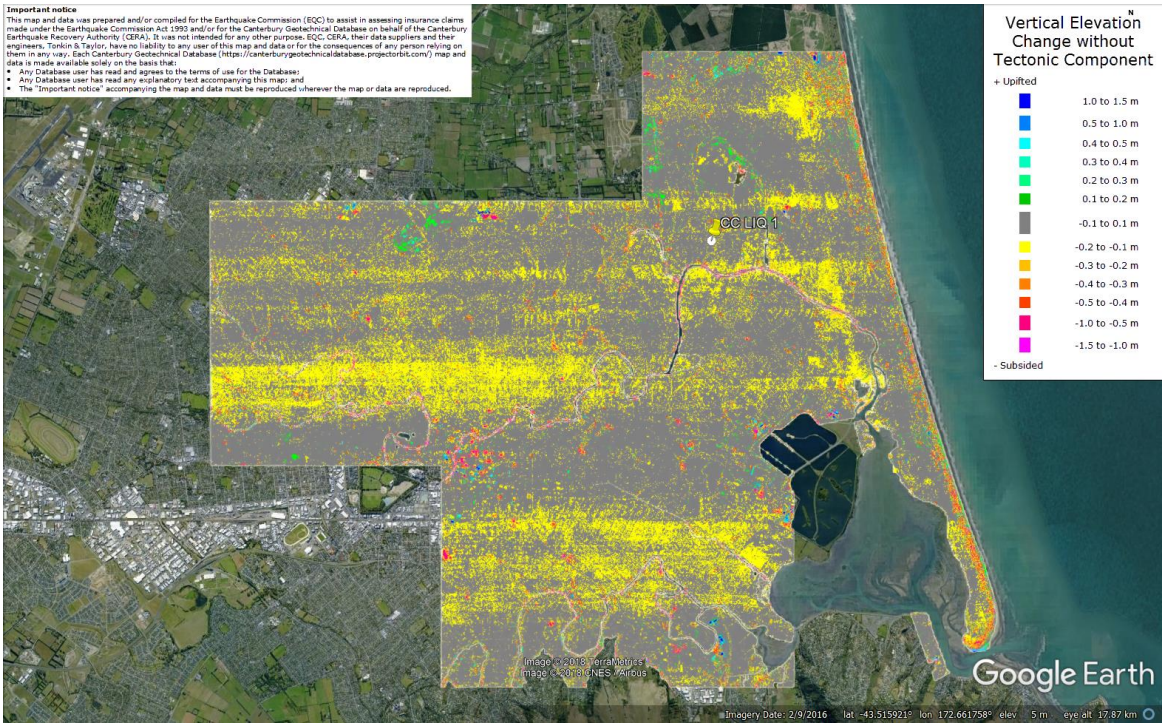

Figure 21: Vertical Ground Movements (Surface – Tectonic) for Dec 2011 Earthquake – the site is not in the apparent zone of overestimated or underestimated ground surface subsidence.

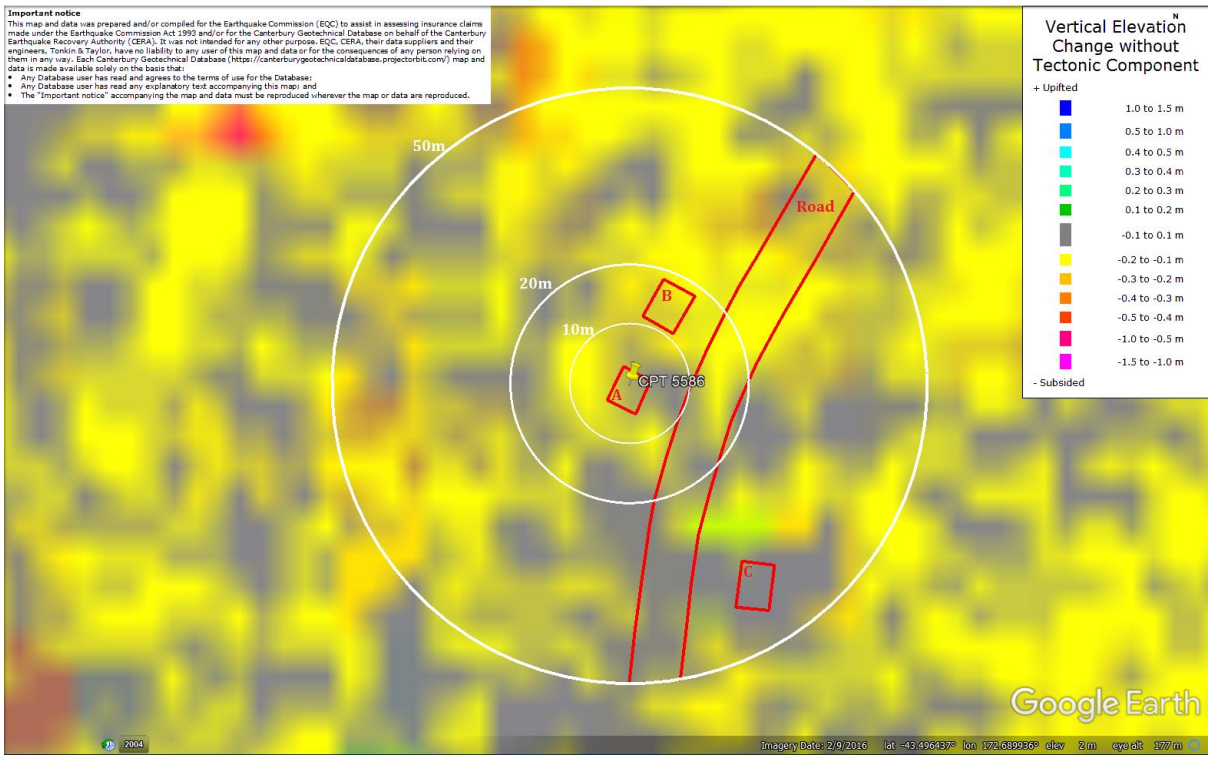

Figure 22: Ground surface subsidence without tectonic component for Sep 2010 Earthquake according to the LiDAR DEM.

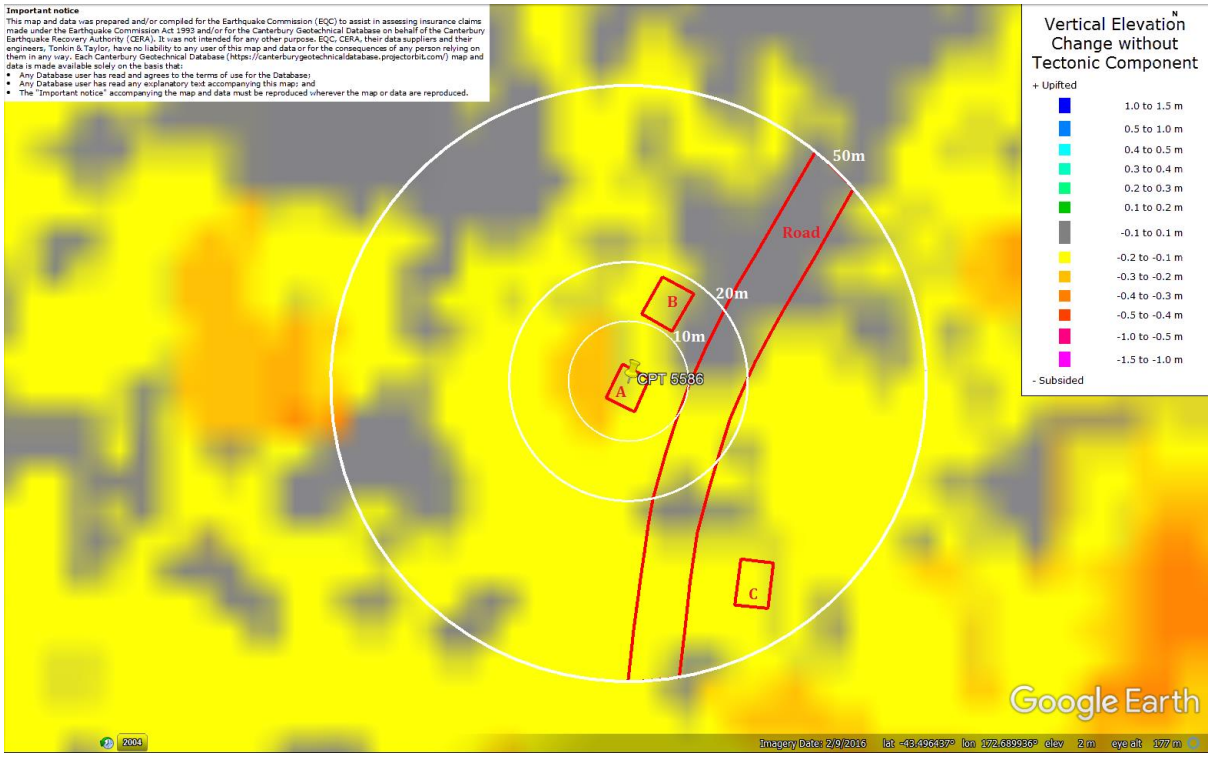

Figure 23: Ground surface subsidence without tectonic component for Feb 2011 Earthquake according to the LiDAR DEM.

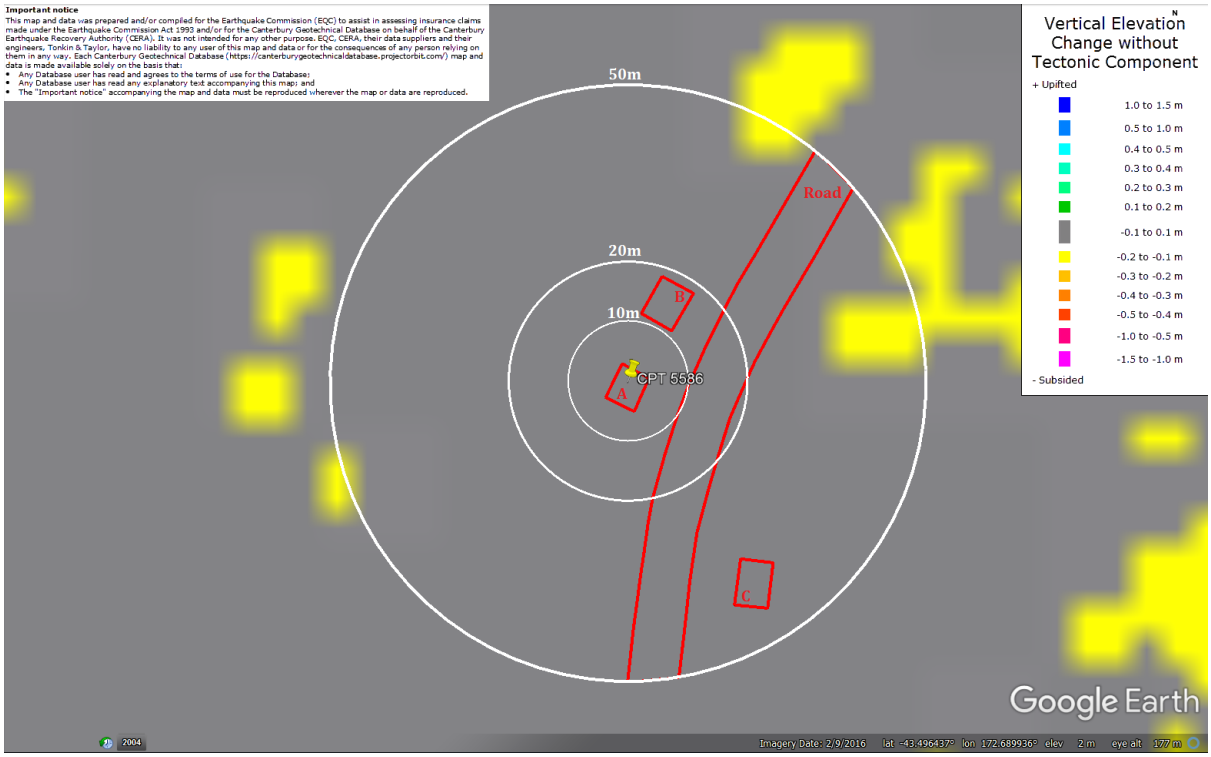

Figure 24: Ground surface subsidence without tectonic component for June 2011 Earthquake according to the LiDAR DEM.

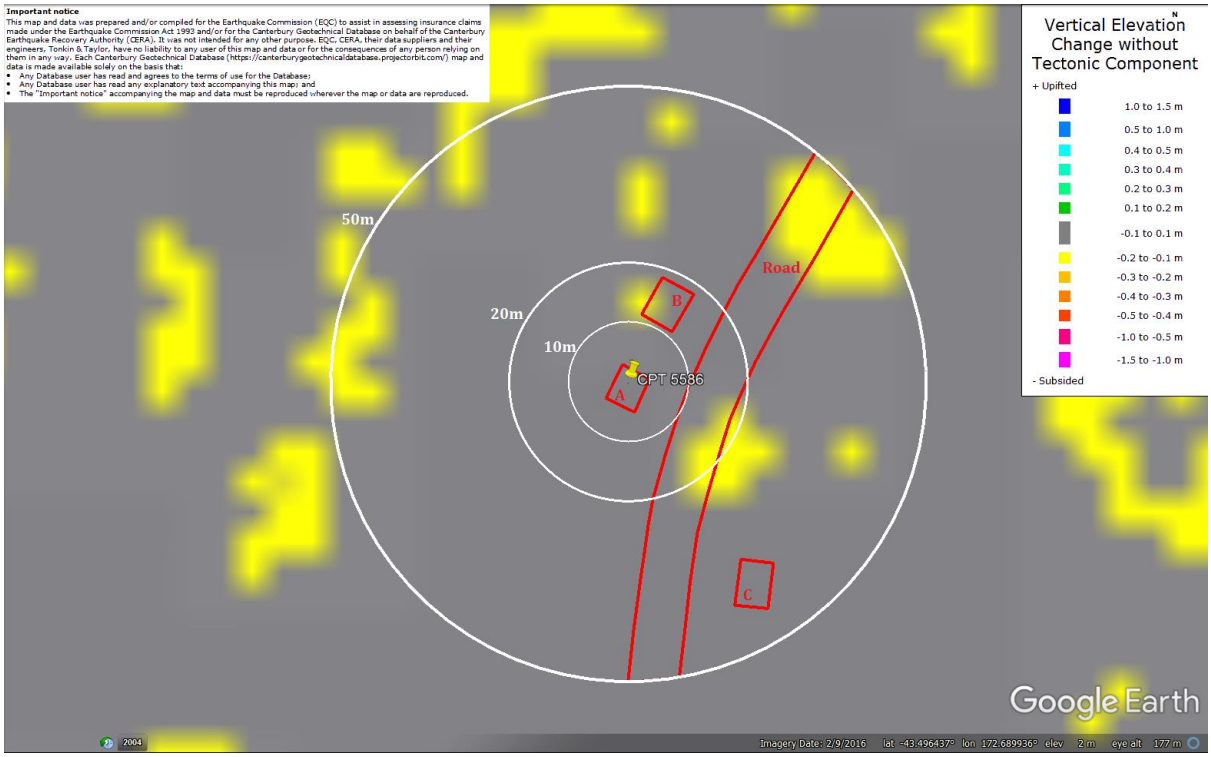

Figure 25: Ground surface subsidence without tectonic component for Dec 2011 Earthquake according to the LiDAR DEM.

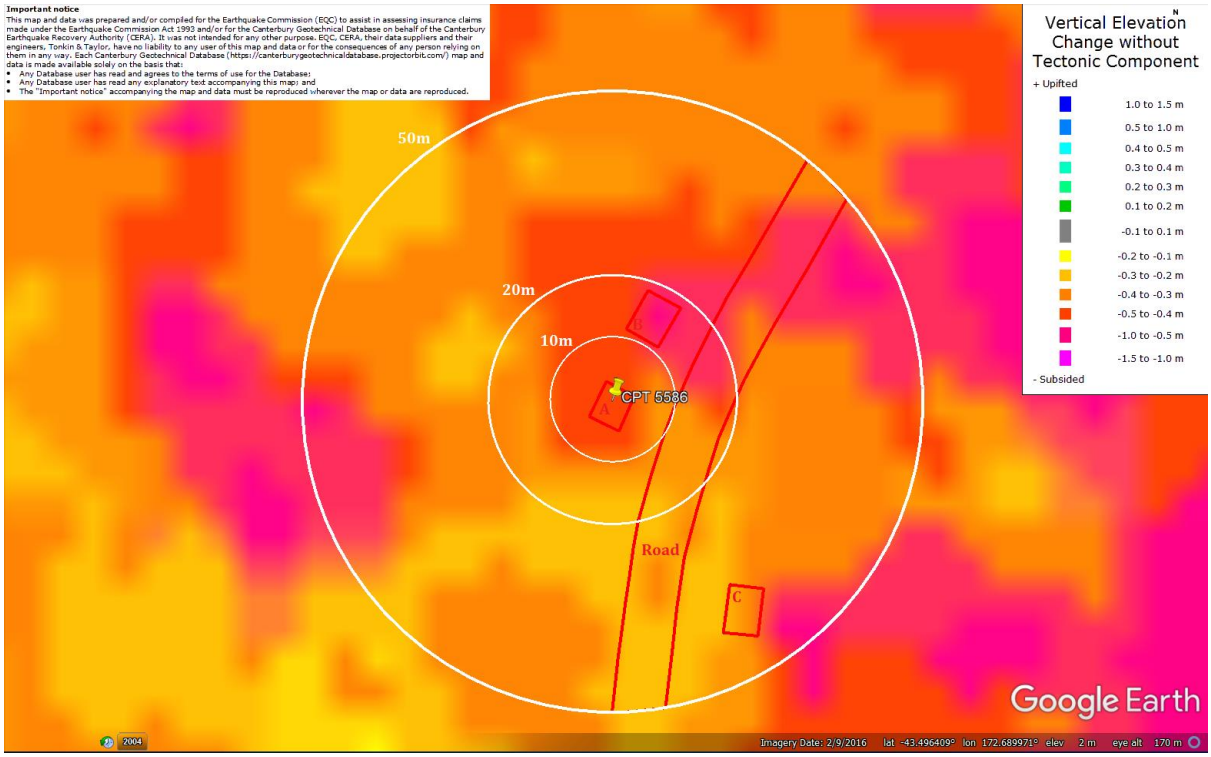

Figure 26: Ground surface subsidence without tectonic component for Canterbury Earthquake Sequence according to the LiDAR DEM.

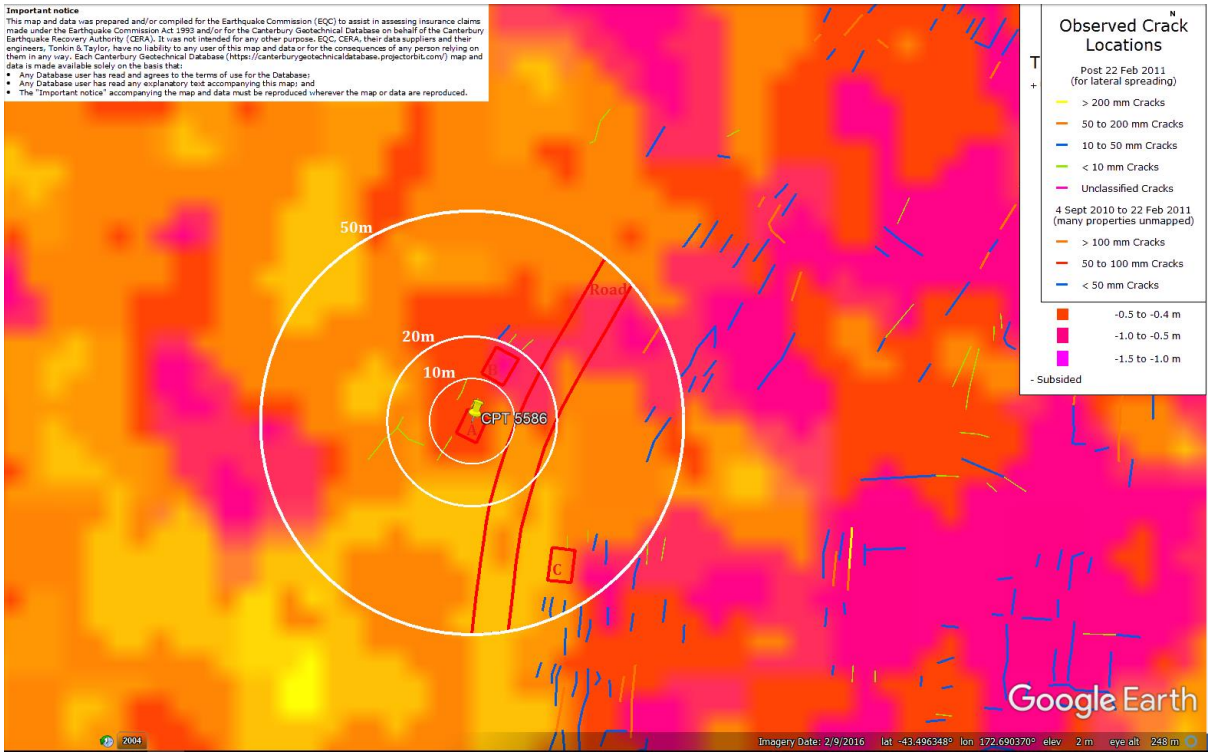

Figure 27: No lateral spreading for Canterbury Earthquake Sequence.

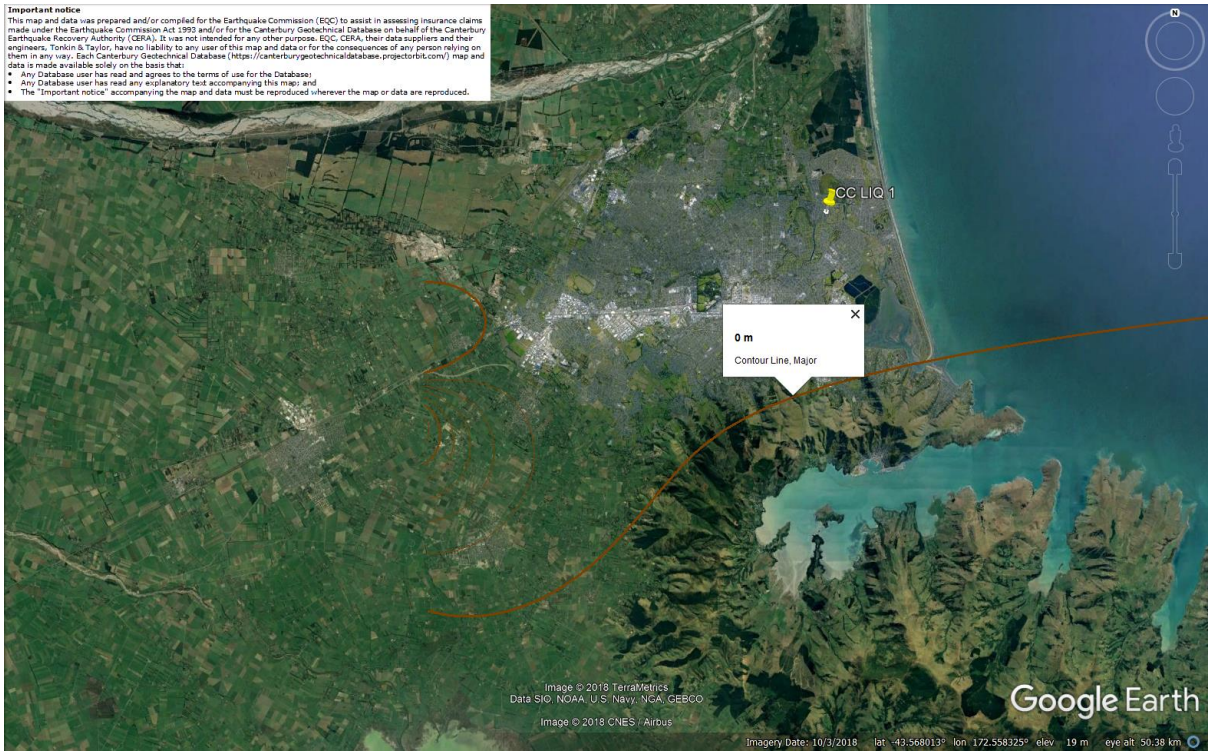

Figure 28: Vertical tectonic movements for Sep 2010 Earthquake.

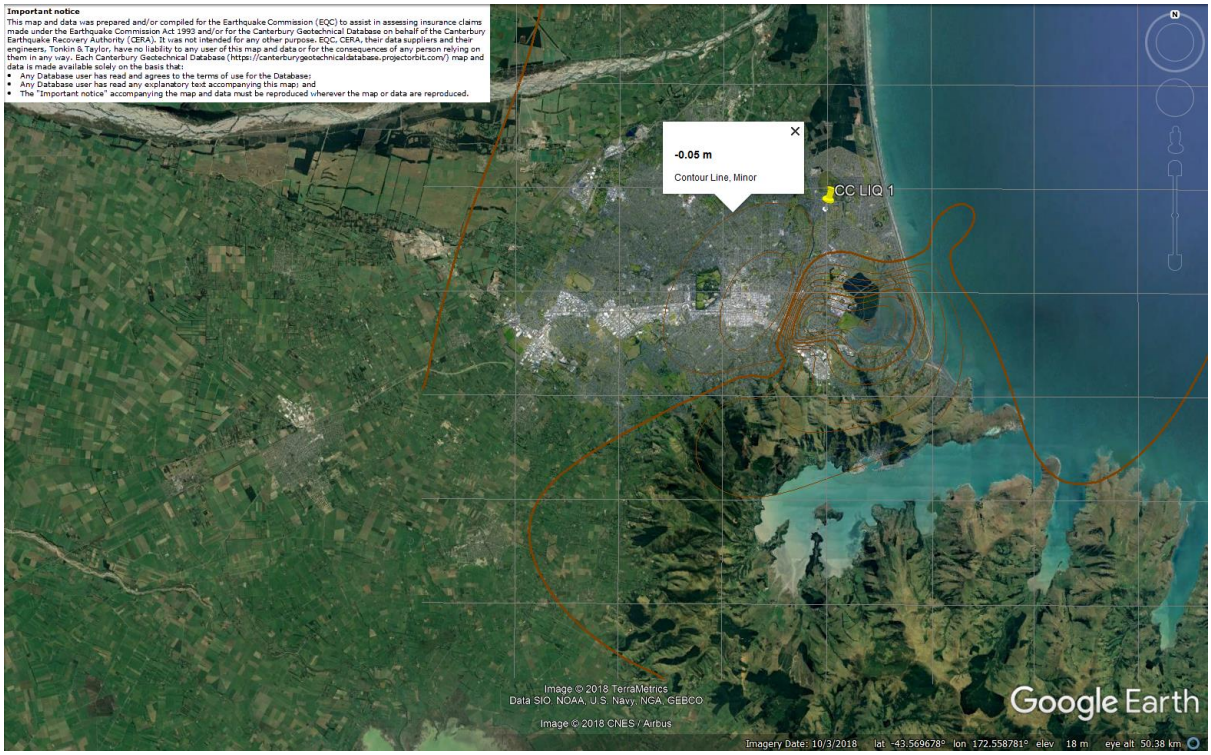

Figure 29: Vertical tectonic movements for Feb 2011 Earthquake.

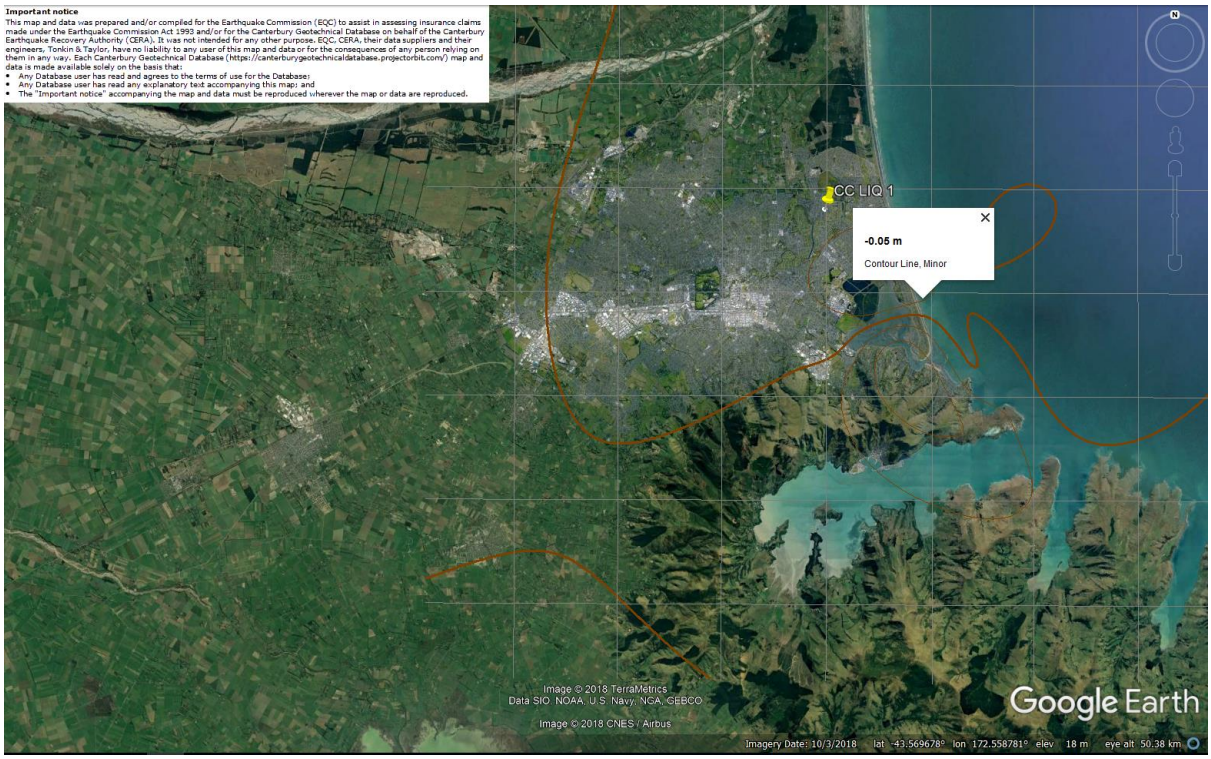

Figure 30: Vertical tectonic movements for June 2011 Earthquake.

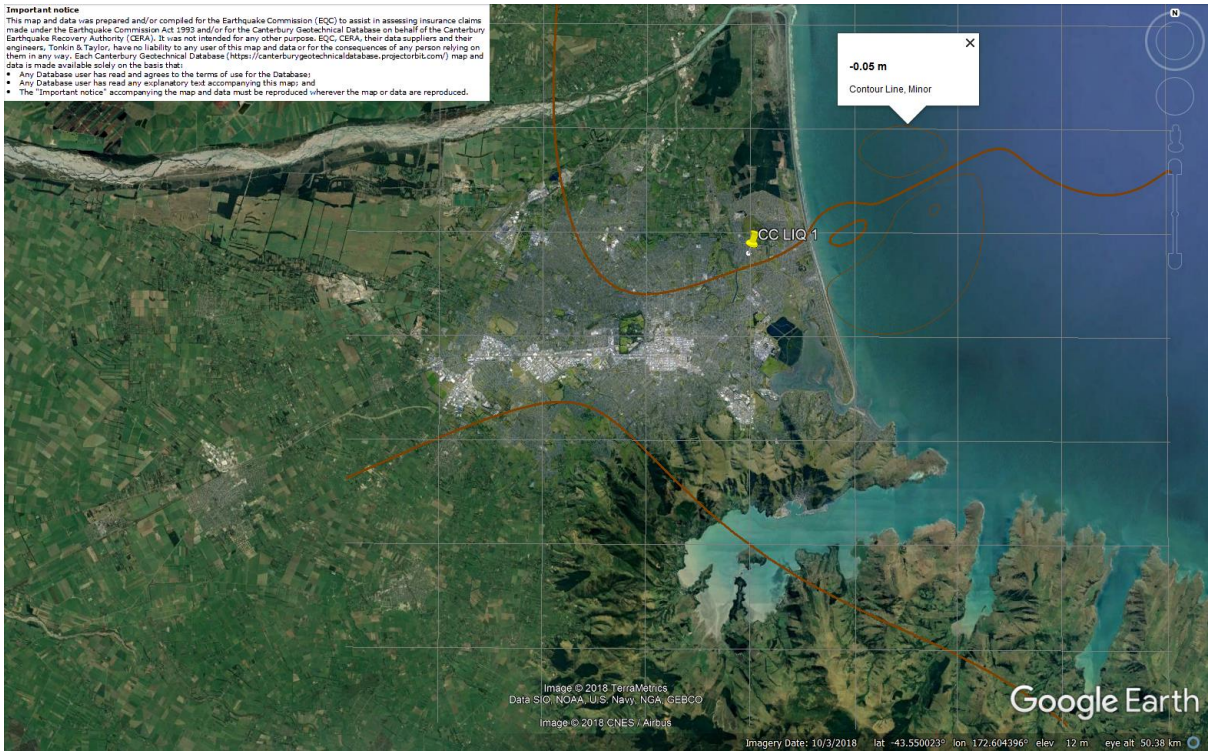

Figure 31: Vertical tectonic movements for Dec 2011 Earthquake.

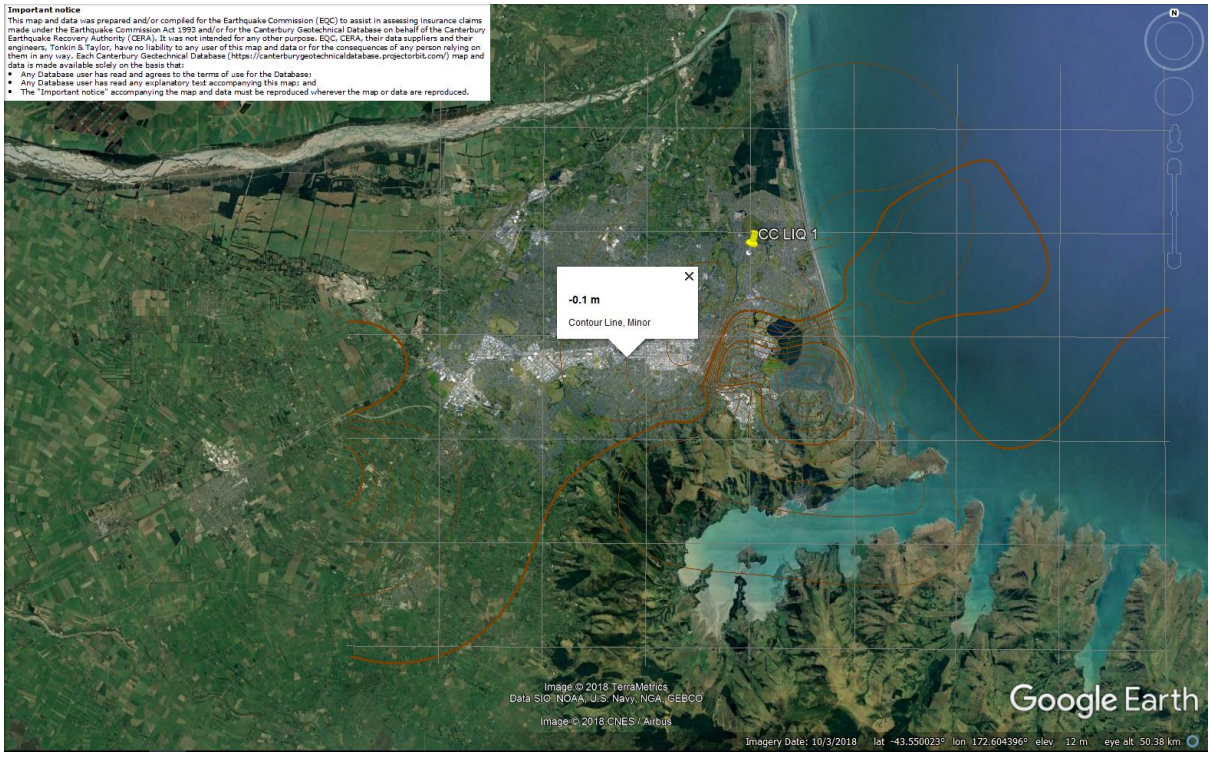

Figure 32: Vertical tectonic movements for Canterbury Earthquake Sequence.

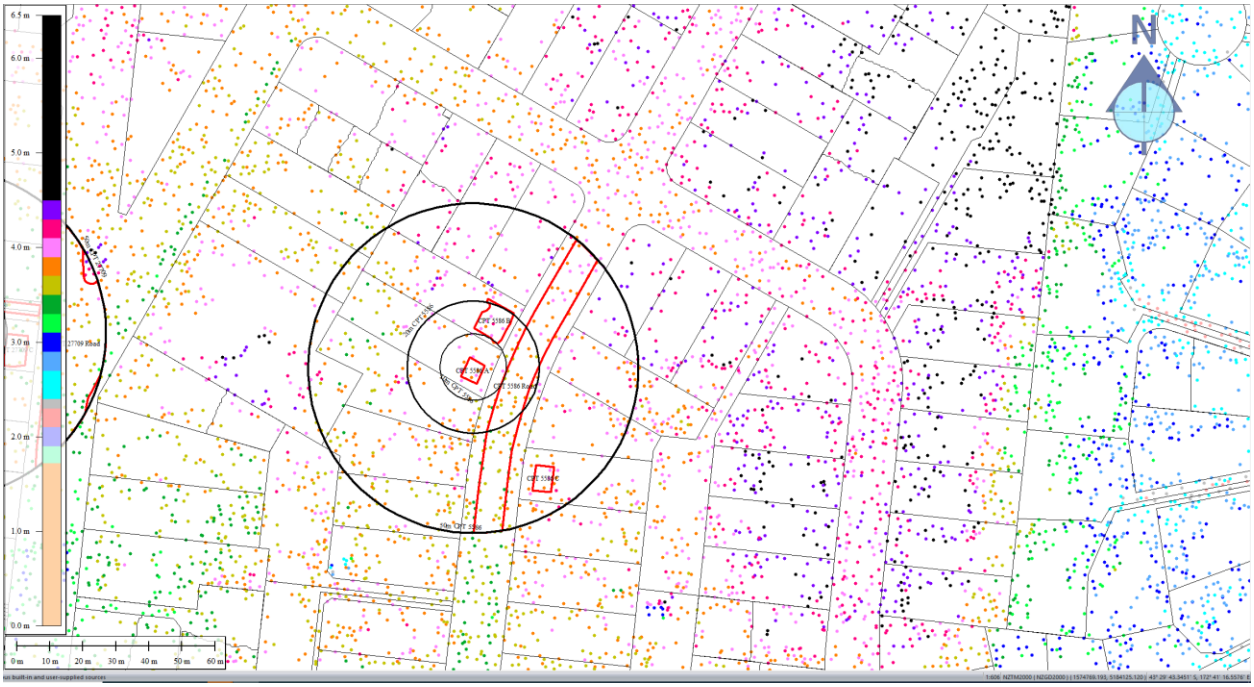

Figure 33: Jul 2003 LiDAR survey.

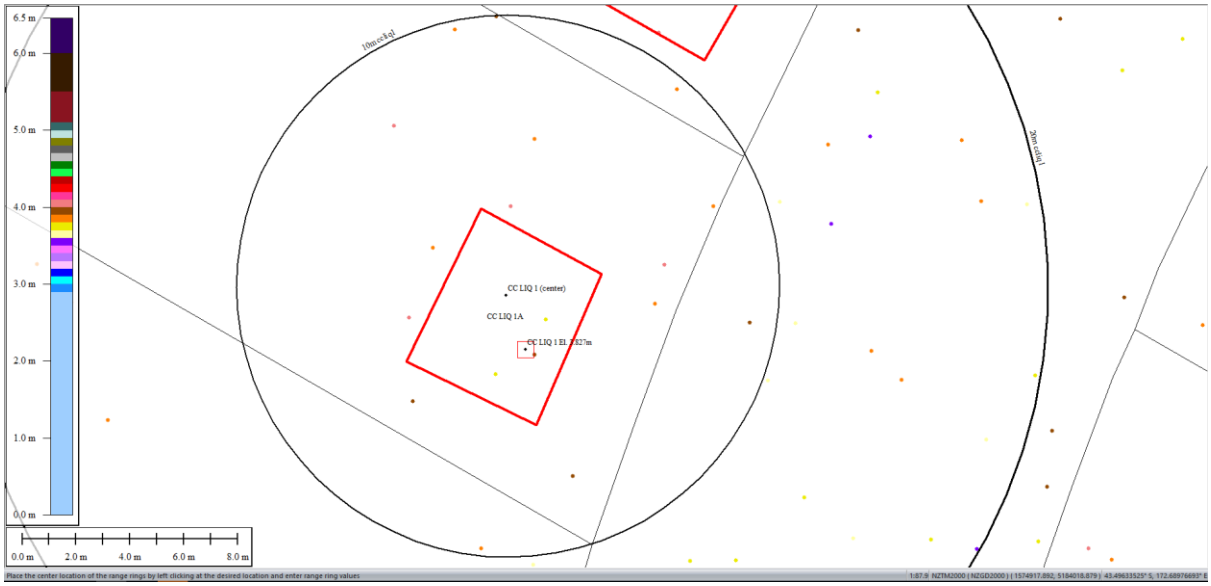

Figure 34: Ground surface elevation averaged over 10-m, 20-m, and 50-m buffers for Patch A for Jul 2003 LiDAR survey.

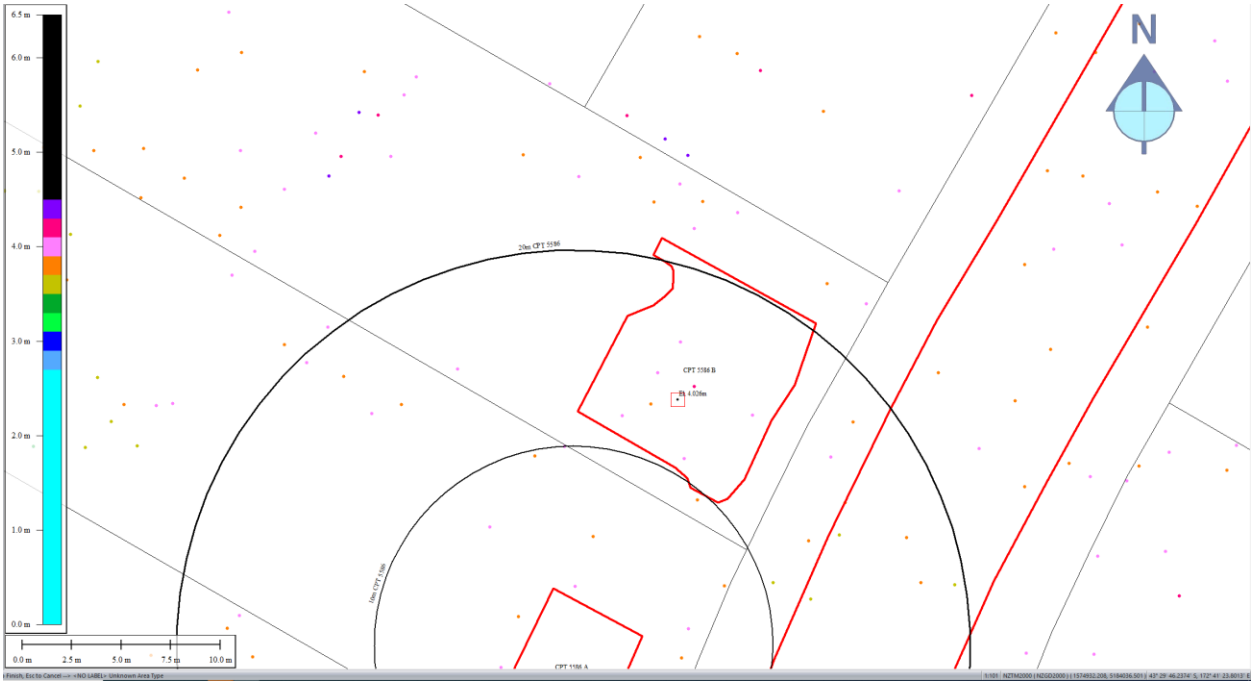

Figure 35: Ground surface elevation averaged over 20-m and 50-m buffers for Patch B for Jul 2003 LiDAR survey.

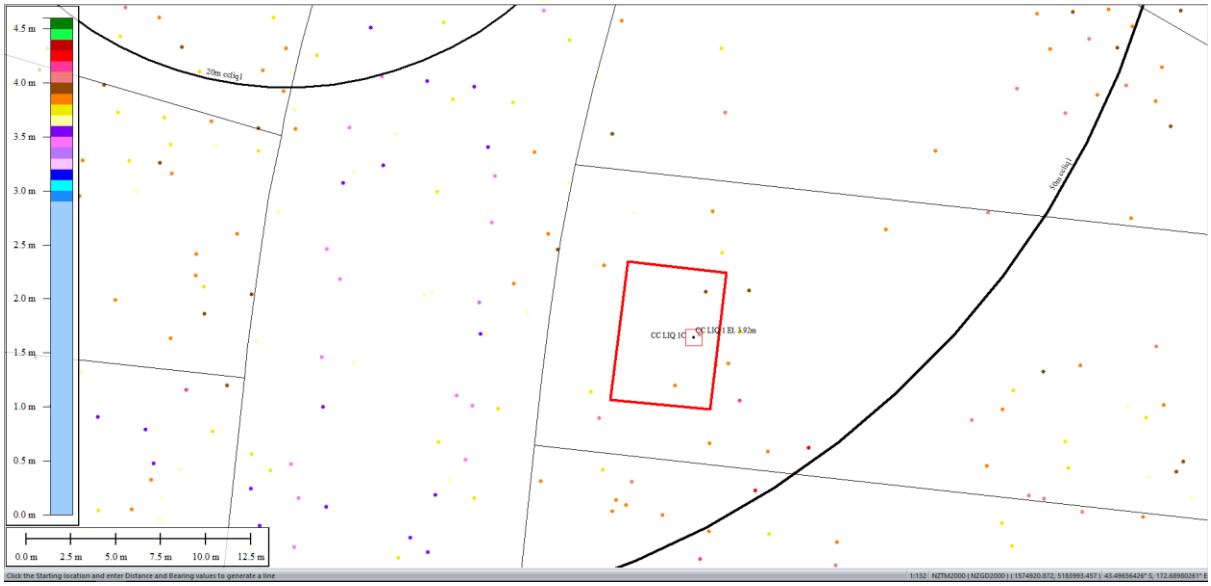

Figure 36: Ground surface elevation averaged over 50-m buffer for Patch C for Jul 2003 LiDAR survey.

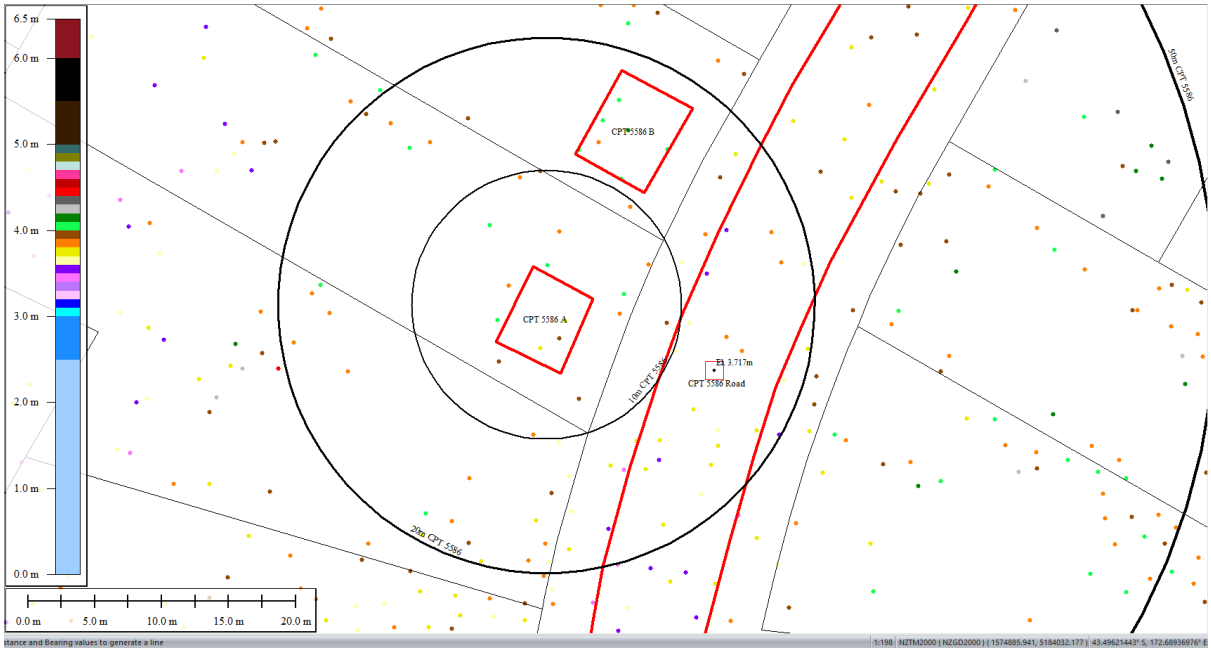

Figure 37: Ground surface elevation averaged over 20-m buffer for Road for Jul 2003 LiDAR survey.

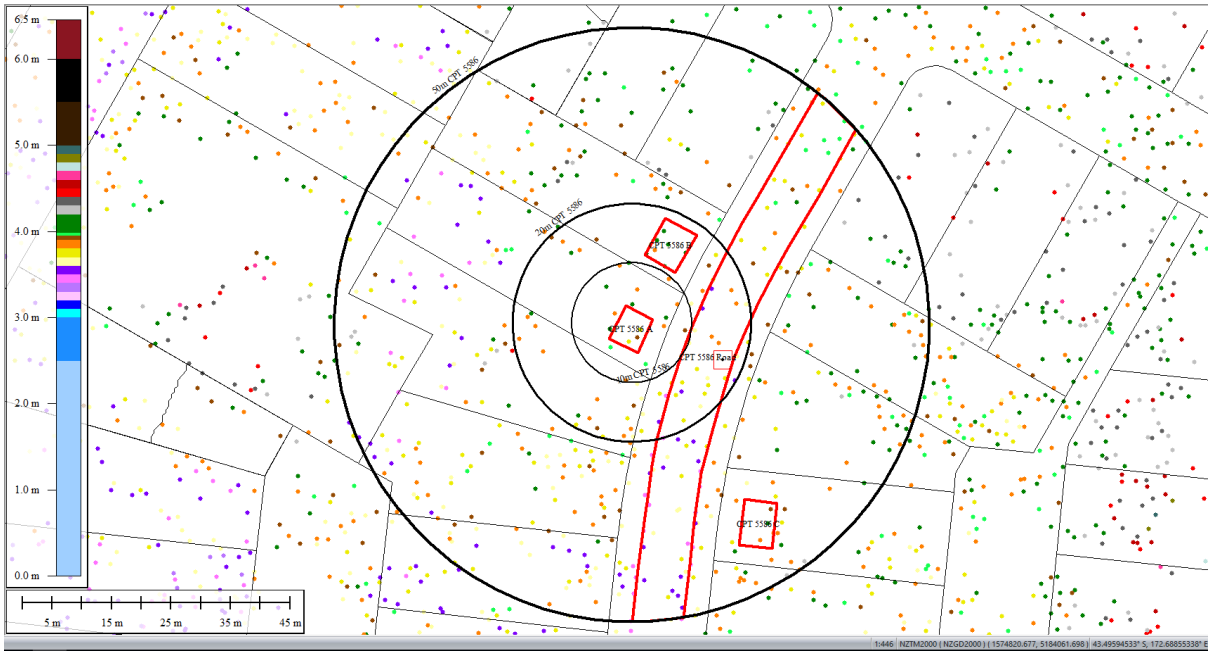

Figure 38: Ground surface elevation averaged over 50-m buffer for Road for Jul 2003 LiDAR survey.

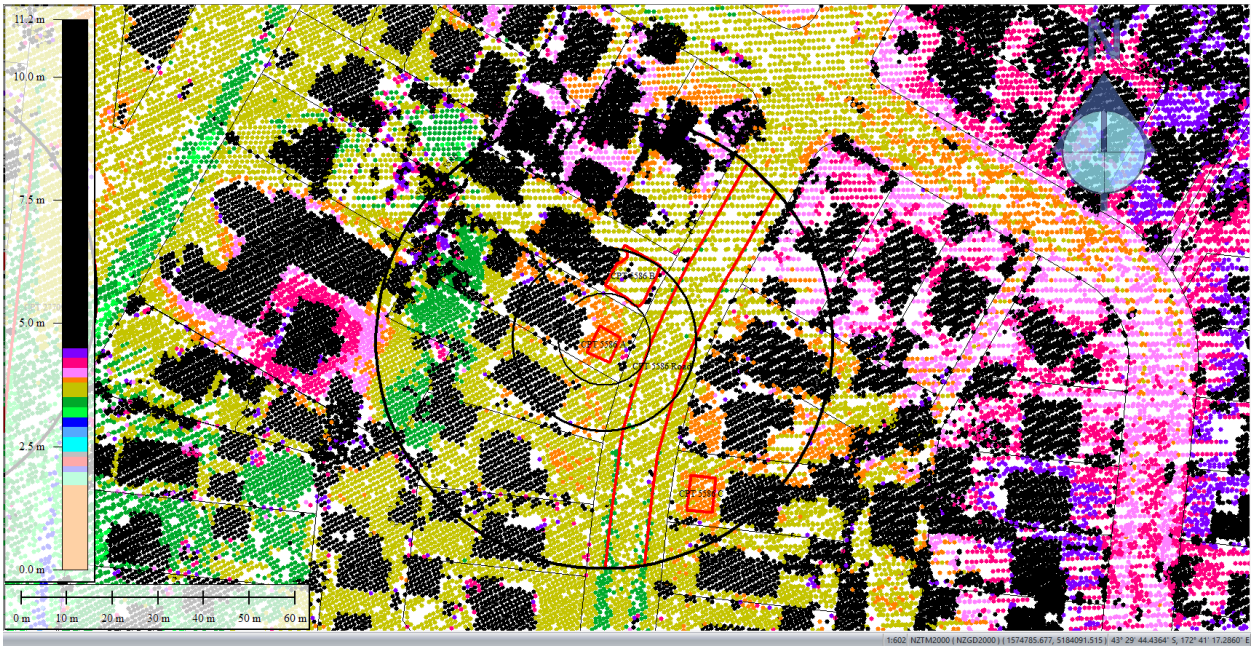

Figure 39: Sep 5, 2010 LiDAR survey.

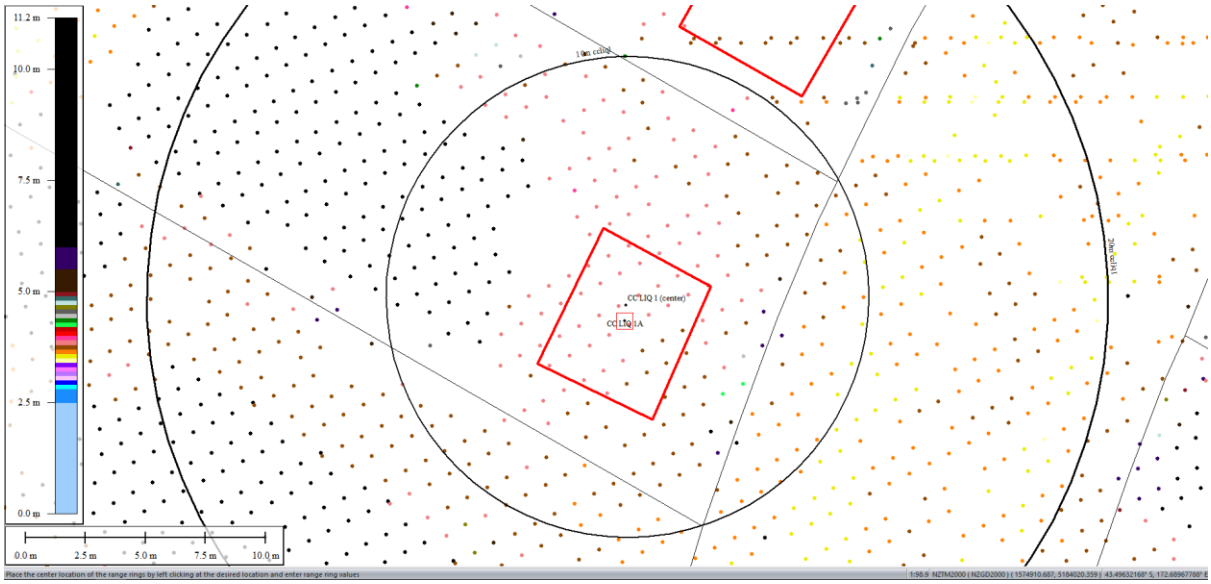

Figure 40: Ground surface elevation averaged over 10-m, 20-m, and 50-m buffers for Patch A for Sep 5, 2010 LiDAR survey.

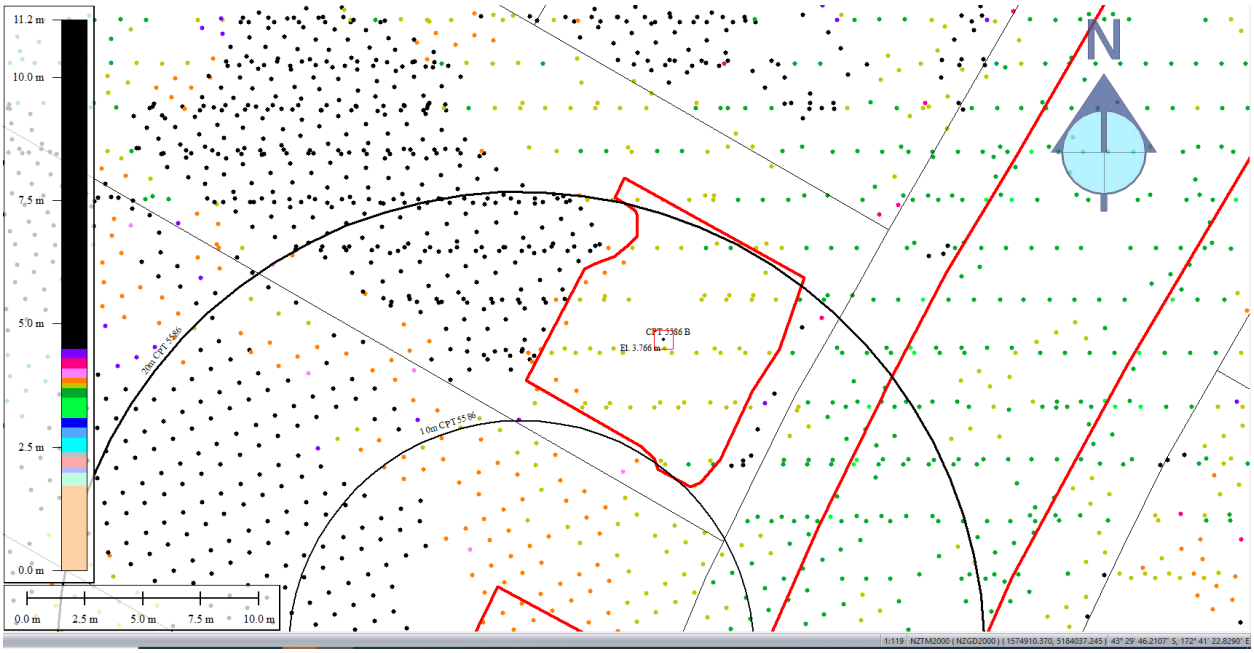

Figure 41: Ground surface elevation averaged over 20-m and 50-m buffers for Patch B for Sep 5, 2010 LiDAR survey.

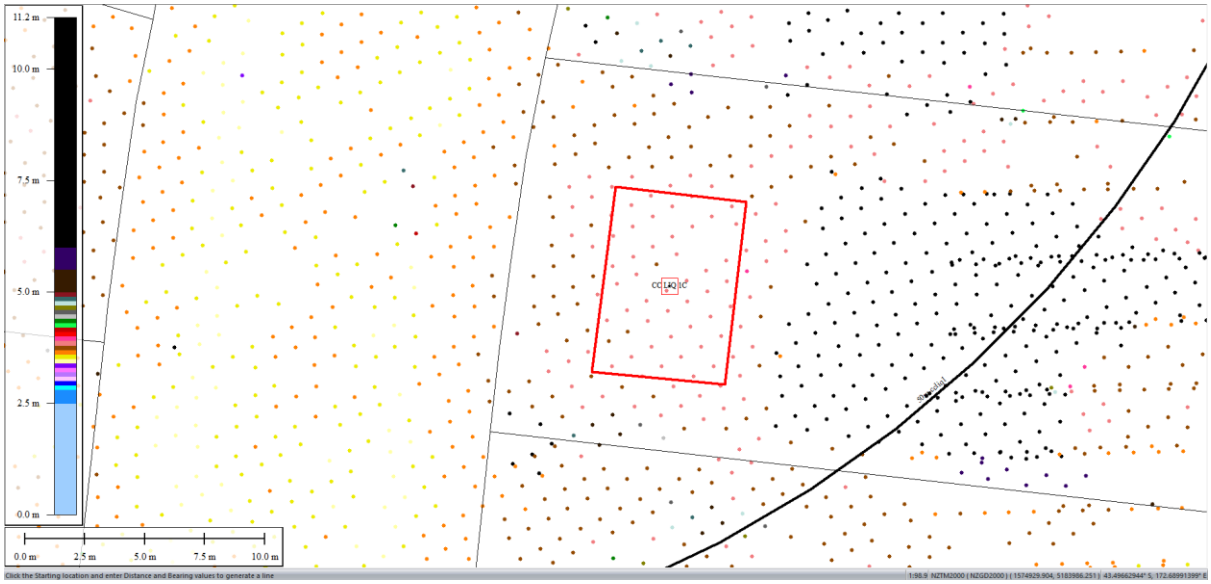

Figure 42: Ground surface elevation averaged over 50-m buffer for Patch C for Sep 5, 2010 LiDAR survey.

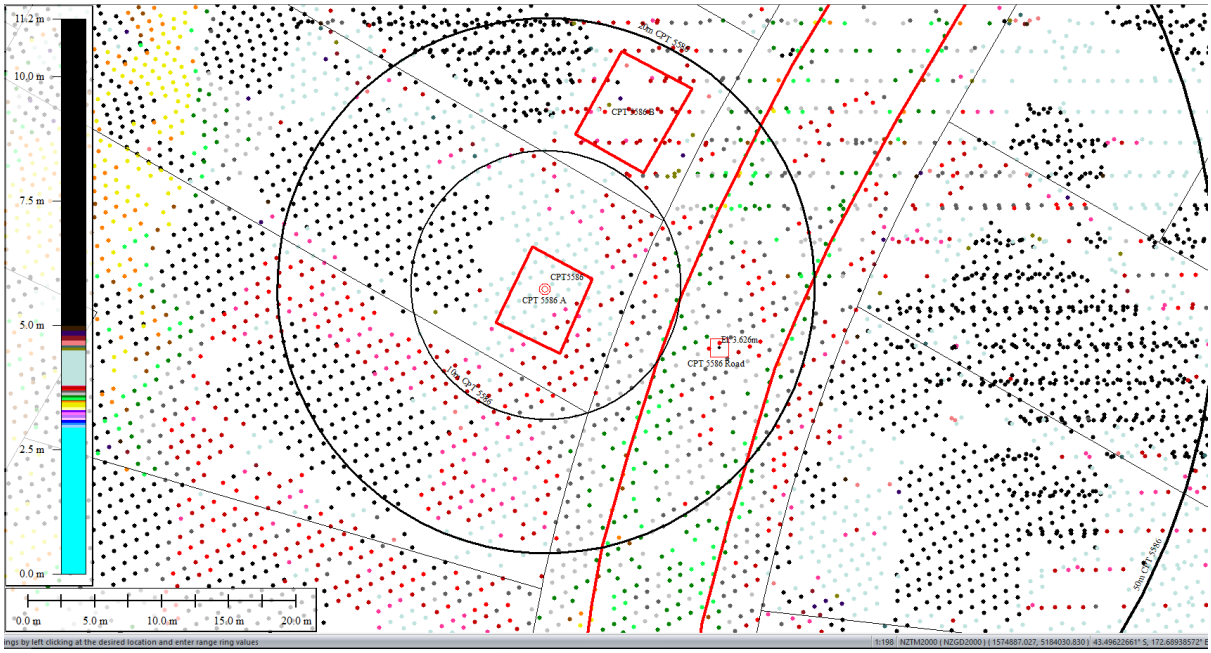

Figure 43: Ground surface elevation averaged over 20-m buffer for Road for Sep 5, 2010 LiDAR survey.

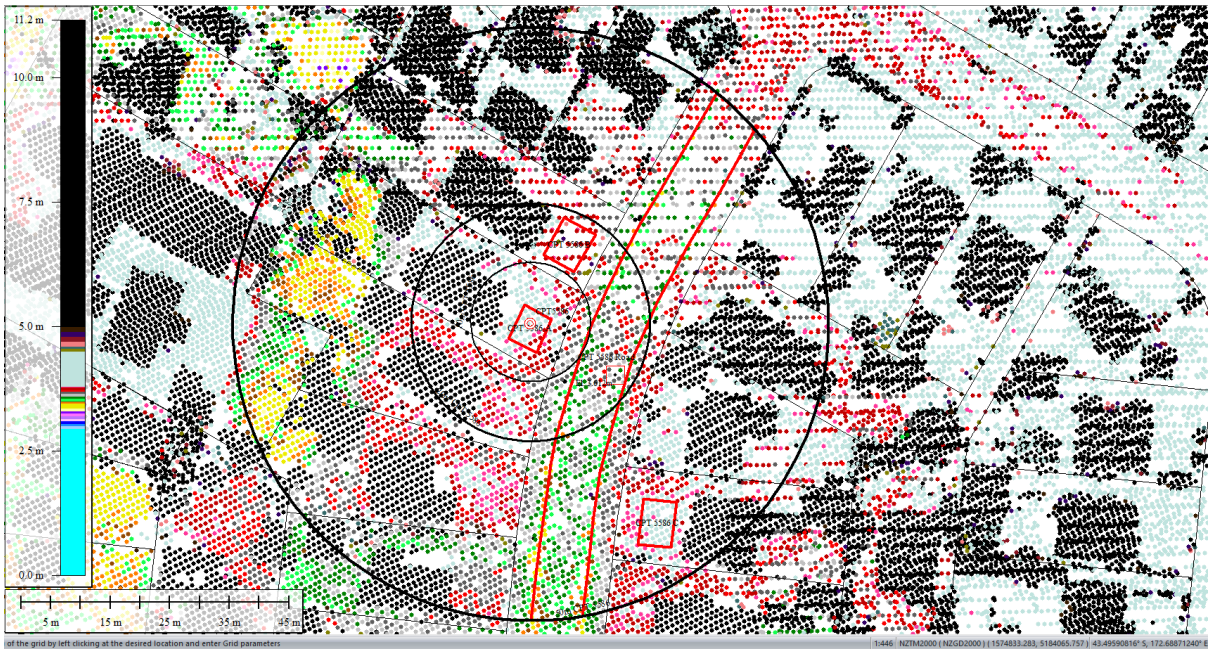

Figure 44: Ground surface elevation averaged over 50-m buffer for Road for Sep 5, 2010 LiDAR survey.

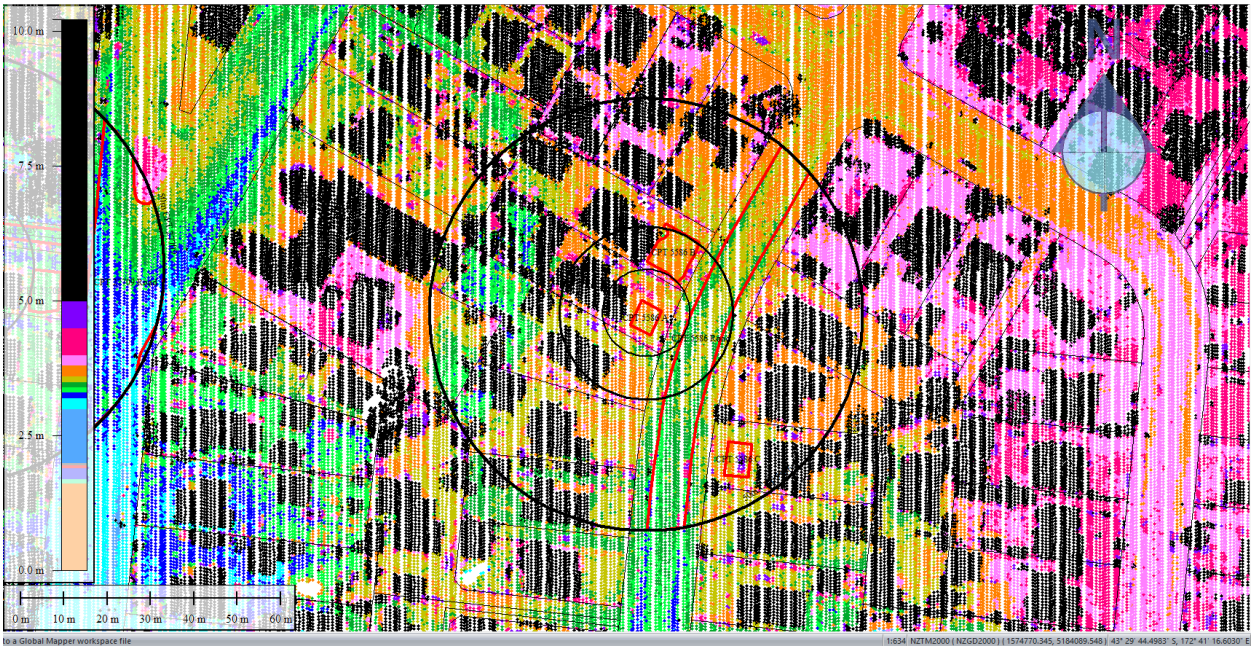

Figure 45: Mar 2011 LiDAR survey.

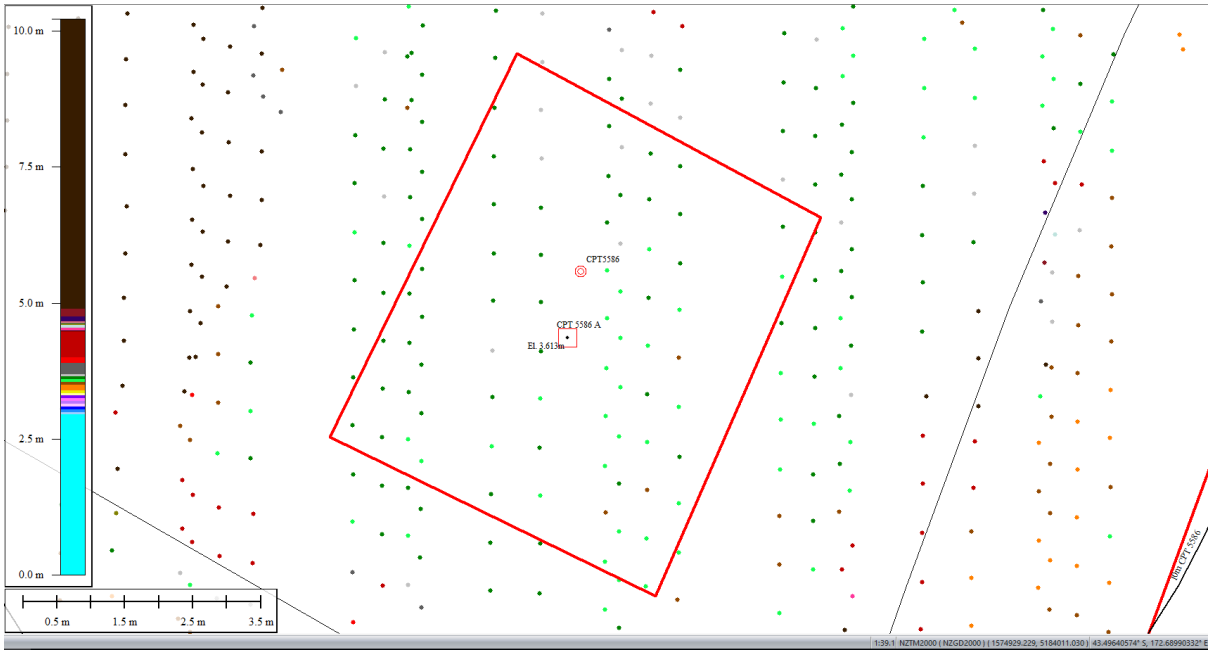

Figure 46: Ground surface elevation averaged over 10-m, 20-m, and 50-m buffers for Patch A for Mar 2011 LiDAR survey.

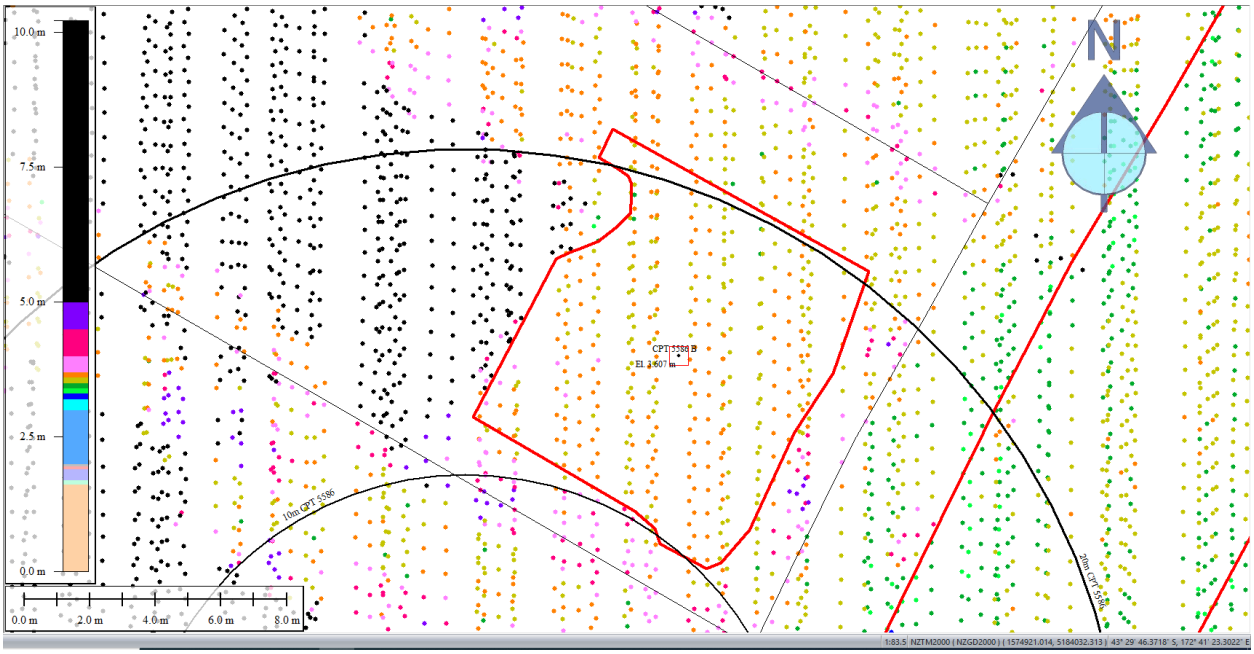

Figure 47: Ground surface elevation averaged over 20-m and 50-m buffers for Patch B for Mar 2011 LiDAR survey.

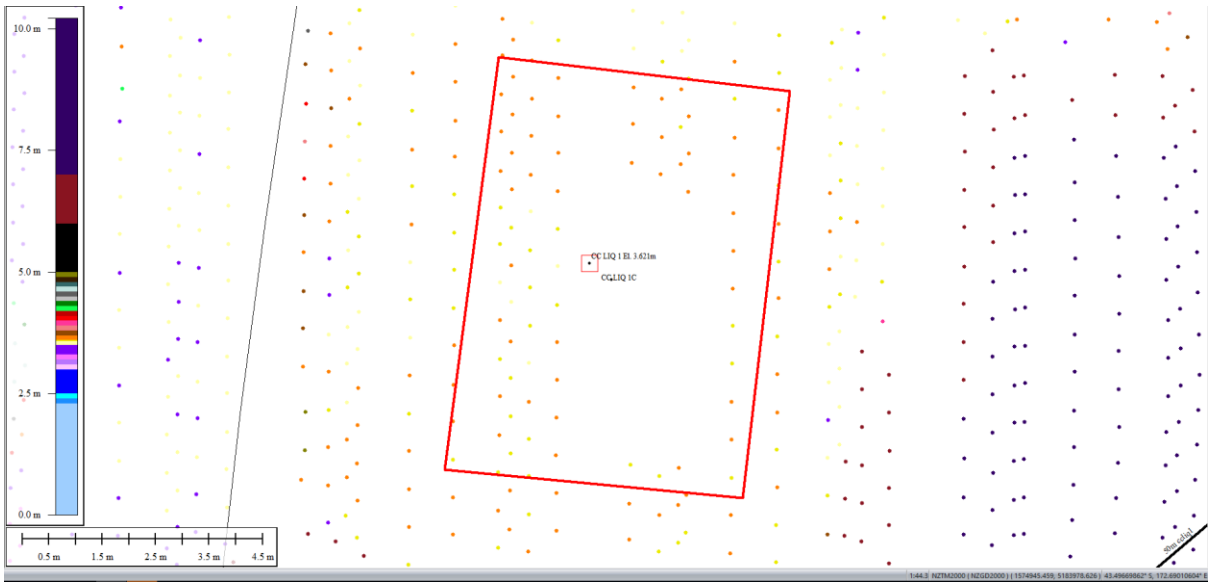

Figure 48: Ground surface elevation averaged over 50-m buffer for Patch C for Mar 2011 LiDAR survey.

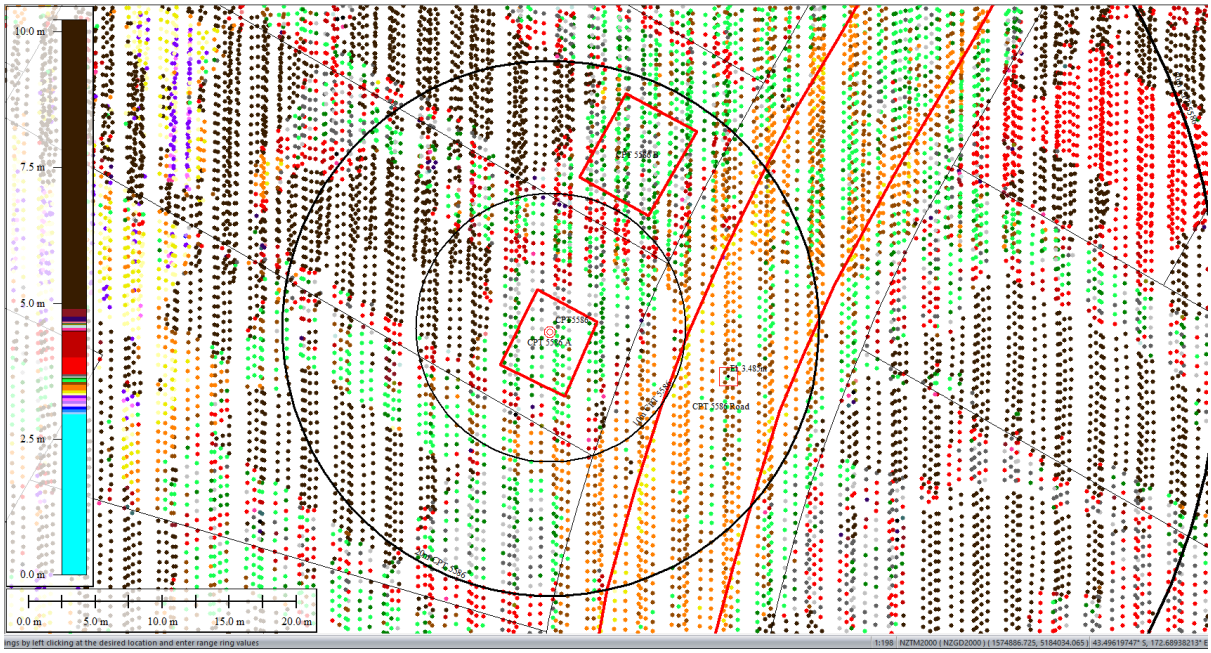

Figure 49: Ground surface elevation averaged over 20-m buffer for Road for Mar 2011 LiDAR survey.

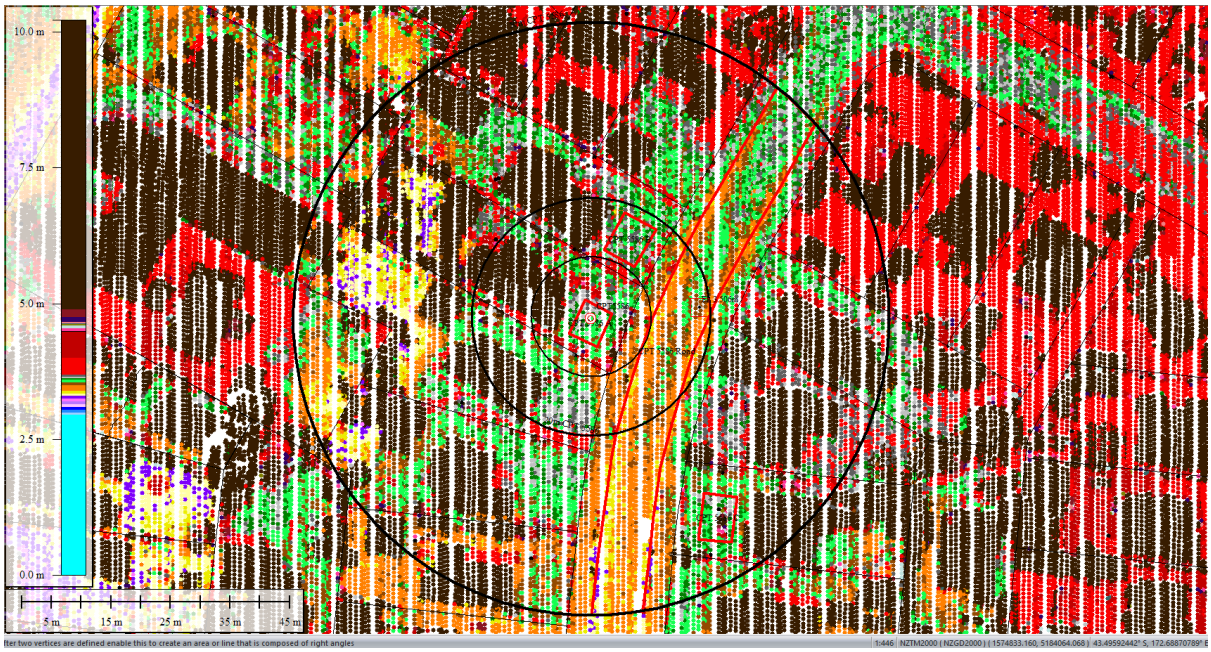

Figure 50: Ground surface elevation averaged over 50-m buffer for Road for Mar 2011 LiDAR survey.

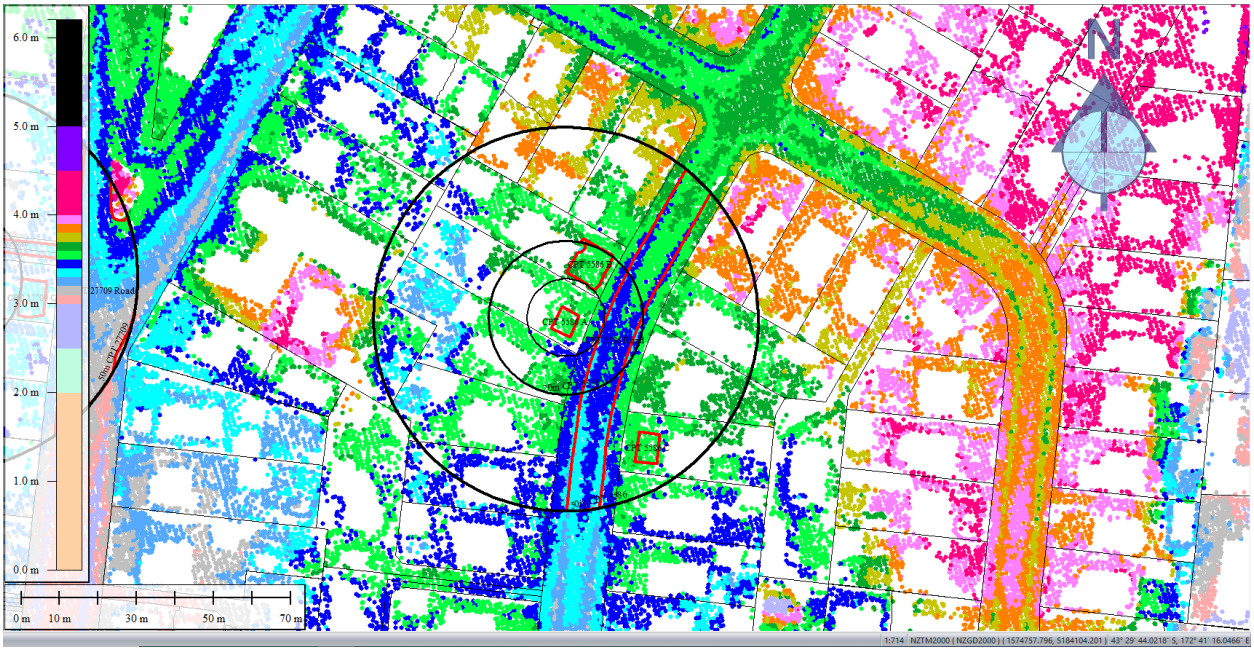

Figure 51: May 2011 LiDAR survey.

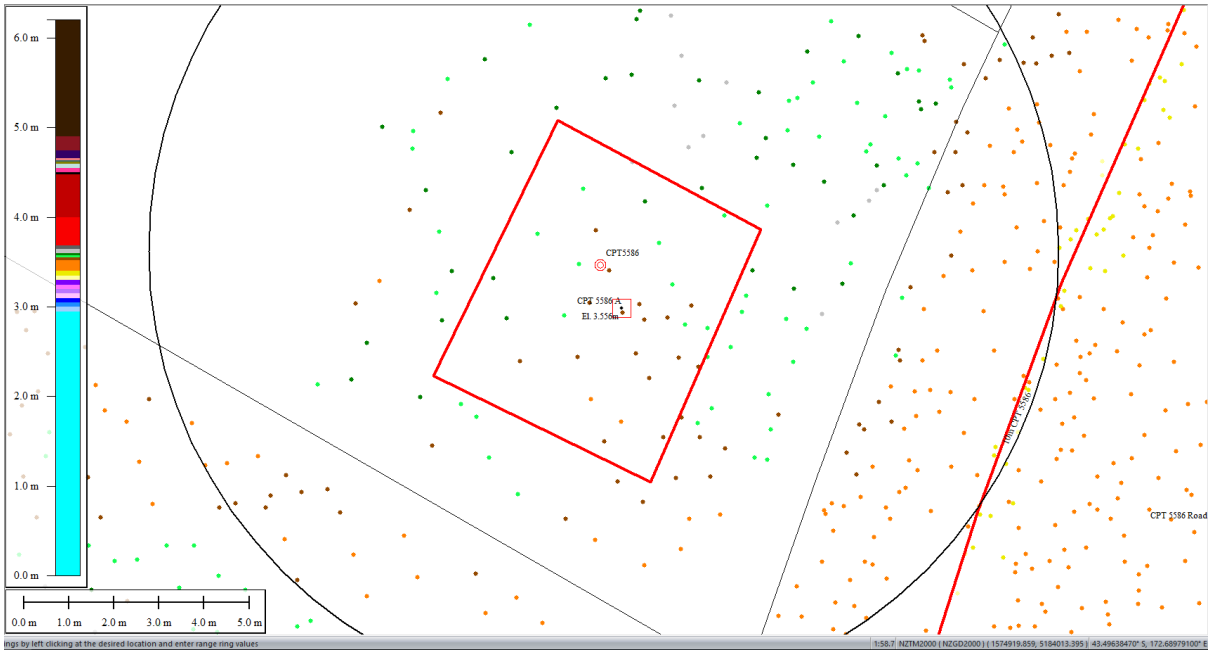

Figure 52: Ground surface elevation averaged over 10-m, 20-m, and 50-m buffers for Patch A for May 2011 LiDAR survey.

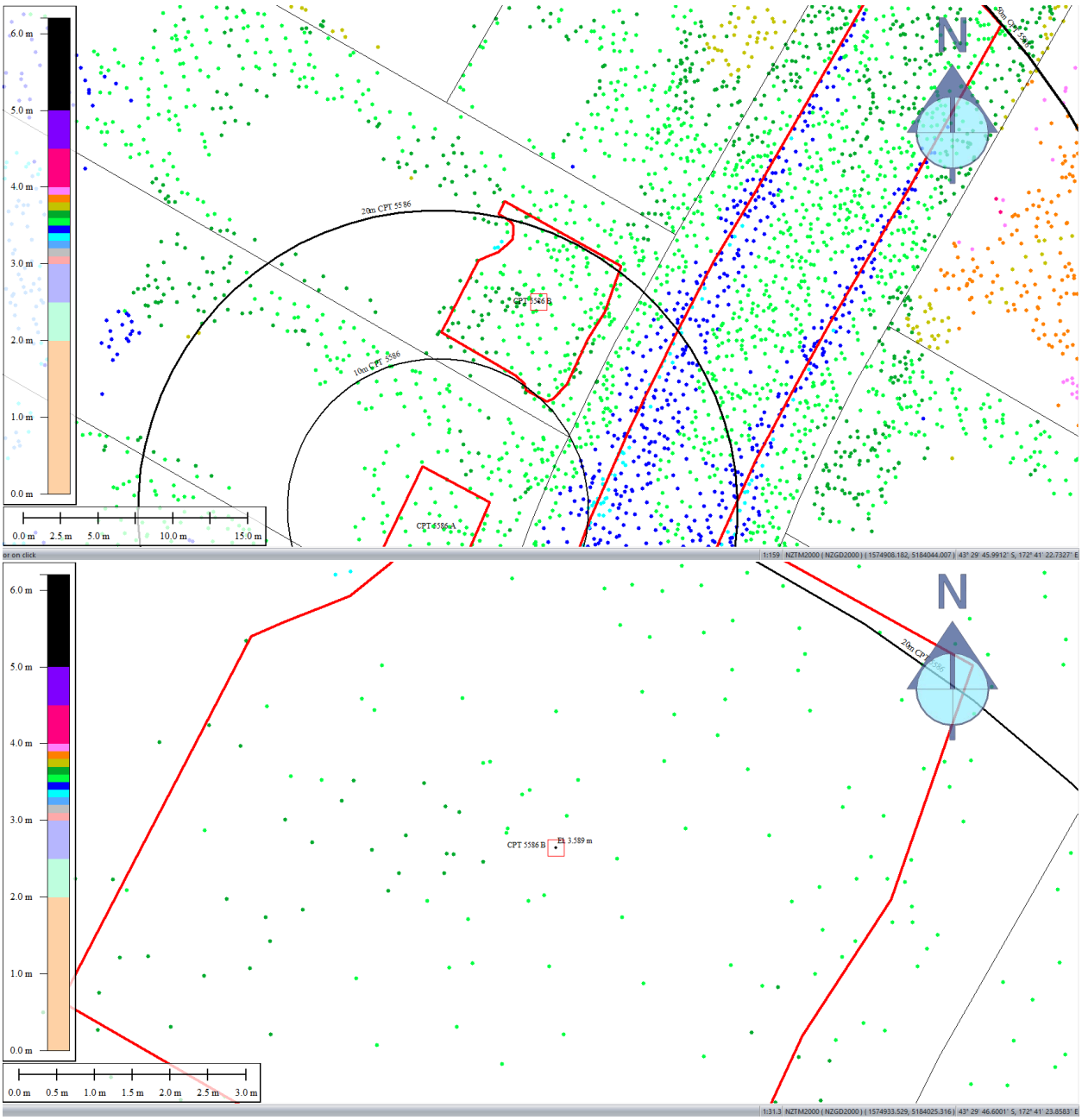

Figure 53: Ground surface elevation averaged over 20-m and 50-m buffers for Patch B for May 2011 LiDAR survey.

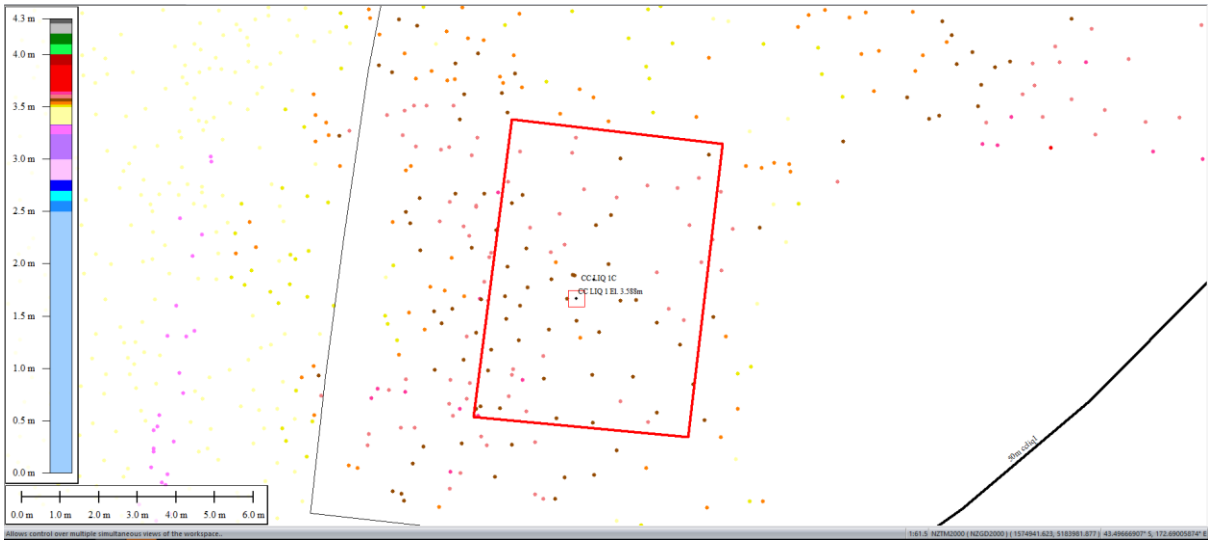

Figure 54: Ground surface elevation averaged over 50-m buffer for Patch C for May 2011 LiDAR survey.

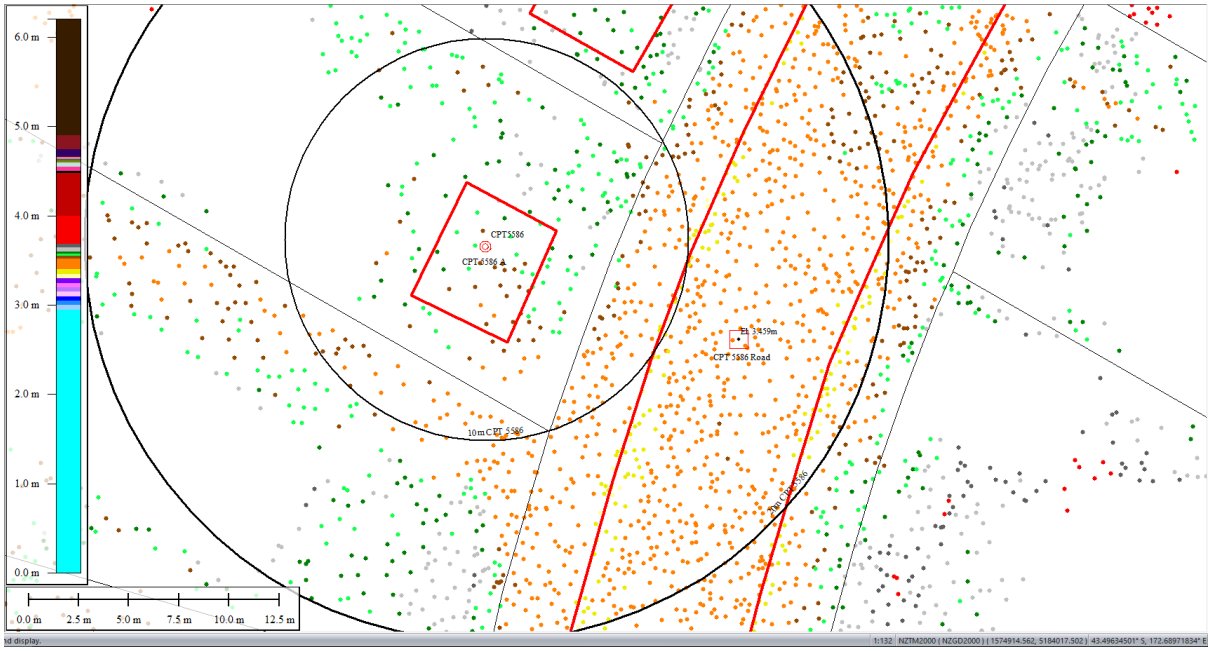

Figure 55: Ground surface elevation averaged over 20-m buffer for Road for May 2011 LiDAR survey.

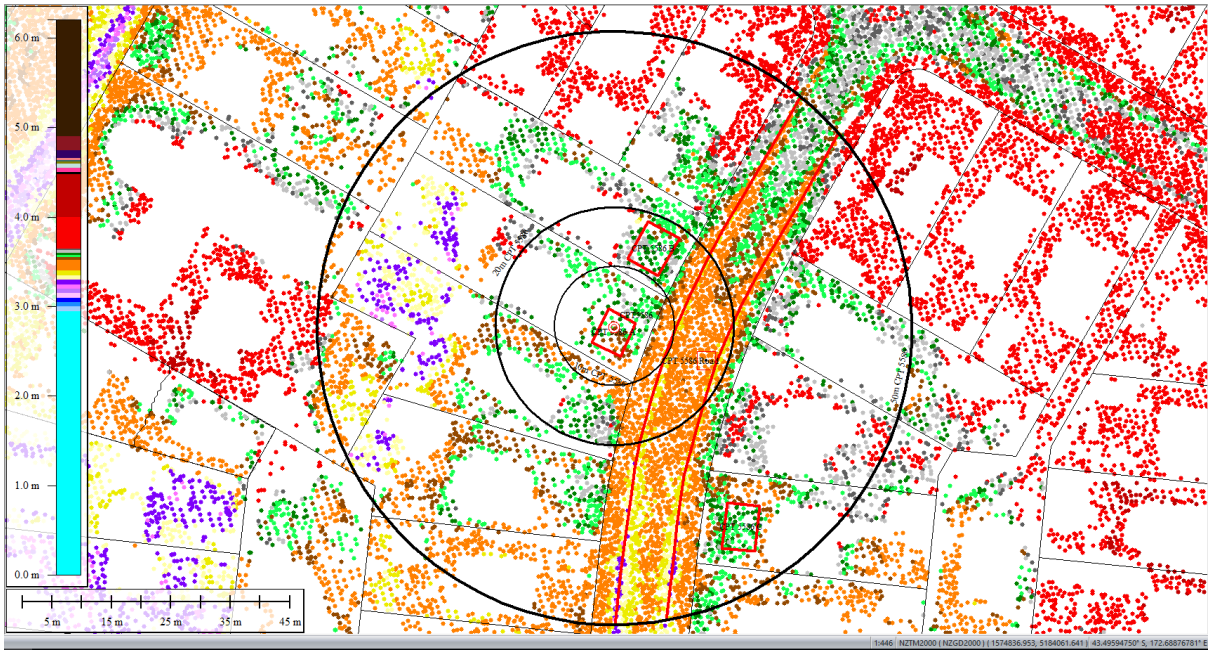

Figure 56: Ground surface elevation averaged over 50-m buffer for Road for May 2011 LiDAR survey.

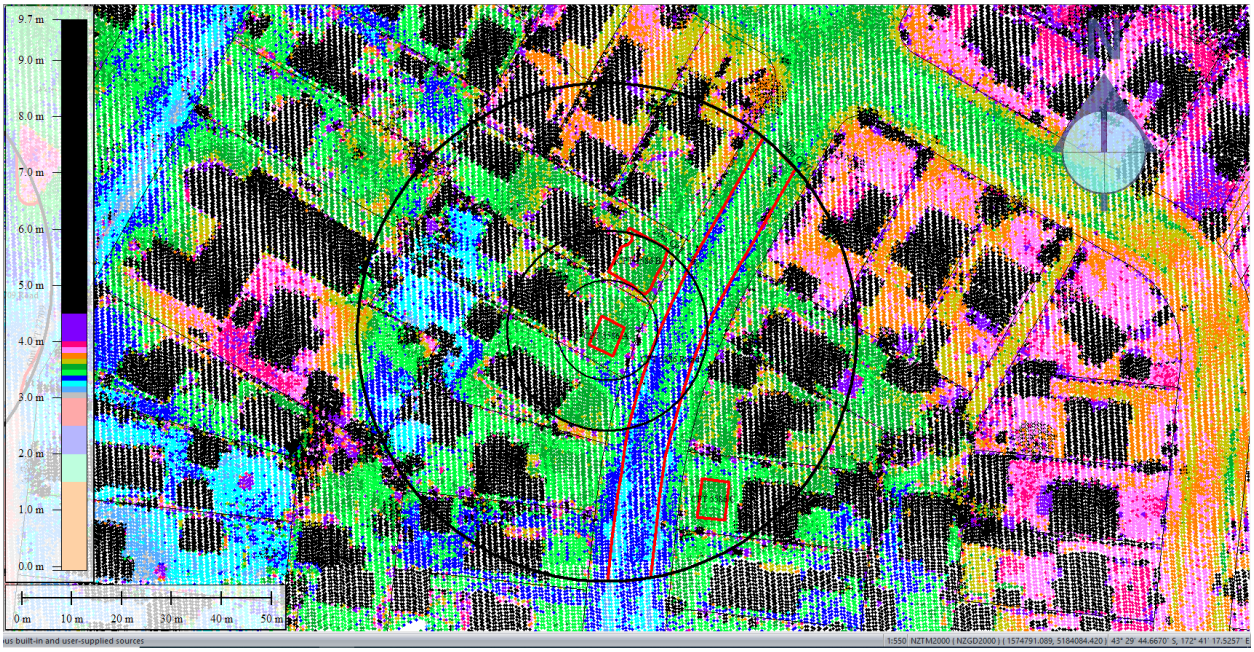

Figure 57: Sep 2011 LiDAR survey.

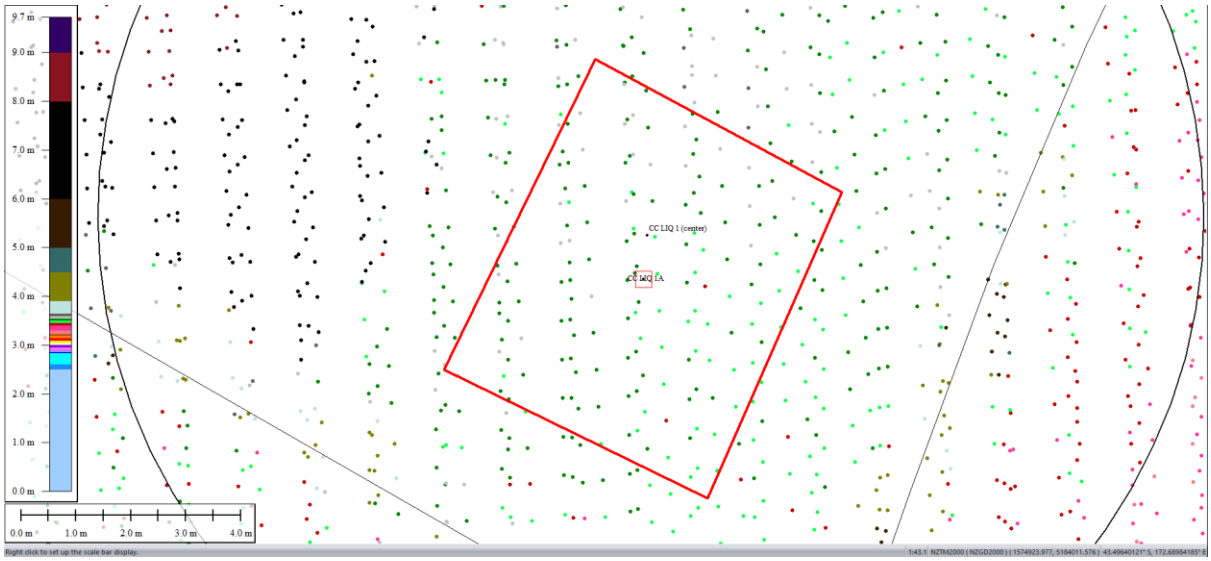

Figure 58: Ground surface elevation averaged over 10-m, 20-m, and 50-m buffers for Patch A for Sep 2011 LiDAR survey.

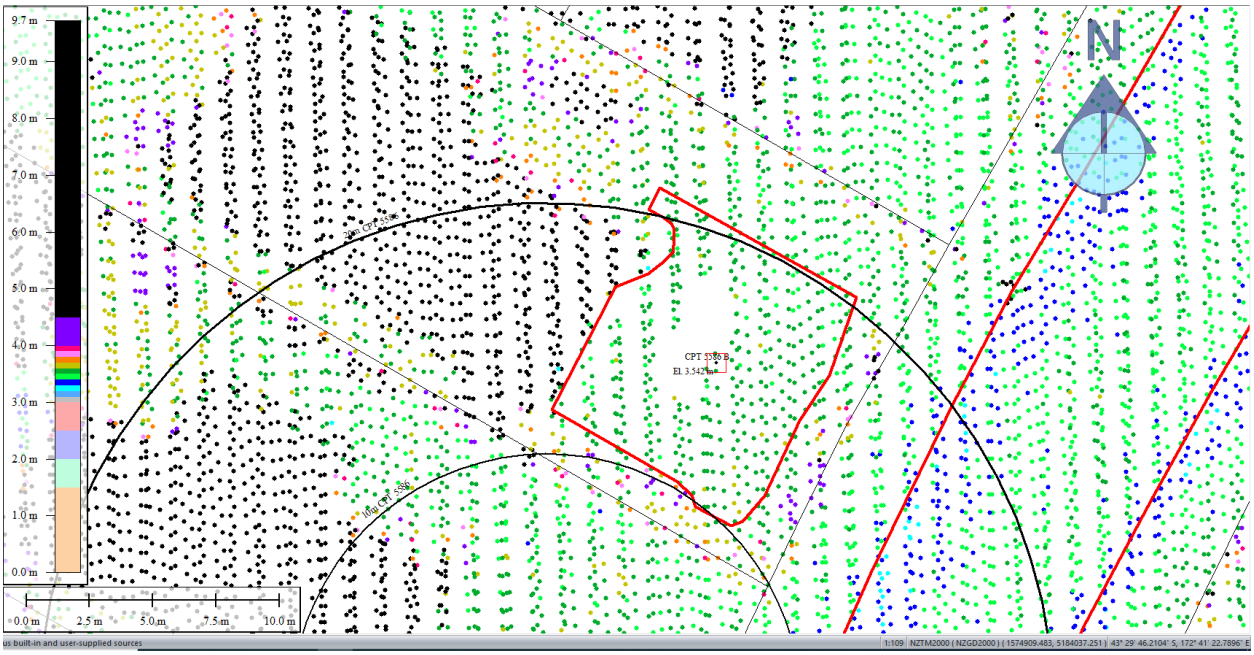

Figure 59: Ground surface elevation averaged over 20-m and 50-m buffers for Patch B for Sep 2011 LiDAR survey.

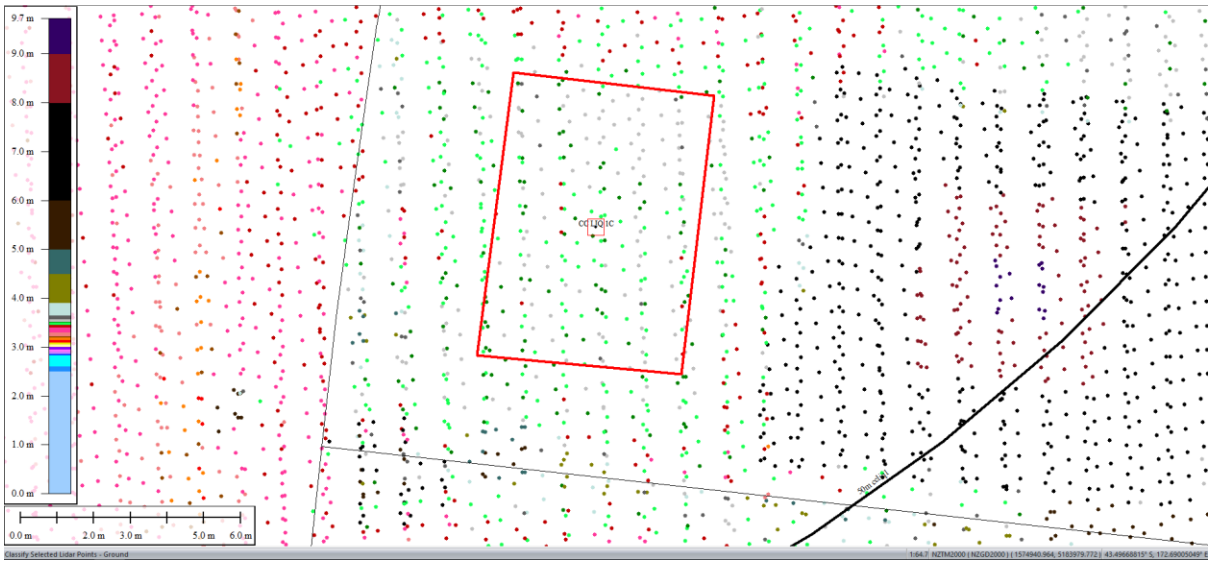

Figure 60: Ground surface elevation averaged over 50-m buffer for Patch C for Sep 2011 LiDAR survey.

Figure 61: Ground surface elevation averaged over 20-m buffer for Road for Sep 2011 LiDAR survey.

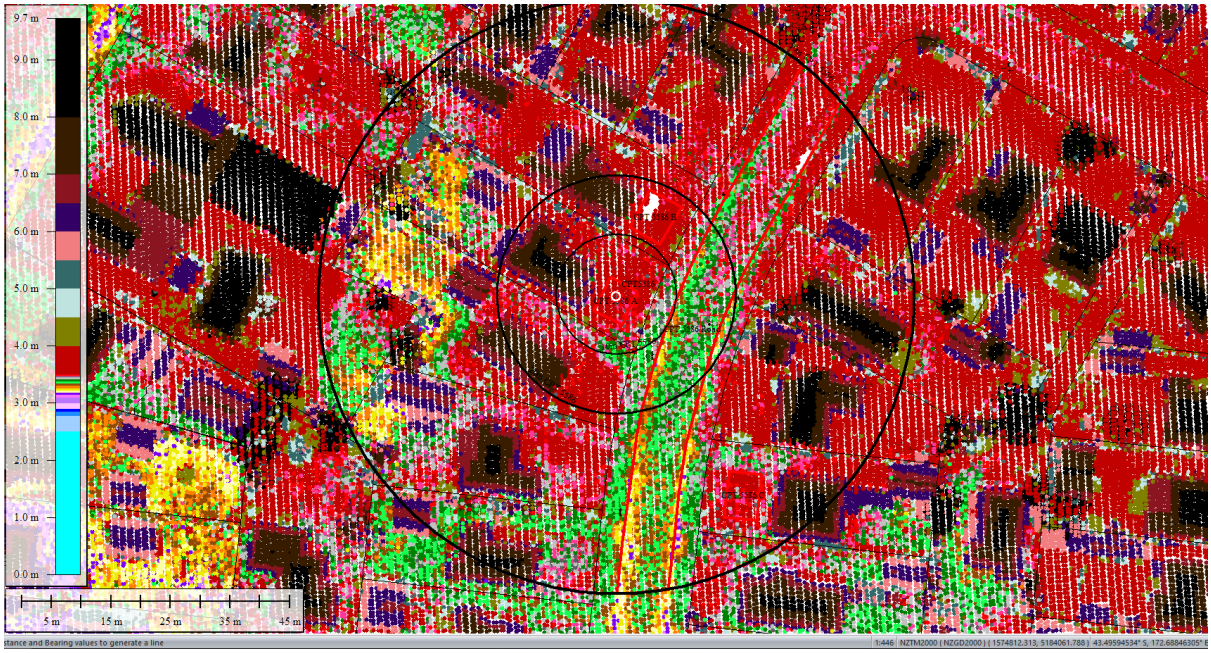

Figure 62: Ground surface elevation averaged over 50-m buffer for Road for Sep 2011 LiDAR survey.

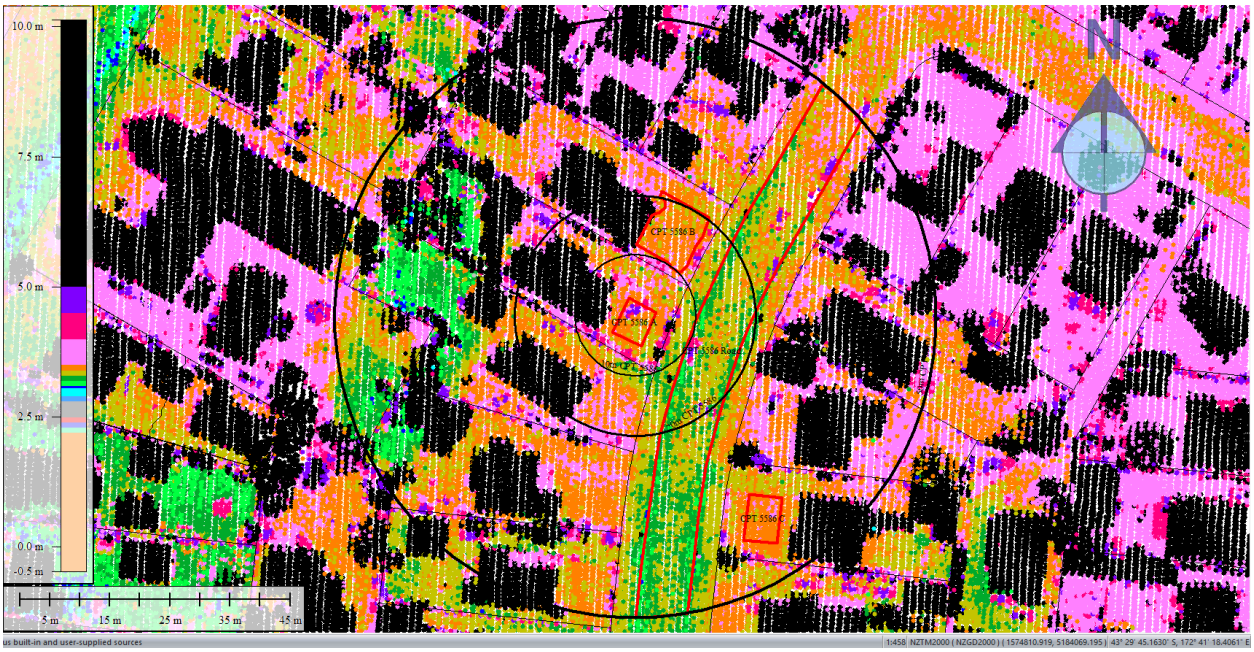

Figure 63: Feb 2012 LiDAR survey.

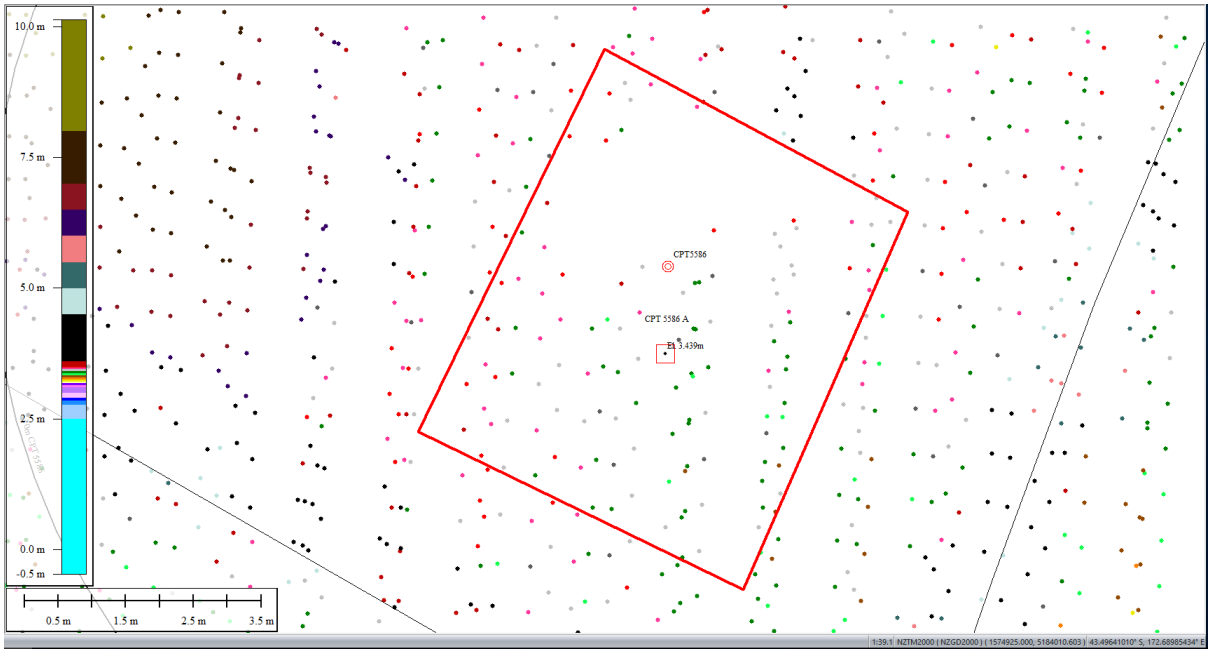

Figure 64: Ground surface elevation averaged over 10-m, 20-m, and 50-m buffers for Patch A for Feb 2012 LiDAR survey.

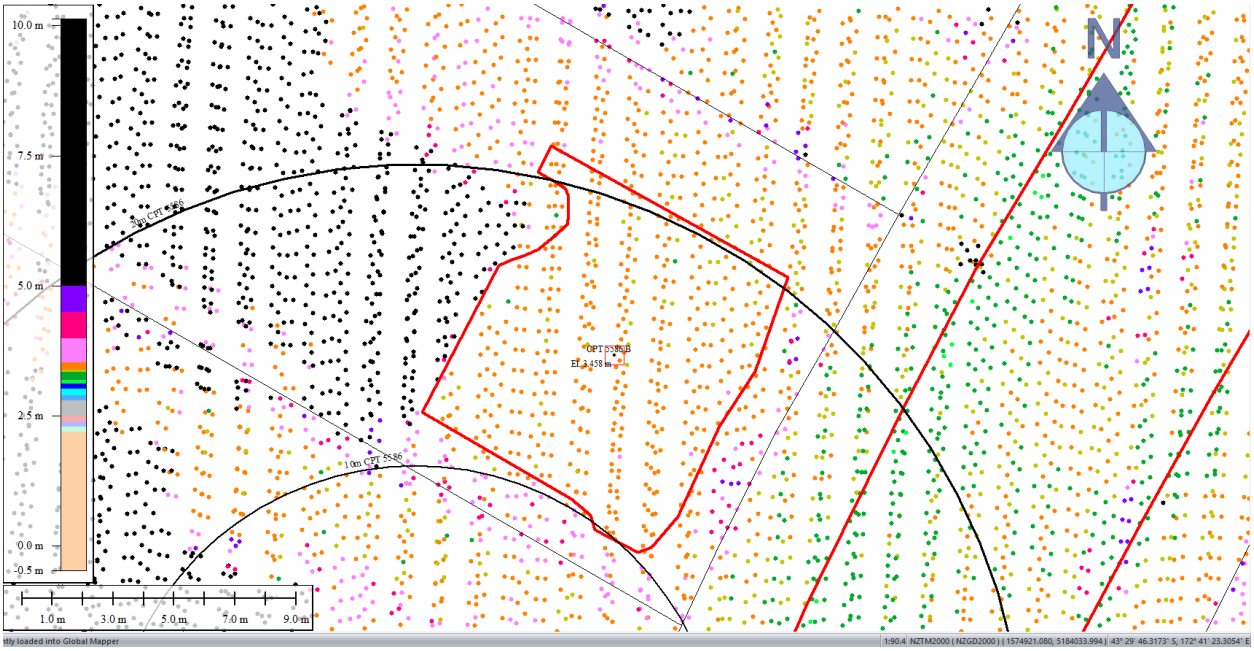

Figure 65: Ground surface elevation averaged over 20-m and 50-m buffers for Patch B for Feb 2012 LiDAR survey.

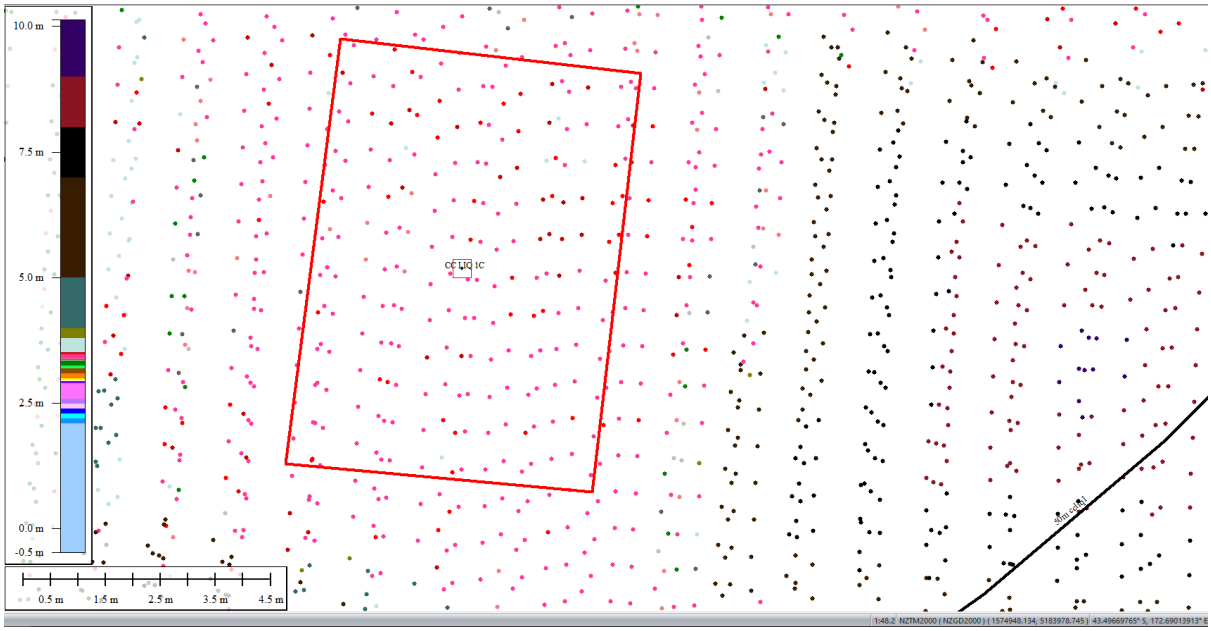

Figure 66: Ground surface elevation averaged over 50-m buffer for Patch C for Feb 2012 LiDAR survey.

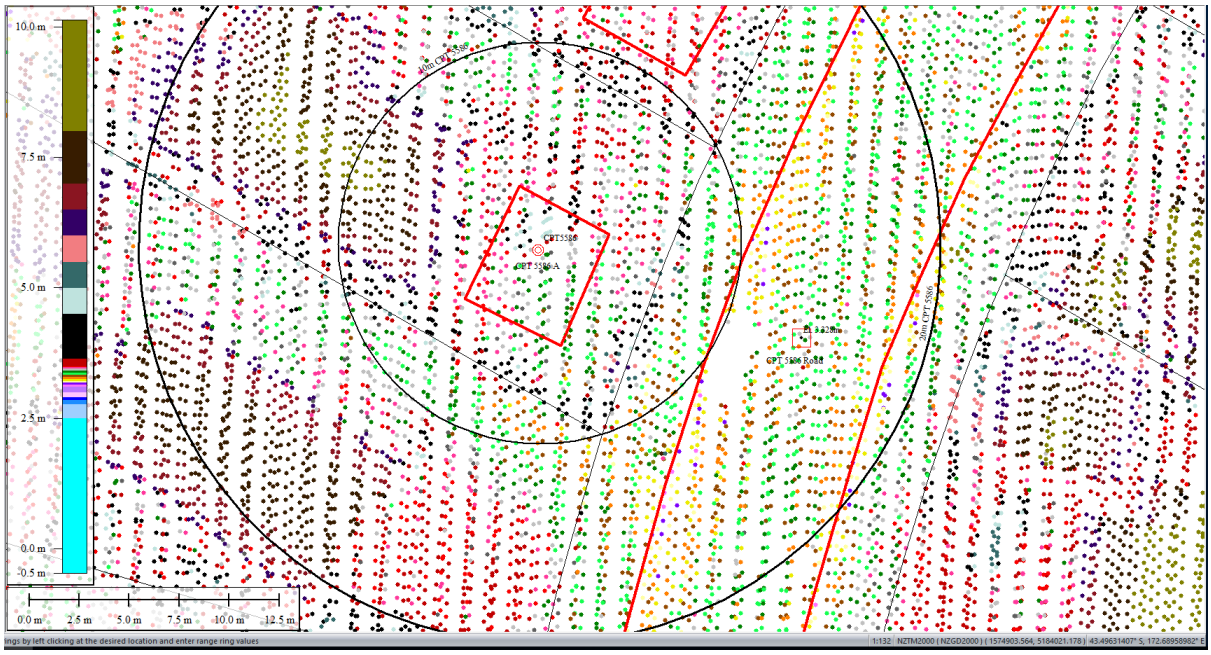

Figure 67: Ground surface elevation averaged over 20-m buffer for Road for Feb 2012 LiDAR survey.

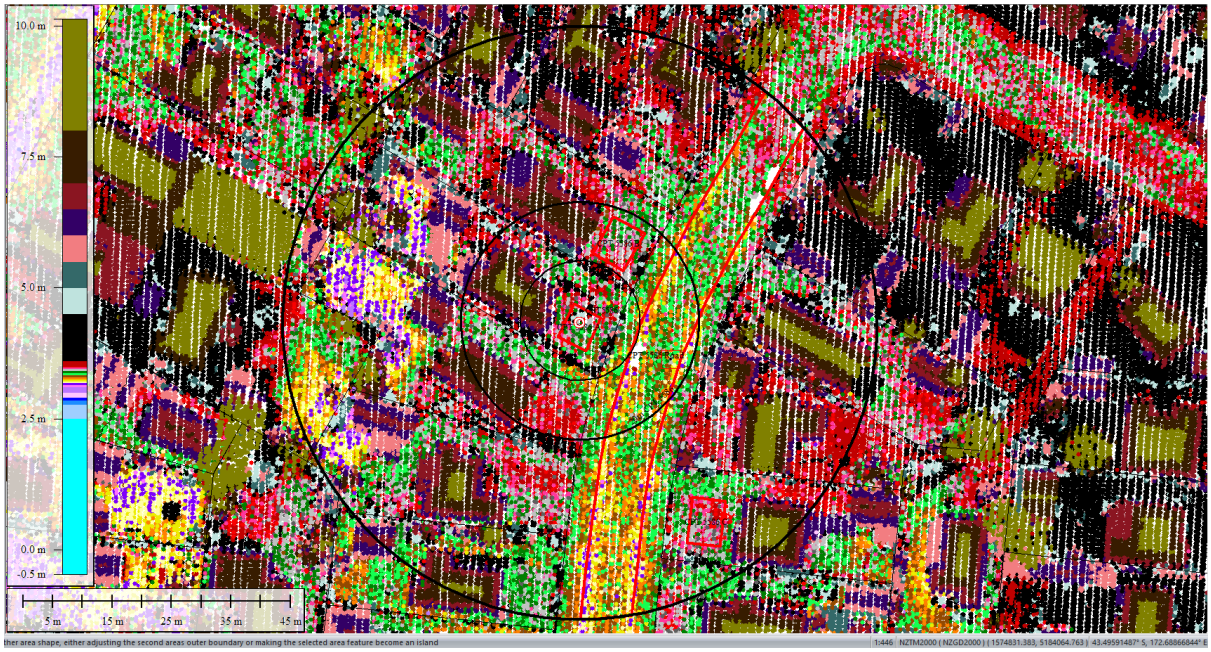

Figure 68: Ground surface elevation averaged over 50-m buffer for Road for Feb 2012 LiDAR survey.

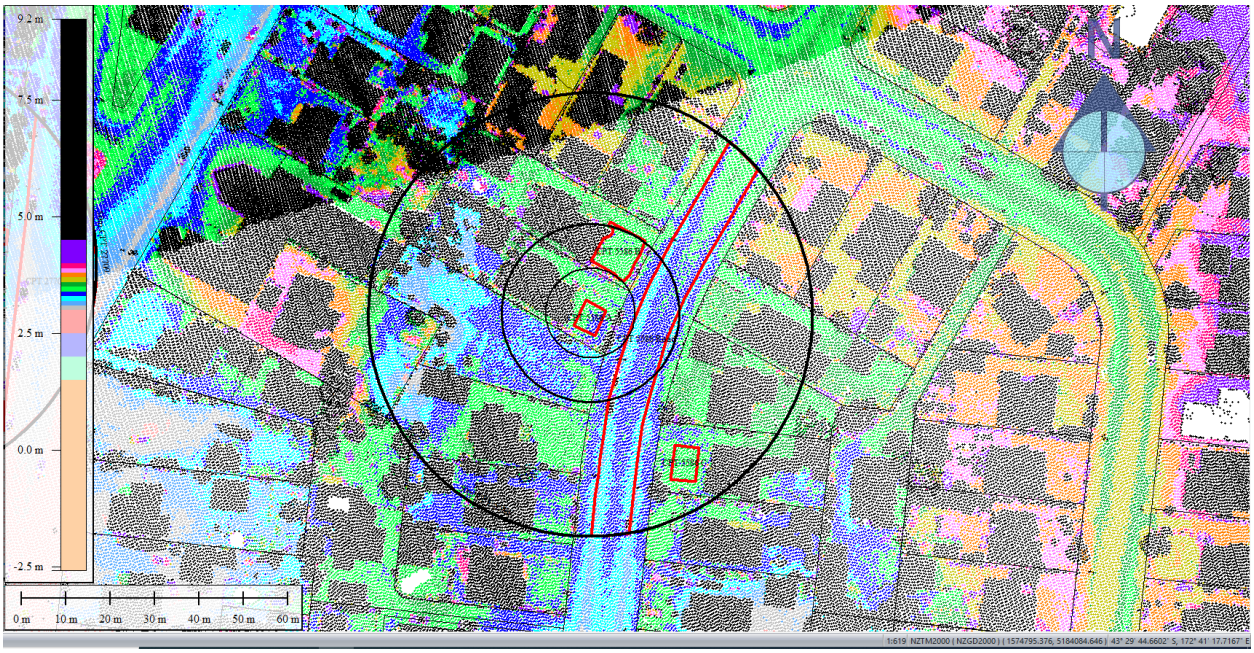

Figure 69: Oct 2015 LiDAR survey.

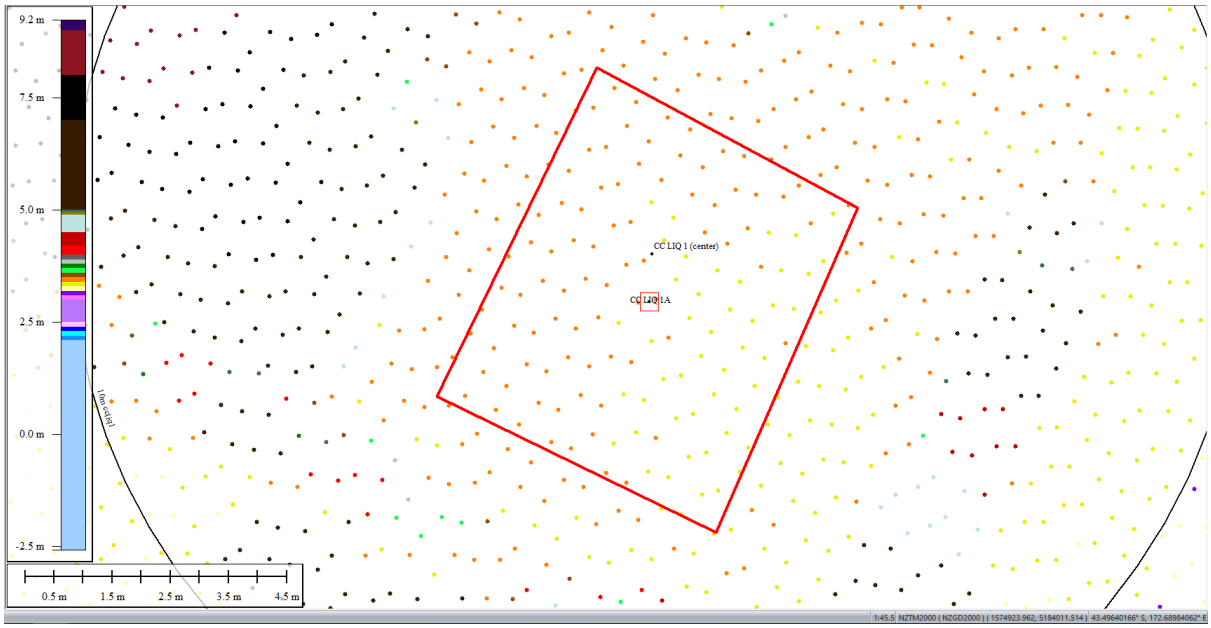

Figure 70: Ground surface elevation averaged over 10-m, 20-m, and 50-m buffers for Patch A for Oct 2015 LiDAR survey.

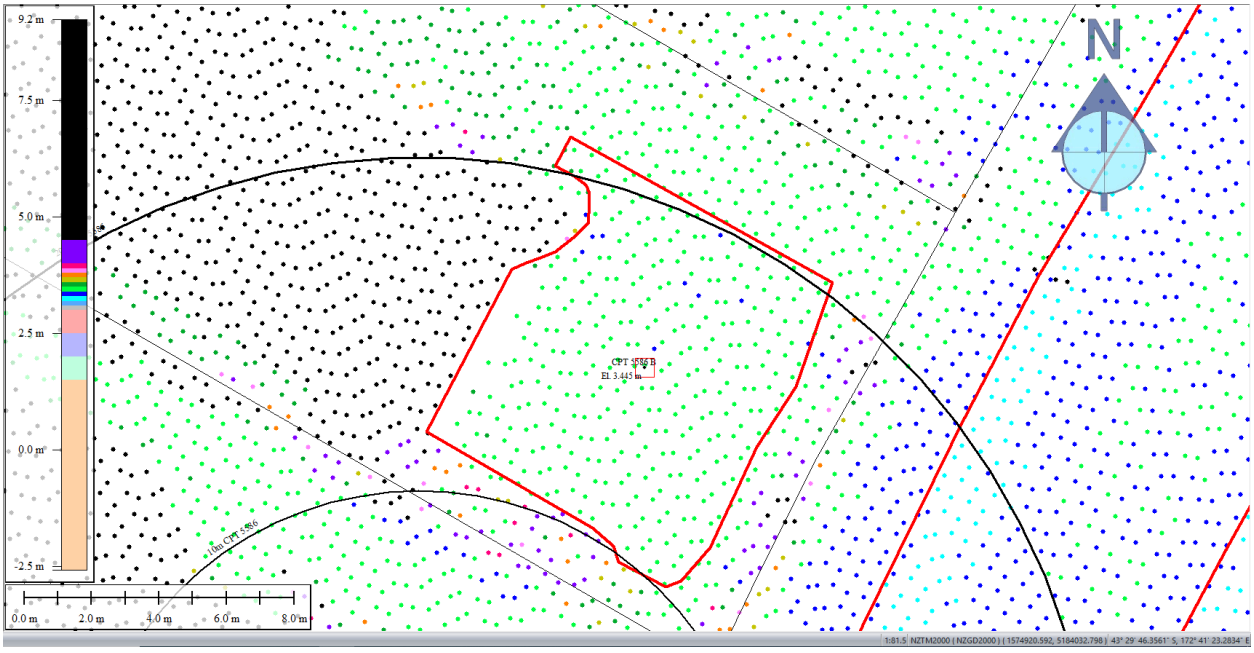

Figure 71: Ground surface elevation averaged over 20-m and 50-m buffers for Patch B for Oct 2015 LiDAR survey.

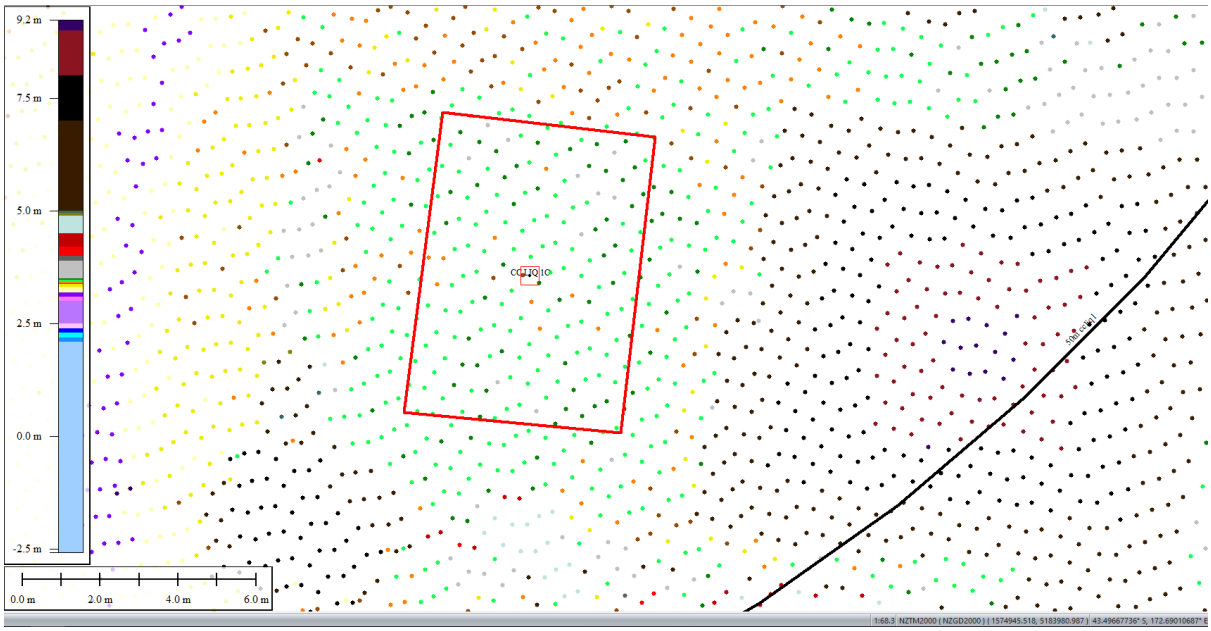

Figure 72: Ground surface elevation averaged over 50-m buffer for Patch C for Oct 2015 LiDAR survey.

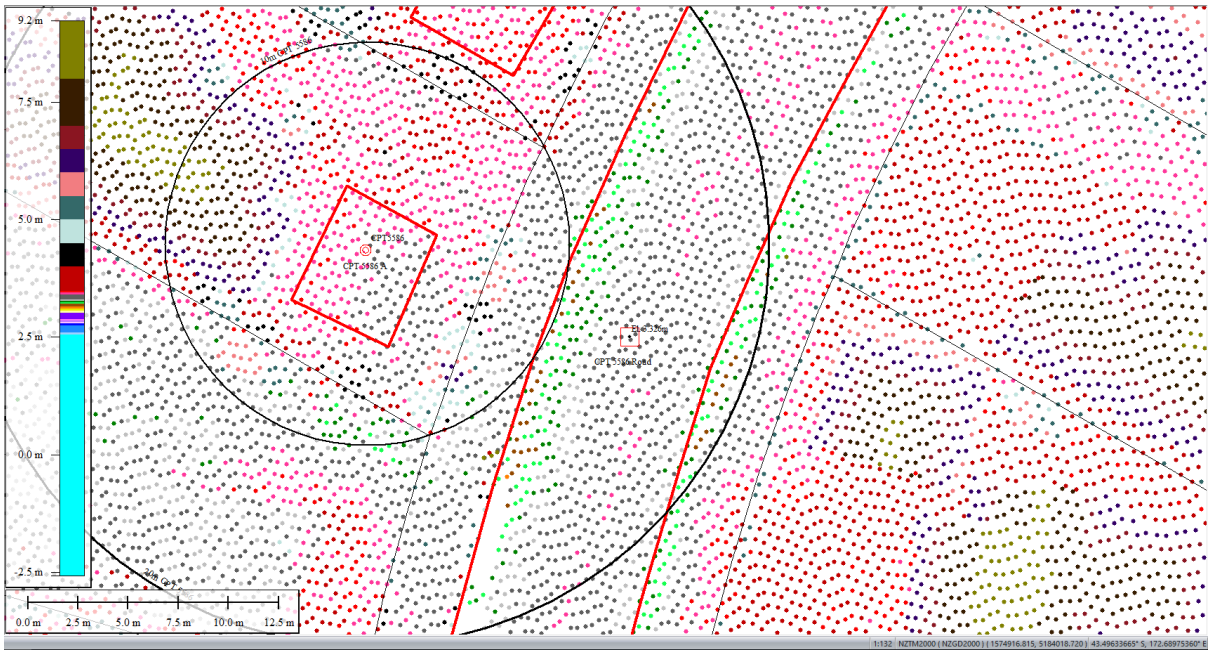

Figure 73: Ground surface elevation averaged over 20-m buffer for Road for Oct 2015 LiDAR survey.

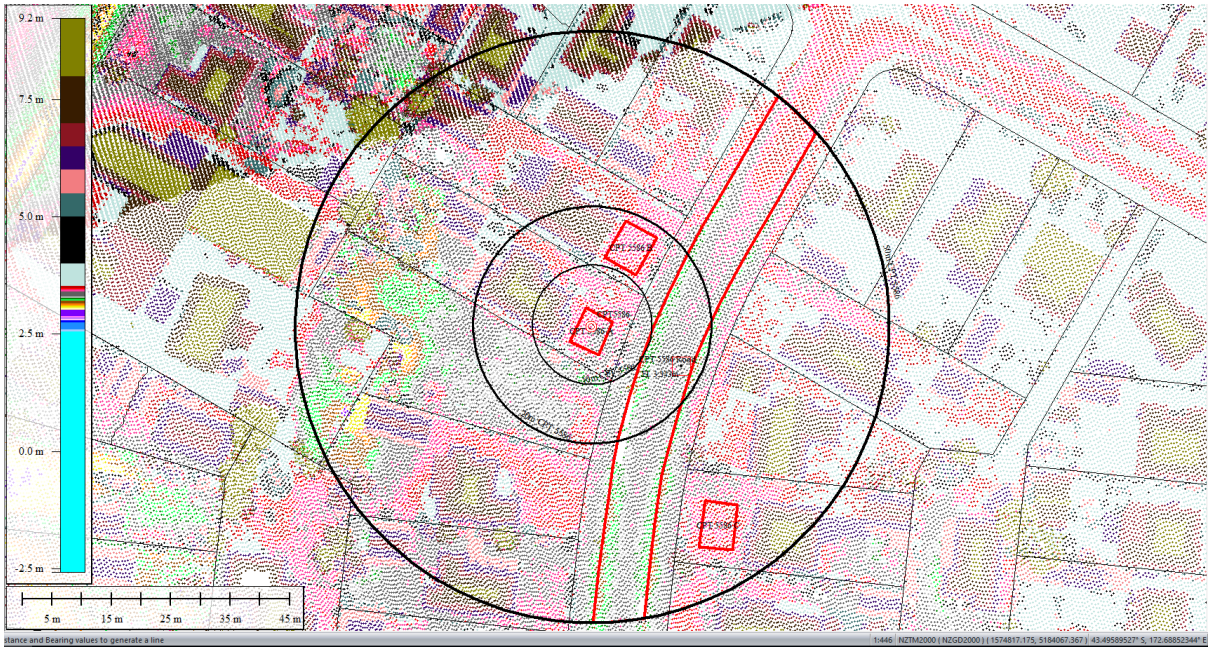

Figure 74: Ground surface elevation averaged over 50-m buffer for Road for Oct 2015 LiDAR survey.

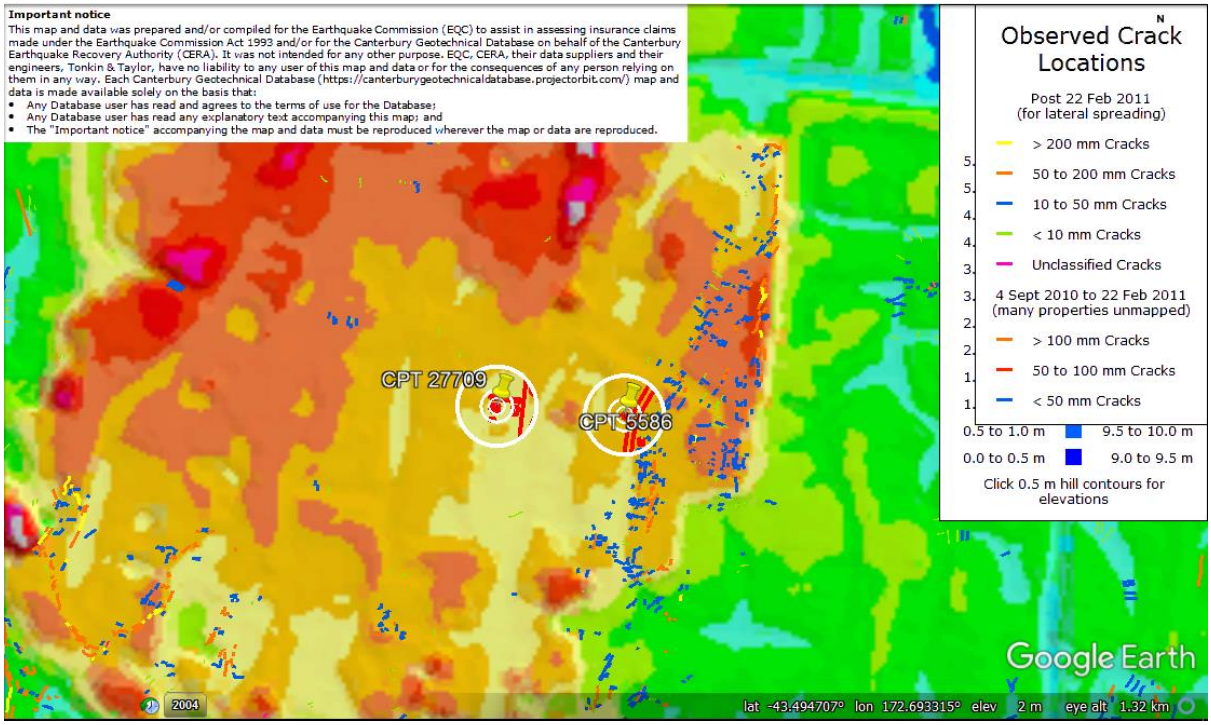

Figure 75: Ground surface elevation difference between the road and properties (Sep 2010 LiDAR DEM).

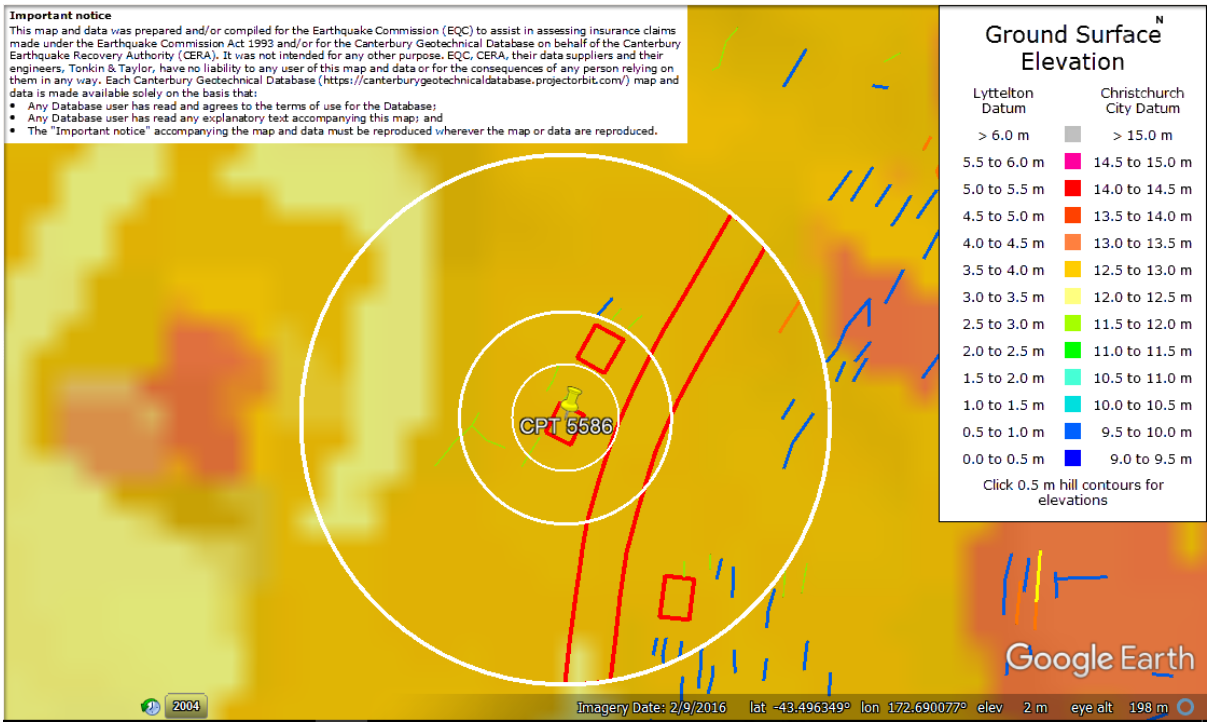

Figure 76: Enlarged view of ground surface elevation difference between the road and properties (Sep 2010 LiDAR DEM).

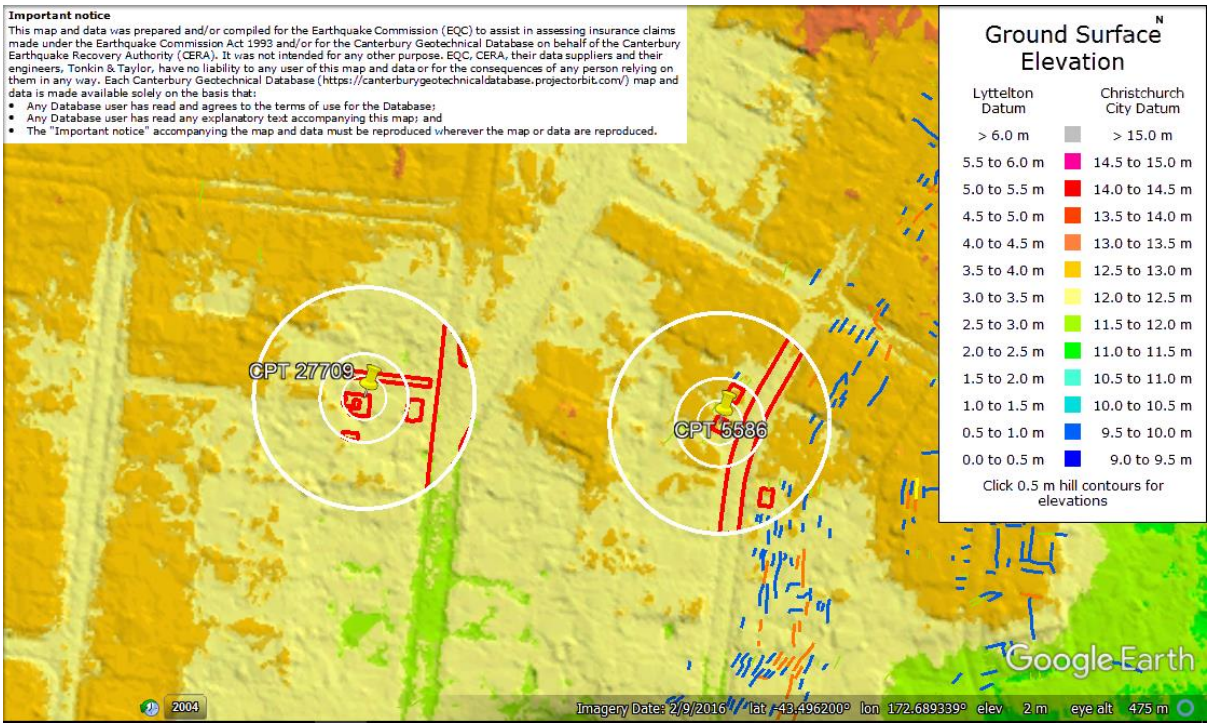

Figure 77: Enlarged view of ground surface elevation difference between the road and properties (Sep 2011 LiDAR DEM).

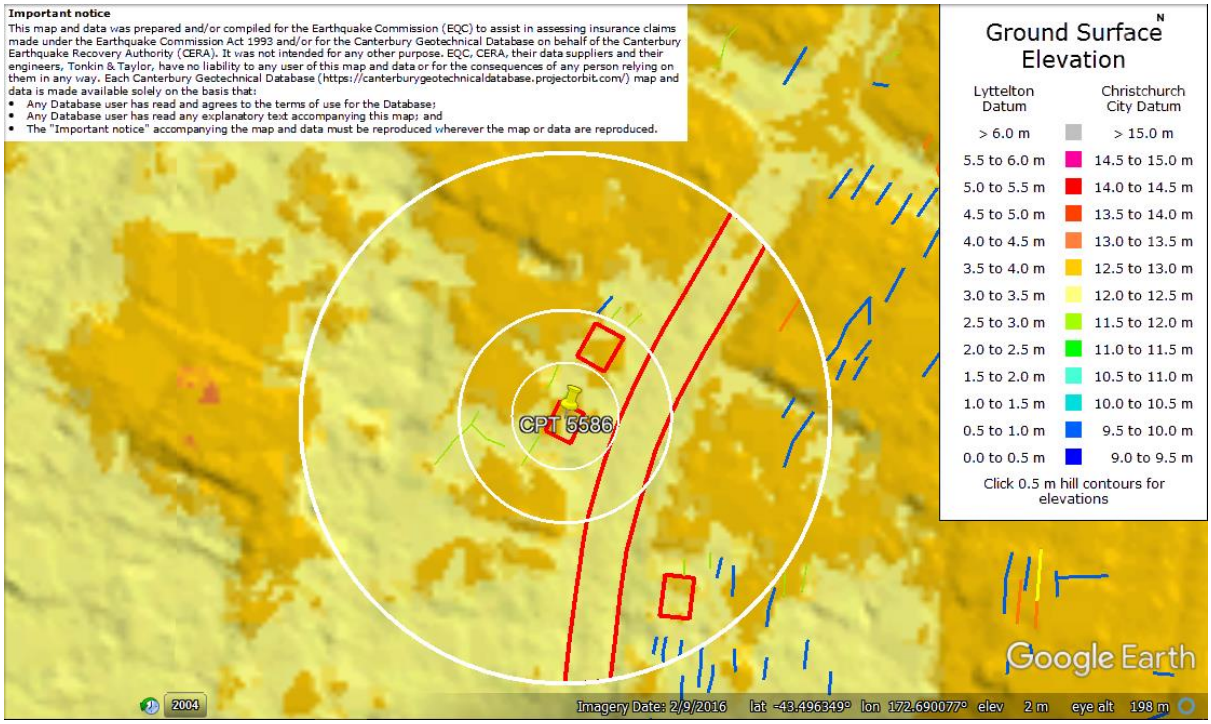

Figure 78: Ground surface elevation difference between the road and properties (Sep 2011 LiDAR DEM).

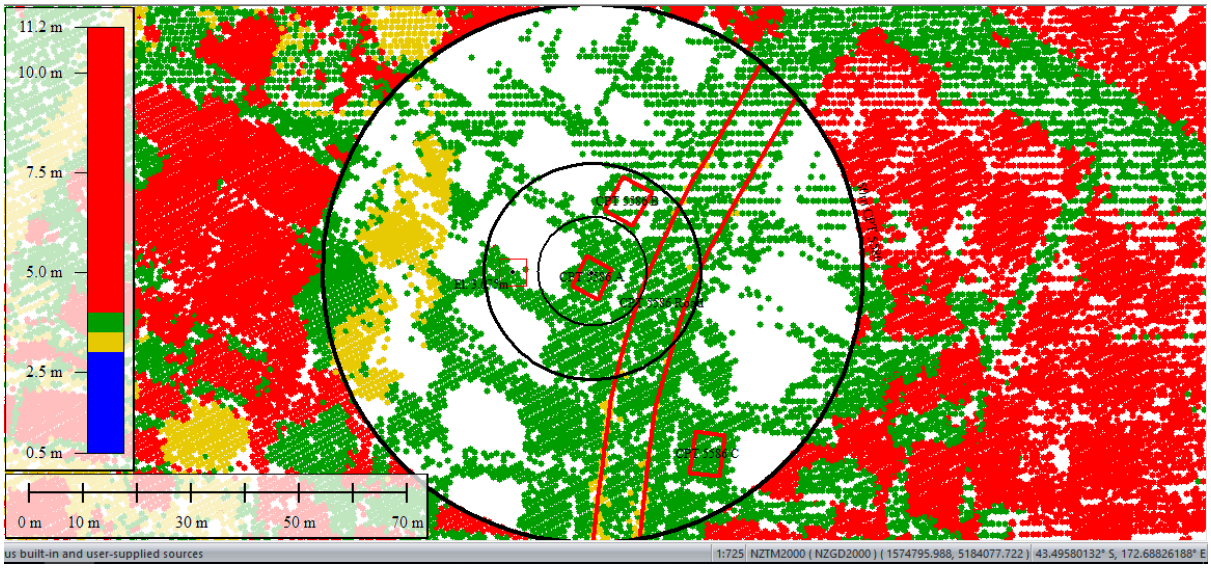

Figure 79: Ground surface elevation averaged over the properties in the east relative to the road for Sept 2010.

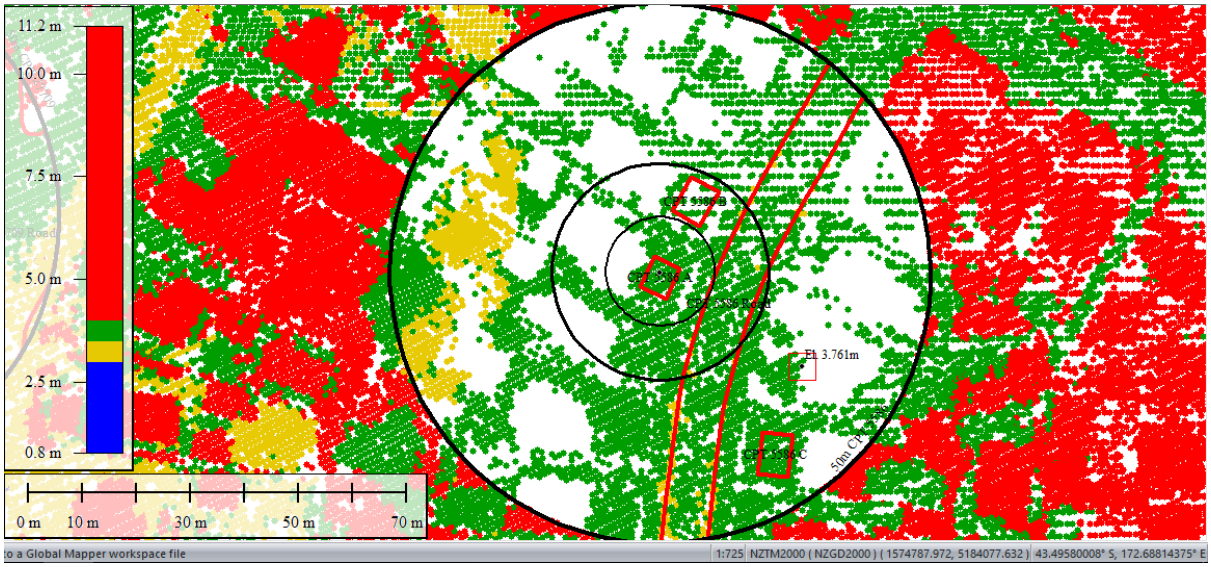

Figure 80: Ground surface elevation averaged over the properties in the west relative to the road for Sept 2010.

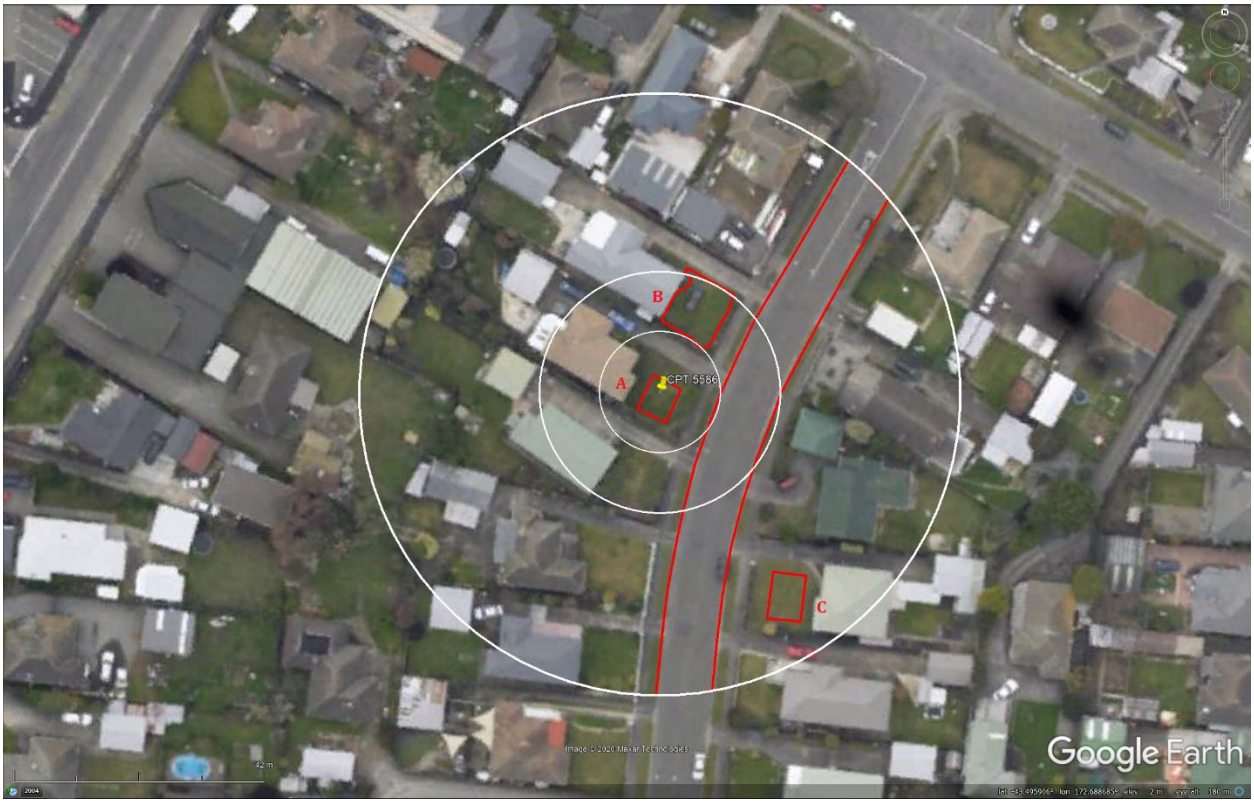

Figure 81: Aerial photograph showing no ejecta at the site for Sep-10 EQ.

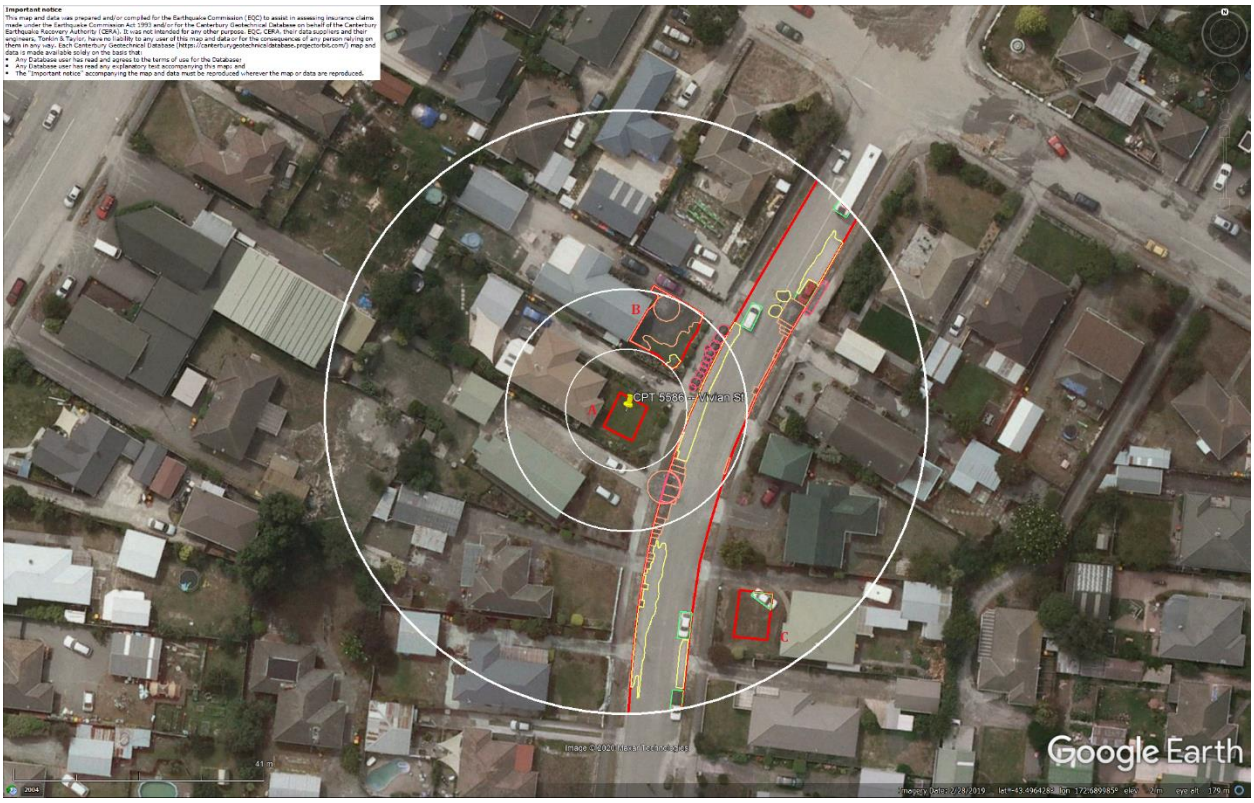

Figure 82: Aerial photograph showing the ejecta outline at the site for Feb-11 EQ.

Figure 83: Aerial photograph acquired on 16 Jun 2011 showing the ejecta outline at the site for Jun-11 EQ.

Figure 84: Aerial photograph acquired on 14-15 Jun 2011 showing ejecta at the site for Jun-11 EQ.

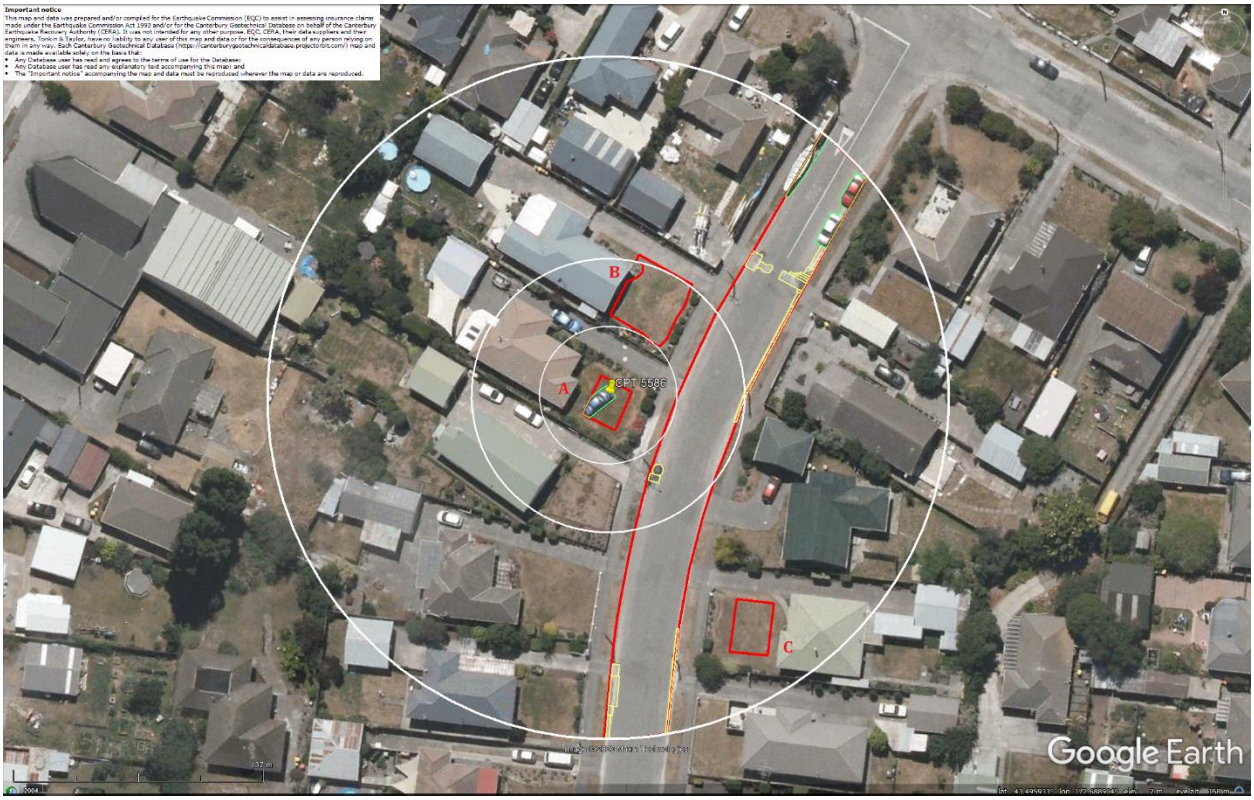

Figure 85: Aerial photograph showing the ejecta outline at the site for Dec-11 EQ.

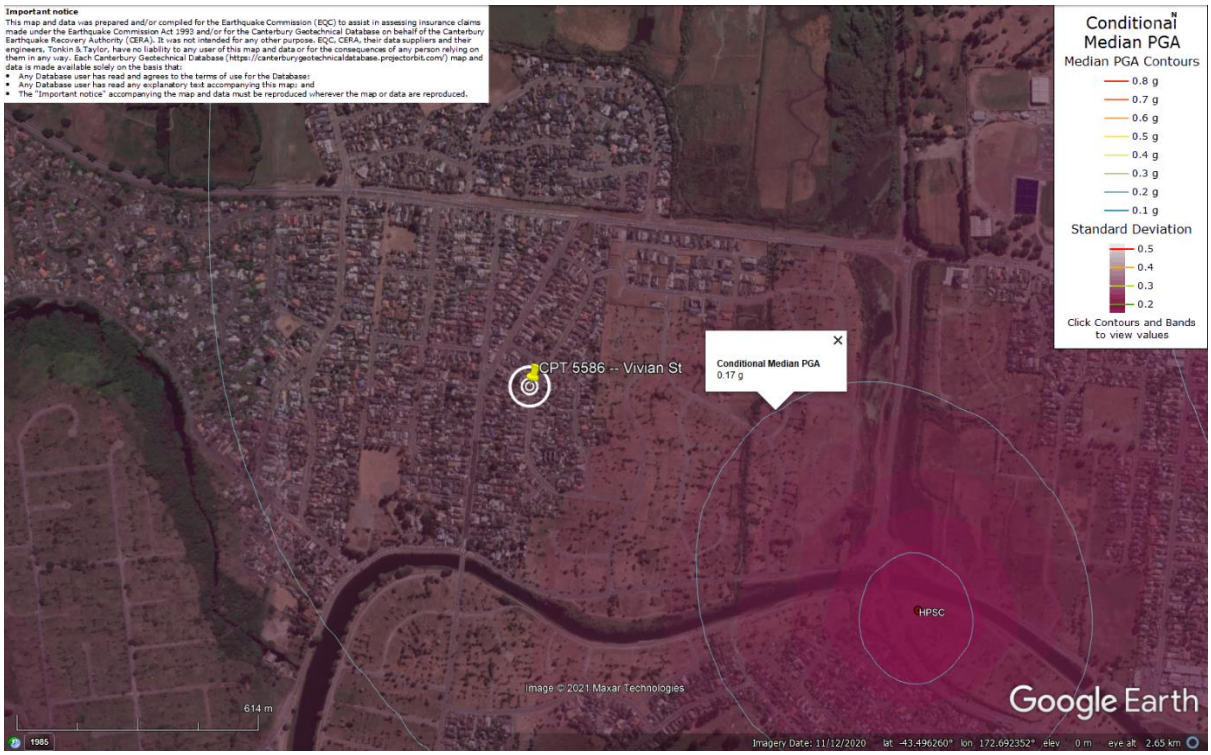

Figure 86: PGA for Sep-10 EQ (st. dev. = 0.300-0.325 ln units).

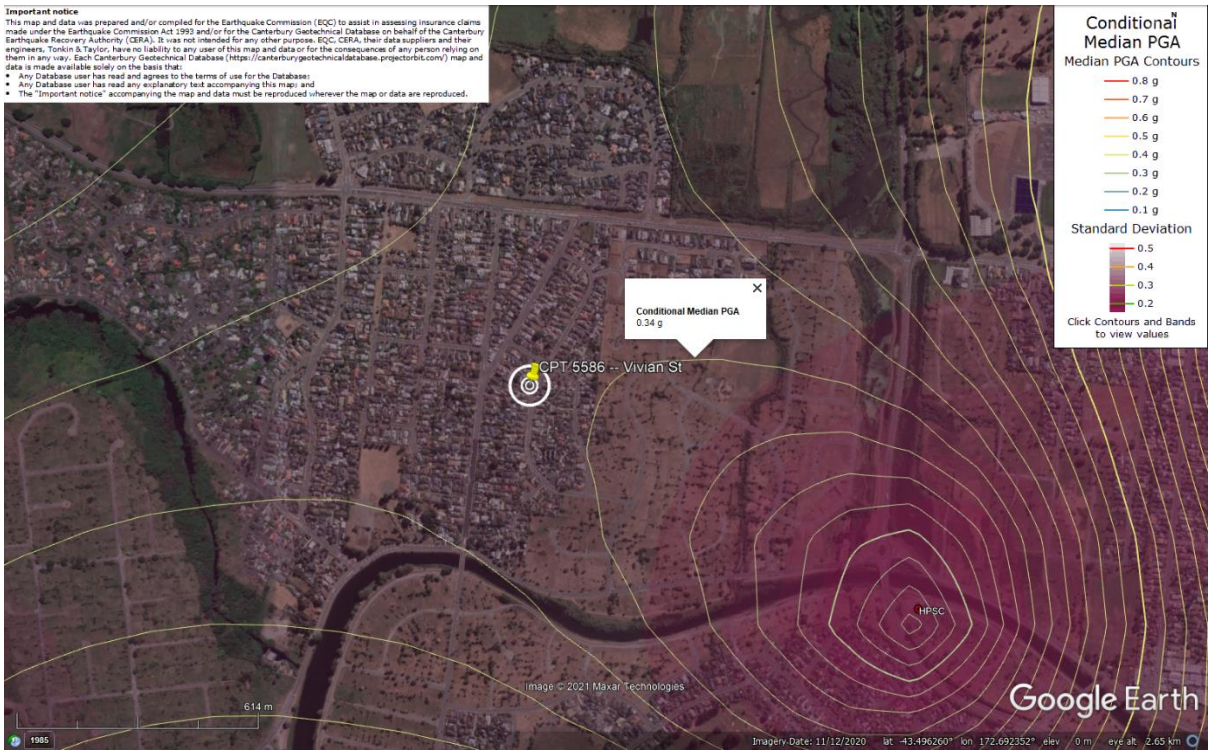

Figure 87: PGA for Feb-11 EQ (st. dev. = 0.325-0.350 ln units).

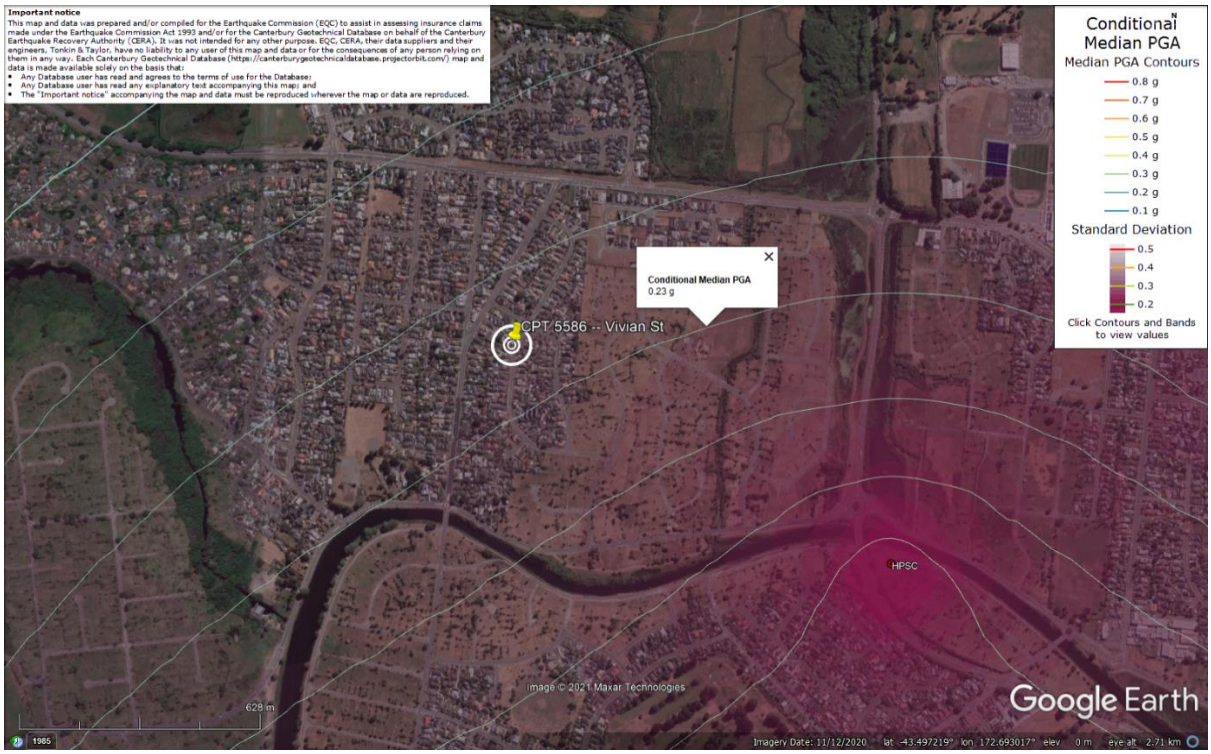

Figure 88: PGA for Jun-11 EQ (st. dev. = 0.325-0.375 ln units).

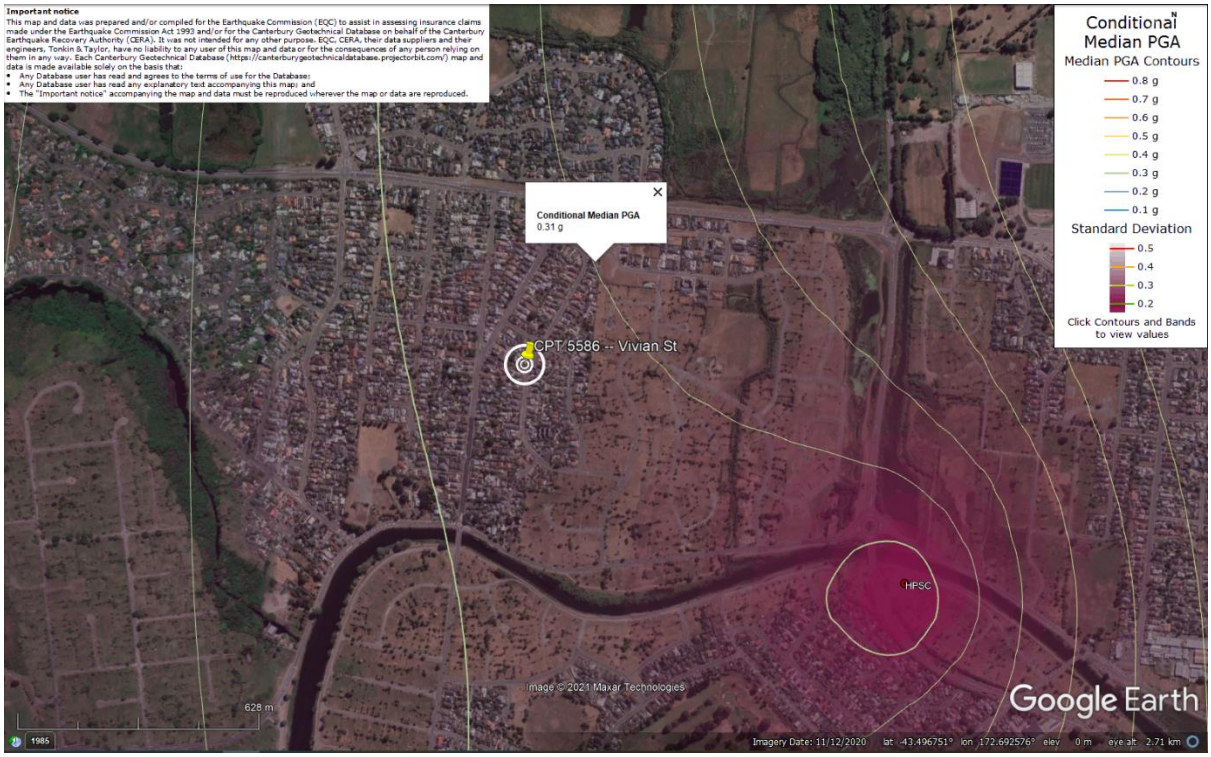

Figure 89: PGA for Dec-11 EQ (st. dev. = 0.350-0.375 ln units).

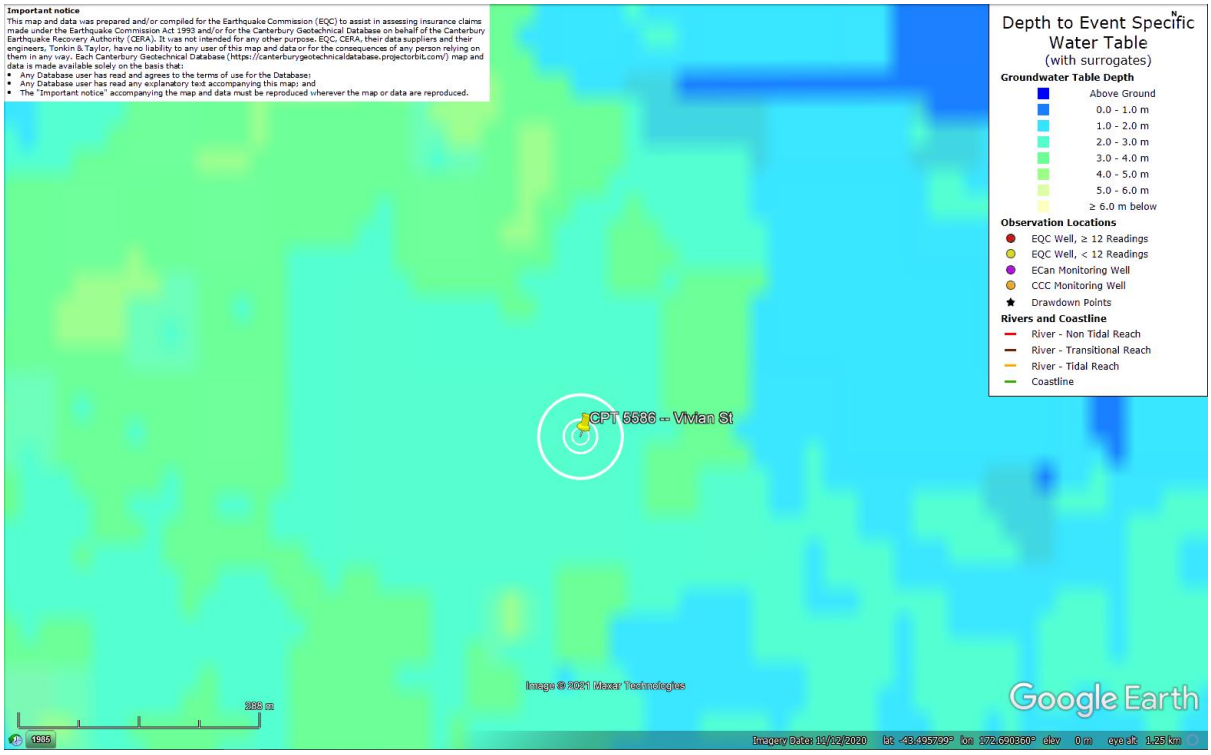

Figure 90: Depth to groundwater table for Sep-10 EQ.

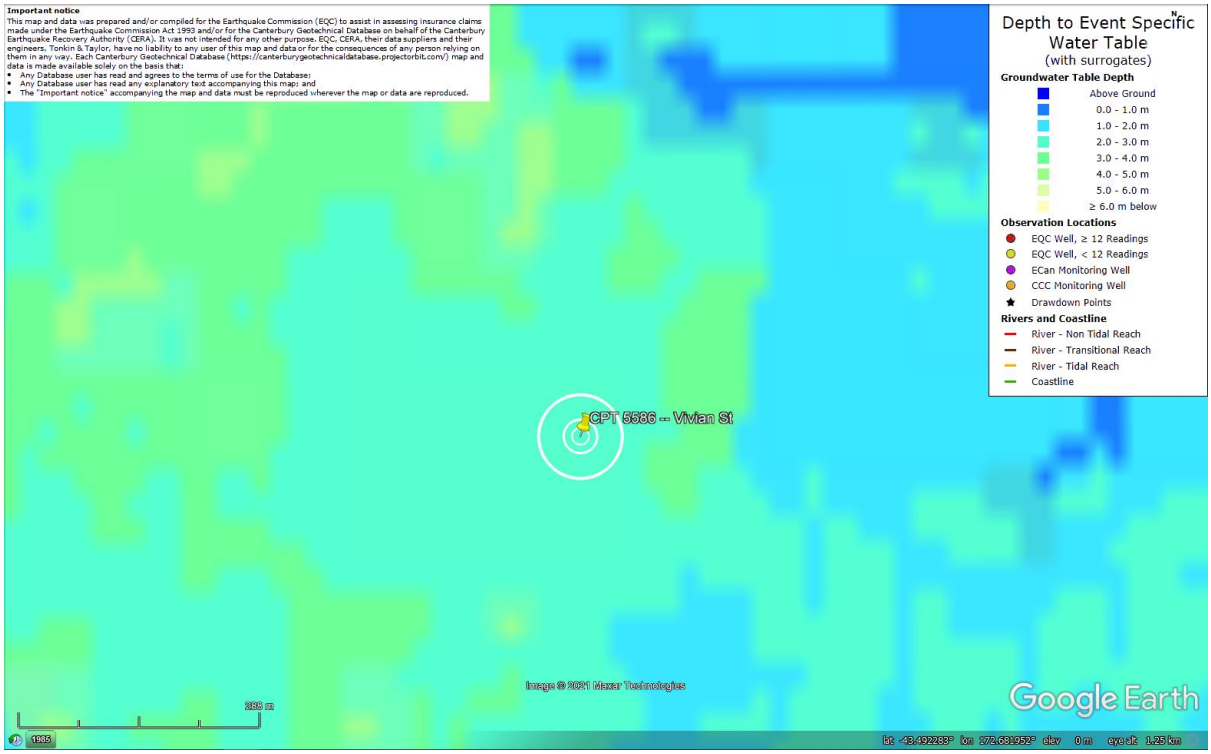

Figure 91: Depth to groundwater table for Feb-11 EQ.

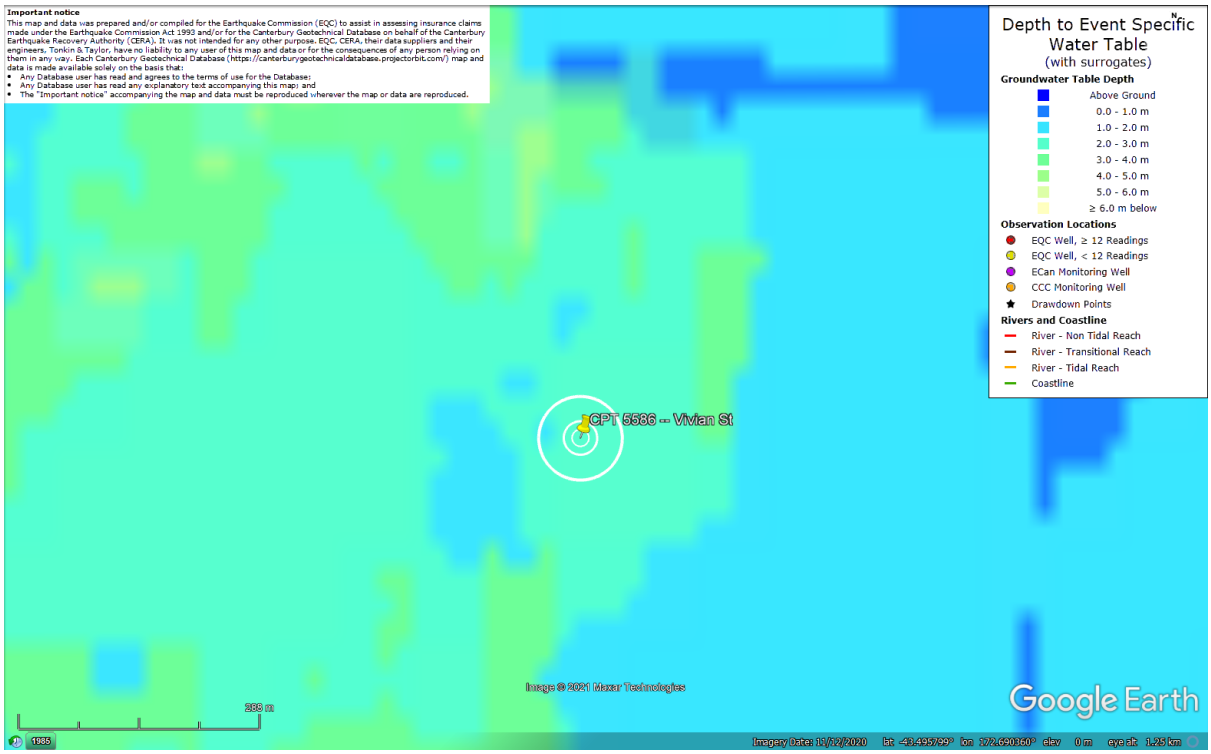

Figure 92: Depth to groundwater table for Jun-11 EQ.

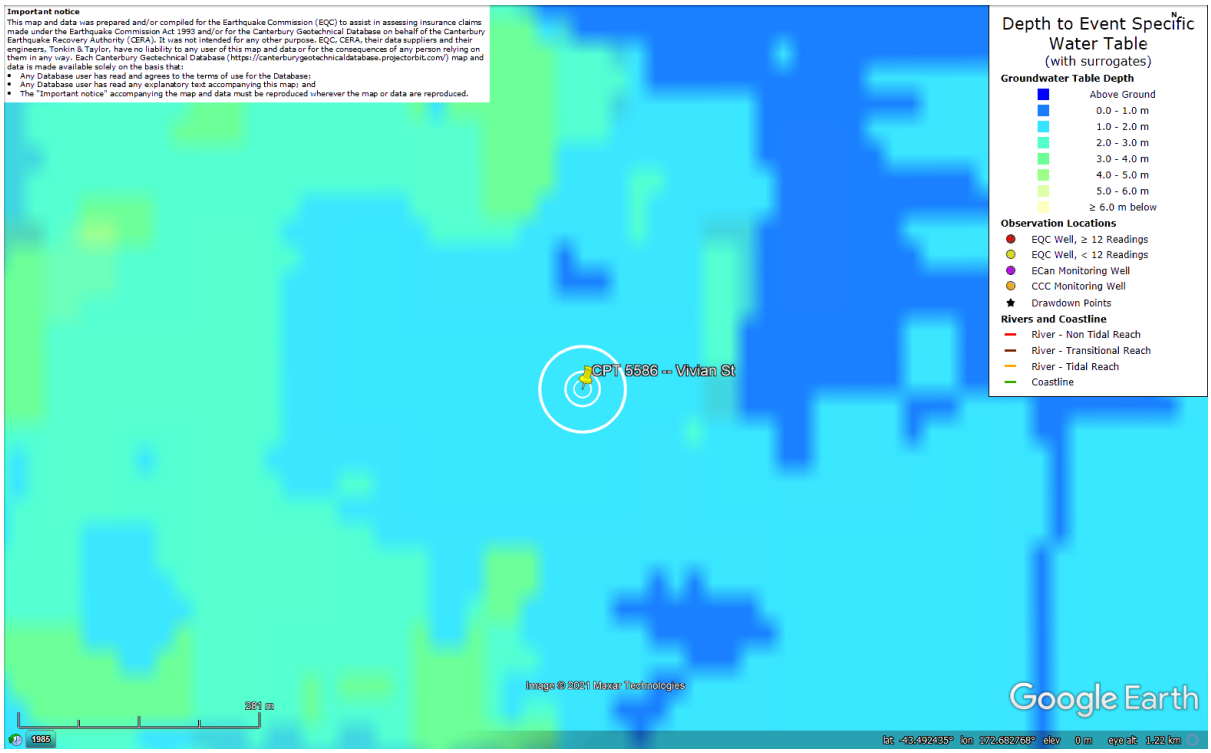

Figure 93: Depth to groundwater table for Dec-11 EQ.

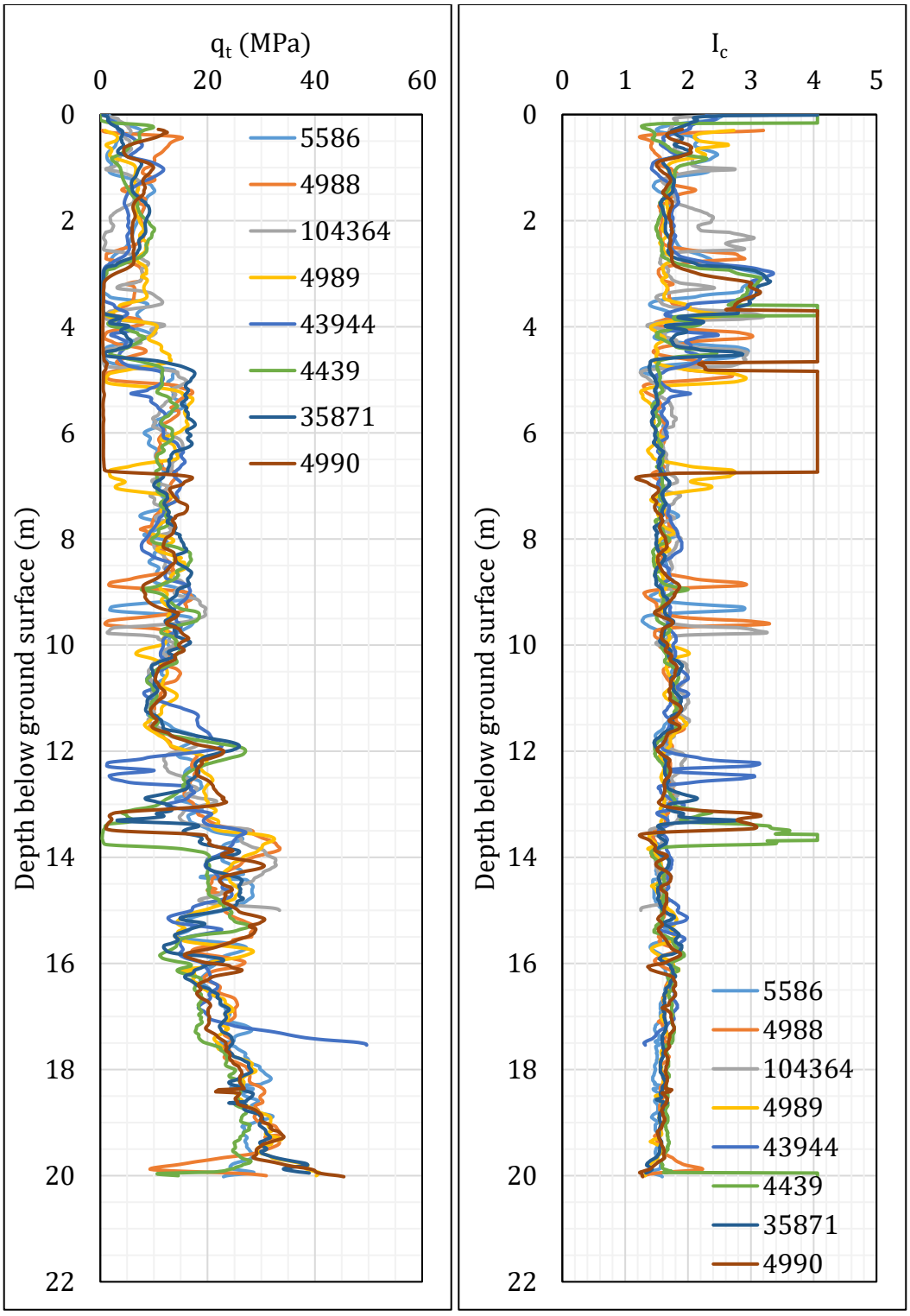

Figure 94: q_t and I_c profiles.

Note 6: The selection of CPTs for the area considered for settlement assessment (Figure 1) is based on the proximity of the CPTs to the considered areas. In accordance with that, the following table shows CPTs that were used for the volumetric settlement analysis in *Cliq v.3.0.3.2*, a CPT soil liquefaction software developed by GeoLogismiki. (The average volumetric settlements were reported in Table 8.)

Table 12: CPT profiles used in volumetric settlement analysis for areas selected for settlement assessment.

CPT ID No.	Patch A	Patch B	Patch C	Road
5586	✓	✓		✓
4988	✓	✓		✓
43944			✓	✓
35871		✓		✓
4990				✓
4439				✓
104364		✓		✓
34026				
4989		✓		
35872				
35873				
43495				

Table 13: CPT-based results.

		CPT ID							
EQ Event	Parameter	5586	4988	104364	4989	43944	4439	35871	4990
Sep-10	S_{V1D} (mm)	9	9	1	6	6	9	5	7
	LSN	2	2	0	1	1	1	1	1
	LPI	0	0	0	0	0	0	0	0
	LPI_{ish}	0	0	0	0	0	0	0	0
	$D_{FS<1}$ (m)	undet.	undet.	undet.	undet.	undet.	undet.	undet.	undet.
Feb-11	S_{V1D} (mm)	86	76	29	68	58	78	51	35
	LSN	14	14	5	10	11	12	9	5
	LPI	5	5	1	4	3	5	3	2
	LPI_{ish}	1	2	0	1	1	1	1	1
	$D_{FS<1}$ (m)	2.62	3.18	undet.	3.50	3.54	2.72	3.76	8.66
Jun-11	S_{V1D} (mm)	27	26	5	19	20	28	17	13
	LSN	5	5	1	3	4	5	3	2
	LPI	1	1	0	0	0	1	0	0
	LPI_{ish}	1	1	0	0	0	1	0	0
	$D_{FS<1}$ (m)	undet.	undet.	undet.	undet.	3.54	3.80	undet.	undet.
Dec-11	S_{V1D} (mm)	89	79	39	71	72	79	52	39
	LSN	16	16	10	13	17	13	10	8
	LPI	6	6	2	4	5	5	3	2
	LPI_{ish}	3	2	1	2	2	2	1	1
	$D_{FS<1}$ (m)	2.52	3.10	1.86	3.48	2.00	2.69	2.55	2.26

Notes: $D_{FS<1}$ = Depth to the first liquefiable layer ($FS_L<1$) that is at least 200-mm thick, as determined by the Boulanger and Idriss (2016) liquefaction-triggering procedure (P_L=50%, C_{FC}=0.13, and $I_{c,cutoff}$ =2.6), and exported from *Cliq v.3.0.3.2*; undet. = the specified soil layer was not detected.

Note 7: Based on the borehole log (BH 8995, Figure 1), the groundwater table is at a depth of 1.95 m below the ground surface. The soil profile consists of (1) topsoil to a depth of 0.3 m, (2) poorly graded sand, SP, of the Christchurch formation to a depth of 2.7 m, (3) silty sand, SM, of the Christchurch formation with roughly 60% of low-plasticity (PI=11) fines to a depth of 3.6 m, and (4) denser, poorly graded sand, SP, of the Christchurch formation with the median fines content of 10% (for a range of 8-16% fines) to a depth of 20 m.

Note 8: The ejecta-induced free-field settlement provided in Table 11 is an areal average settlement due to ejecta, which is based on the total settlement assessment area, A_T (provided in Table 9 and repeated in Table 14). However, the considered area was not always covered completely with ejecta; thus, it is important to provide the localized ejecta-induced settlement, too. The localized settlement due to ejecta is estimated using photographic evidence only as

$$S_{E,P\_localized} = \frac{V_E}{A_E}$$

where V_E is the total volume of ejecta within A_T and A_E is the total coverage area of ejecta within A_T. Please note that the areal ejecta-induced settlement provided in Table 14 as S_{E,P_areal} is the same as $S_{E,P}$ in Table 11, which was estimated as

$$S_{E,P\_areal} = S_{E,P} = \frac{V_E}{A_T}$$

where V_E is the total volume of ejecta within A_T and A_T is the total settlement assessment area.

Table 14a: Areal and localized ejecta-induced settlement estimates for Patch B (20-m and 50-m buffers) based on photographic evidence.

Earthquake Event	A_T (m^2)	A_E (m^2)	V_E (m^3)	S_{E,P_areal} (mm)	$S_{E,P\_localized}$ (mm)
Sep-10	87.0	0	0	0	0
Feb-11	87.0	64.5	4.6-9.6	80±30	110±40
Jun-11	87.0	0	0	0	0
Dec-11	87.0	0	0	0	0

Notes: S_{E,P_areal} = $S_{E,P}$ reported in Table 11 = areal ejecta-induced settlement; $S_{E,P\_localized}$ = localized ejecta-induced settlement; A_T = total settlement assessment area; V_E = total volume of ejecta within A_T; A_E = total area of ejecta within A_T; The estimates of both areal and localized ejecta-induced settlement are rounded to the nearest 5; Final plus/minus values are also rounded to the nearest 5.

Table 14b: Areal and localized ejecta-induced settlement estimates for Road (20-m buffer) based on photographic evidence.

Earthquake Event	A_T (m^2)	A_E (m^2)	V_E (m^3)	S_{E,P_areal} (mm)	$S_{E,P\_localized}$ (mm)
Sep-10	223	0	0	0	0
Feb-11	223	64.2	4.6-6.2	25±5	85±10
Jun-11	236	127	9.0-9.3	40±5	70±5
Dec-11	240	5.2	0.1-0.2	<5	30±10

Notes: S_{E,P_areal} = $S_{E,P}$ reported in Table 11 = areal ejecta-induced settlement; $S_{E,P\_localized}$ = localized ejecta-induced settlement; A_T = total settlement assessment area; V_E = total volume of ejecta within A_T; A_E = total area of ejecta within A_T; The estimates of both areal and localized ejecta-induced settlement are rounded to the nearest 5; Final plus/minus values are also rounded to the nearest 5.

Table 14c: Areal and localized ejecta-induced settlement estimates for Road (50-m buffer) based on photographic evidence.

Earthquake Event	A_T (m^2)	A_E (m^2)	V_E (m^3)	S_{E,P_areal} (mm)	$S_{E,P\_localized}$ (mm)
Sep-10	785	0	0	0	0
Feb-11	779	213	7.0-10.1	10±5	40±5
Jun-11	829	413	10.5-12.4	15±5	30±5
Dec-11	812	45.2	0.6-1.2	<5	20±5

Notes: S_{E,P_areal} = $S_{E,P}$ reported in Table 11 = areal ejecta-induced settlement; $S_{E,P\_localized}$ = localized ejecta-induced settlement; A_T = total settlement assessment area; V_E = total volume of ejecta within A_T; A_E = total area of ejecta within A_T; The estimates of both areal and localized ejecta-induced settlement are rounded to the nearest 5; Final plus/minus values are also rounded to the nearest 5.

Summary 2:

- **The best estimate of the localized ejecta-induced free-field ground settlement at the Vivian St site for the SEP 2010, FEB 2011, JUN 2011, and DEC 2011 earthquake is 0 mm, 110±40 mm, 0 mm, and 0 mm, respectively.**
- **The best estimate of the localized ejecta-induced settlement of the road at the Vivian St site for the SEP 2010, FEB 2011, JUN 2011, and DEC 2011 earthquake is 0 mm, 85±10 mm, 70±5 mm, and 30±10 mm, respectively.**

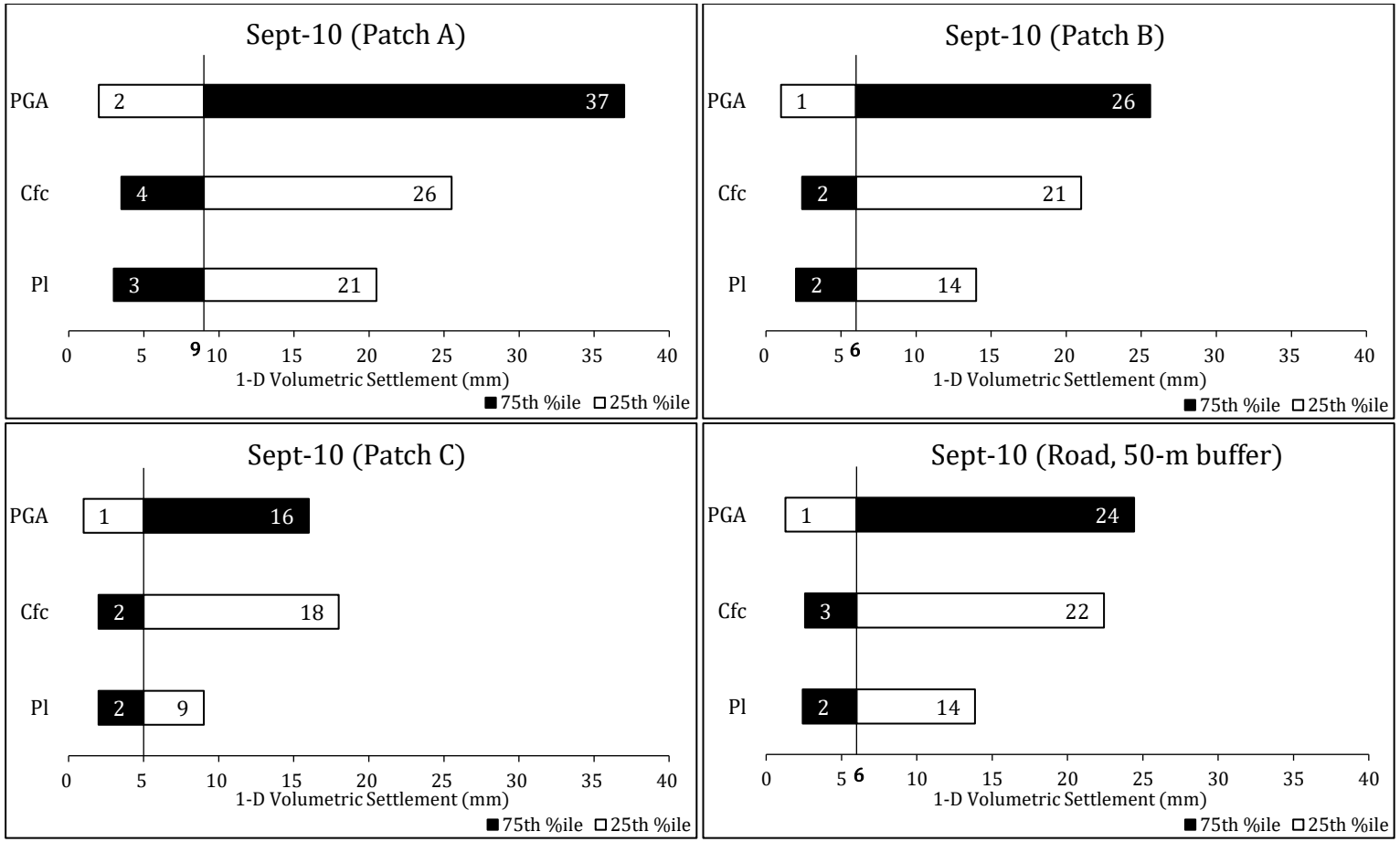

Figure 95: Sensitivity of volumetric settlement (Zhang et al. 2002) to PGA, C_{FC}, and P_L for Sep-10 EQ event. (The baseline case is the 50th %ile.)

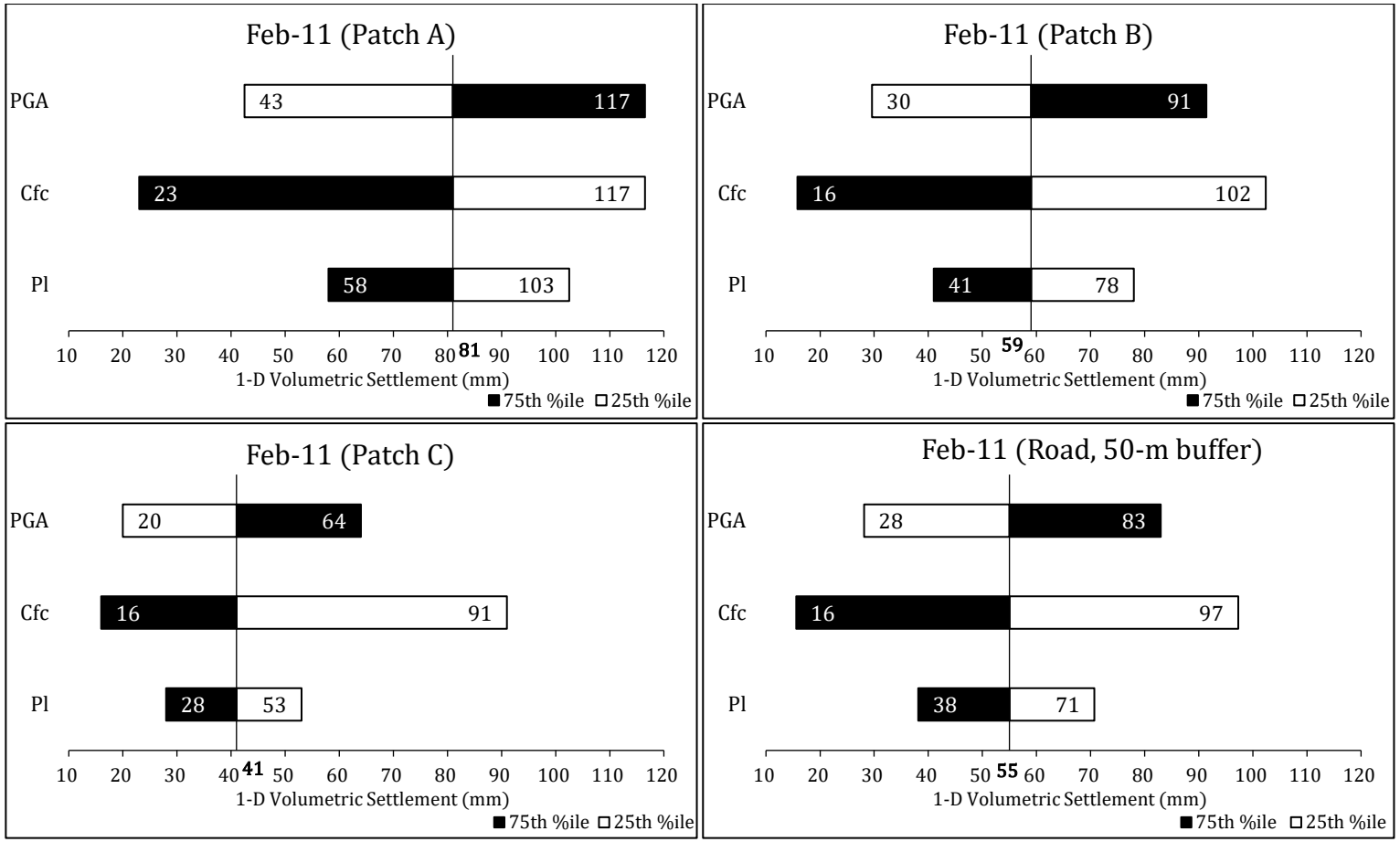

Figure 96: Sensitivity of volumetric settlement (Zhang et al. 2002) to PGA, C_{FC}, and P_L for Feb-11 EQ event. (The baseline case is the 50th %ile.)

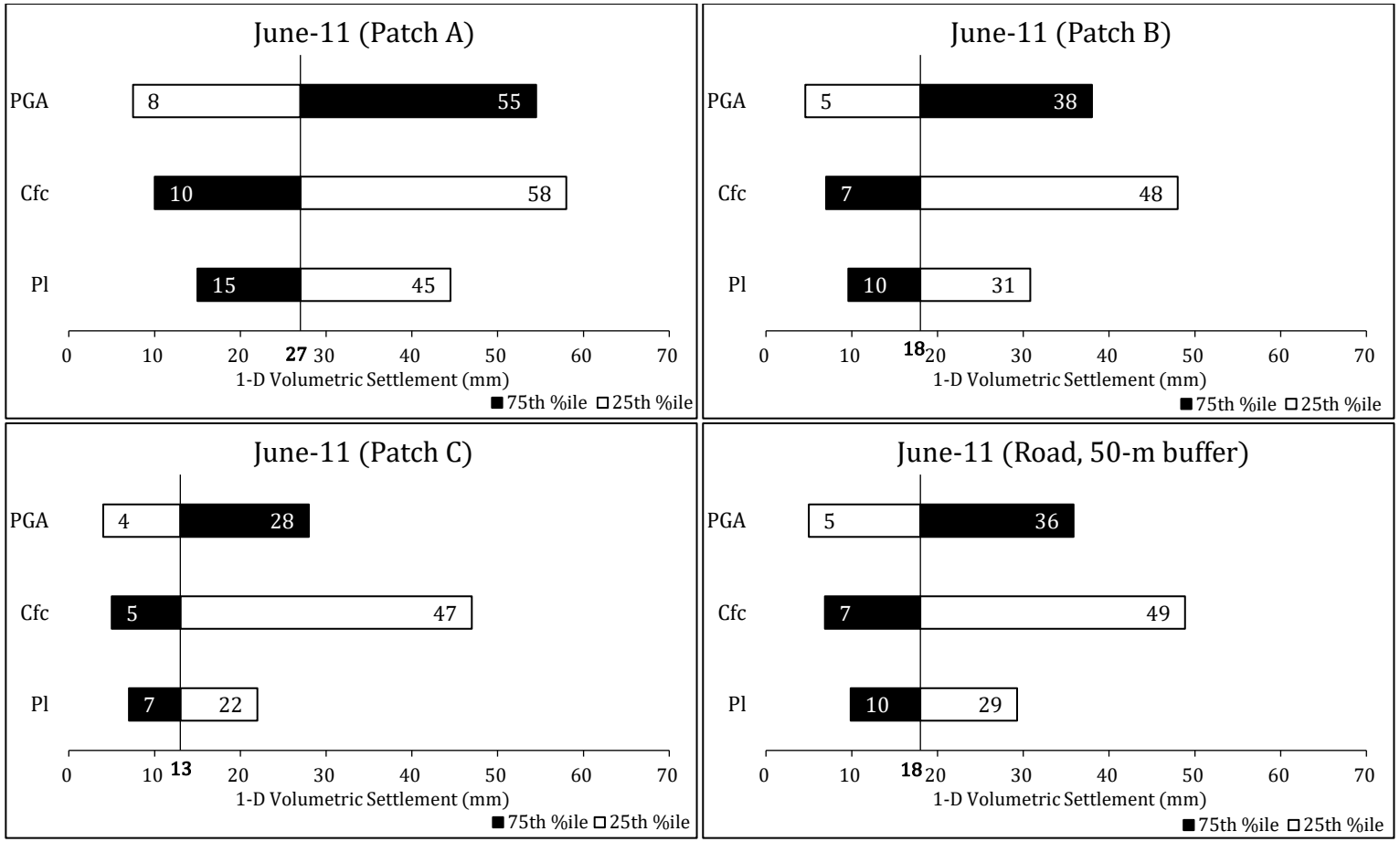

Figure 97: Sensitivity of volumetric settlement (Zhang et al. 2002) to PGA, C_{FC}, and P_L for Jun-11 EQ event. (The baseline case is the 50th %ile.)

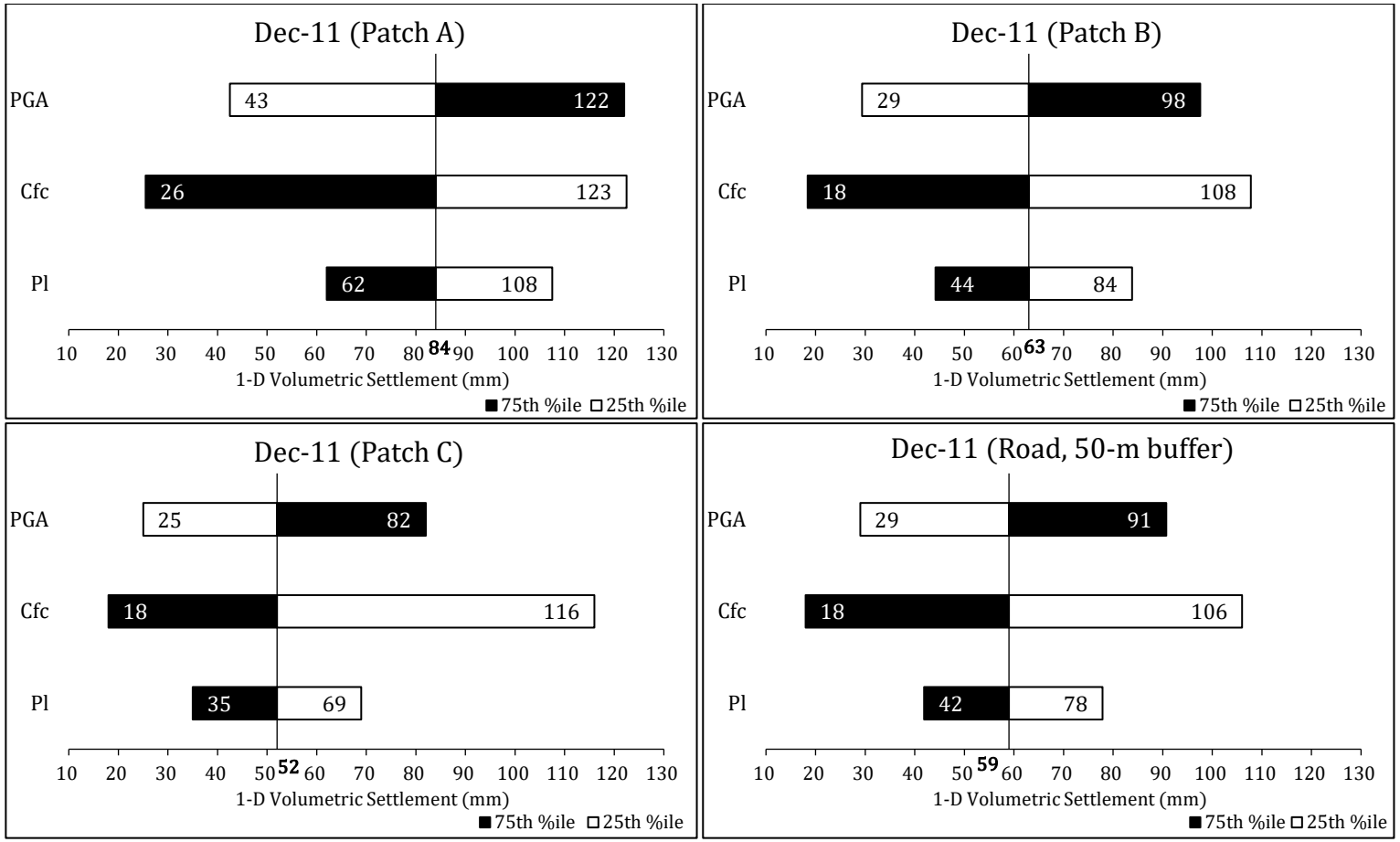

Figure 98: Sensitivity of volumetric settlement (Zhang et al. 2002) to PGA, C_{FC}, and P_L for Dec-11 EQ event. (The baseline case is the 50th %ile.)